

**Universidade do Minho**  
Escola de Ciências

Luís Miguel Mesquita da Silva Ferreira

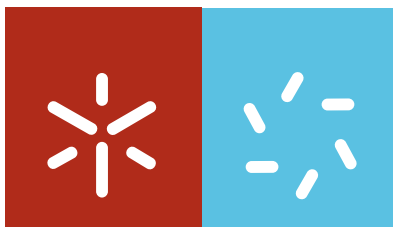
**Applications of Dynamical Systems to  
Economical and Biological Sciences**

**Applications of Dynamical Systems to  
Economical and Biological Sciences**

Luís Miguel Mesquita da Silva Ferreira

UMinho | 2010

Março de 2010



**Universidade do Minho**  
Escola de Ciências

Luís Miguel Mesquita da Silva Ferreira

## **Applications of Dynamical Systems to Economical and Biological Sciences**

Tese de Doutoramento em Ciências  
Área de Conhecimento em Matemática

Trabalho realizado sob a orientação do  
**Professor Doutor Alberto Adrego Pinto**  
e do  
**Professor Doutor Bruno Miguel Paz Mendes de Oliveira**

Março de 2010

---

## DECLARAÇÃO

Nome: Luís Miguel Mesquita da Silva Ferreira

Endereço electrónico: migferreira2@gmail.com    Telefone: 916488882

Número do Bilhete de Identidade: 11696367

Título da tese: **Applications of Dynamical Systems to Economical and Biological Sciences**

Orientadores:

Professor Doutor Alberto Adrego Pinto

Professor Bruno Miguel Paz Mendes de Oliveira

Doutoramento em Ciências, Área de conhecimento Matemática

Março de 2010

É AUTORIZADA A REPRODUÇÃO INTEGRAL DESTA TESE APENAS PARA EFEITOS DE INVESTIGAÇÃO, MEDIANTE DECLARAÇÃO ESCRITA DO INTERESSADO, QUE A TAL SE COMPROMETE;

Universidade do Minho, 2 de Março de 2010

Assinatura:

# Acknowledgments

I would like to thank Alberto Adrego Pinto for his direction and guidance throughout this Thesis and also for his friendship.

To Bruno Oliveira, for all the help, insight and encouragement he provided in the several parts of this Thesis and also for his friendship.

To Flávio Ferreira and to Fernanda Ferreira for their support on the work that is presented here and also for their friendship.

To Diogo for his advice, commentaries, suggestions, for his constant support and, most of all, for his friendship.

To my Mother, Fátima for being the person responsible for my love for Mathematics. Thank you very much.

To my Father, Luís, my Sister, Joana, my brother-in-law, Miguel, my Grandmother, Margarida and to my family for all their support and comprehension.

To Helena for entering my life and bringing something exceptionally beautiful into my everyday routine.

To all my friends, specially to Hugo and Teresa, Nelson and Ana, Miguel and Vera, Frederico and Ana, Eduardo and Sílvia, Miguel and Fabíola, Tiago and Susana, André and Renata, Henrique and Marta, Ulisses and Sofia, Bruno and Ana, Patrício and Malena, and Filipa for giving me the moral strength to proceed with the work I proposed myself to do.

I also acknowledge the financial support from FCT - *Fundação para a Ciência e a Tecnologia* given in the form of PhD scholarship with the reference SFRH/BD/27706/2006.

To University of Minho, in particular to the Mathematics Department of the School of Sciences, for the conditions offered for this project.

To the School of Industrial Studies and Management of the Polytechnic Institute of Porto.

# Abstract

In this PhD thesis, several concepts of distinct areas of Mathematics, such as Dynamical Systems, Game Theory and Statistics are applied to Economical and Biomedical Sciences. The Patent Licensing is studied in a Cournot competition framework, the General Equilibrium Theory is approached in terms of Edgeworthian economies and the subject of Immunology is covered through models with Regulatory T cells.

**Cournot competition Models:** We consider a Cournot competition model with a cost reducing R&D investment program. A new R&D cost reduction investment function inspired by the logistic equation is introduced. We compare the results obtained using our cost reduction investment function with the ones obtained using d'Aspremont and A. Jacquemin's cost reduction investment function. We study the underlying model and find the existence of different Nash investment regions: a competitive Nash investment region, a single Nash investment region and a nil Nash investment region. Moreover, we find regions with multiple Nash investment equilibria. We present an exhaustive characterization of the boundaries of the different economical regions that are found. For low production costs, that can correspond to the production of old technologies, the long term economi-

cal effects are not very sensitive to small changes in the efficiency of the R&D programs neither to small changes in the market structure. However, for high production costs, that can correspond to the production of new technologies, the long term economical effects are very sensitive to small changes in the efficiency of the R&D programs and also to small changes in the market structure.

**Edgeworthian economies Models:** General equilibrium theory assumes an interaction between the participants that is both global and anonymous. The studied models, random matching games, introduce mechanisms of direct exchange in an Edgeworth exchange economy where two goods are traded in a market place. We prove, under the appropriate assumptions, that the expected value of the logarithm of the limiting bilateral Walras equilibrium price is equal to the logarithm of the global Walras equilibrium price. We also consider a modification to this model in which participants have different bargaining skills meaning that participants do not necessarily trade according to their bilateral Walras equilibrium price. The trade occurs such that the more skilled bargainer takes advantage of his edge when exchanging with a less skilled bargainer. When the market has a group of low skilled bargainers and a group of high skilled bargainers, the smaller of these two groups shows a higher median increase on the value of the utilities of the participants. Finally, we let the bargaining skills of the participants be a continuous variable that evolves along the iterations according to one of the following rules: a) the bargaining skills of the pair of participants decrease if they were able to trade and increases otherwise; b) the bargaining skills of the pair of participants increases if they were able to

trade and decreases otherwise. We observe that for rule a) the bargaining skills of each participant converge to one of two possible extreme values, and that for rule b) the bargaining skills of all participants converge to a single intermediate bargaining skill value.

**Immune response Models:** The consequences of regulatory T cell (Treg) inhibition of interleukine 2 secretion are examined by mathematical modeling. We determine the analytic formula that describes the fine balance between Regulatory T cells and T cells at controlled and immune response equilibrium states. We demonstrate that cytokine dependent growth exhibits a quorum T cell population threshold that determines if immune responses develop on activation. We also determine the analytic formulas of T cell proliferation thresholds that allow the study of the sensibility of the quorum growth thresholds controlling immune responses. We introduce an asymmetry reflecting that the difference between the growth and death rates can be higher for the active T cells and Tregs than for the inactive. This asymmetry can be due to the existence of memory T cells and explains why slow increases of the antigenic stimuli do not lead to an immune response, but fast increases provoke an immune response. Finally, we study the bystander proliferation in the immune response model with the asymmetry. An exposure to a pathogen results in an increased proliferation rate of the bystander T cells. If the population of the bystander T cells becomes large enough, autoimmunity can arise, eventually after a long transient period.





# Resumo

Nesta Tese de Doutorado diversos conceitos de áreas distintas da Matemática tais como Sistemas Dinâmicos, Teoria de Jogos e Estatística são aplicados a Ciências Económicas e Biomédicas. O Licenciamento de Patentes é estudado através de modelos de competição de Cournot, a Teoria do Equilíbrio Geral é abordada através de modelos de economias de Edgeworth e na Imunologia são estudados modelos de células T reguladoras.

**Modelos de Competição de Cournot** Consideramos um modelo de competição de Cournot com programas de investigação e desenvolvimento (ID) na redução de custo. É introduzida uma nova função de redução de custo inspirada na função logística. Comparamos os resultados obtidos usando a nossa função de investimento na redução de custo com a função de investimento na redução de custo de d'Aspremont e Jacquemin. Estudamos o modelo correspondente e encontramos a existência de diferentes regiões de investimento: uma região de investimento competitiva, uma região de investimento singular e uma região de investimento nulo. Encontramos ainda uma região com múltiplos equilíbrios de Nash no investimento. Para custos de produção baixos, que podem corresponder a tecnologias antigas, os efeitos económicos a longo prazo não são muito sensíveis a pequenas alterações na

eficiência do programa de investigação e desenvolvimento. Contudo, para custos de produção altos, que podem corresponder a tecnologias mais recentes, os efeitos económicos a longo prazo são muito sensíveis a pequenas alterações na eficiência do programa de investigação e desenvolvimento.

**Modelos de economias Edgeworthianas** A Teoria do Equilíbrio Geral assume uma interacção entre os participantes que é global e anónima. Os modelos estudados, modelos de encontros de trocas aleatórias, introduzem mecanismos de troca directa numa economia de Edgeworth onde dois bens são trocados num mercado. Provamos que, sob as hipóteses apropriadas, o valor esperado do logaritmo do preço de equilíbrio de Walras limite é igual ao logaritmo do preço de equilíbrio de Walras global. Também consideramos uma modificação deste modelo no qual os participantes têm diferentes capacidades de negociação (aptidão) significando que eles nem sempre negociam de acordo com o equilíbrio de Walras bilateral. As trocas ocorrem de modo a que o jogador mais apto tenha vantagem quando a negociar com um jogador menos apto. Quando o mercado tem um grupo de participantes pouco aptos e outro grupo de participantes mais aptos, o mais pequeno dos dois grupos, evidencia um maior aumento na mediana para o valor das utilidades dos participantes. Finalmente, assumimos que a capacidade de negociação dos participantes é uma variável contínua que evolui ao longo das iterações de acordo com uma das seguintes regras: a) as capacidades de negociação do par de participantes decrescem se esse par conseguiu negociar e crescem caso contrário; b) as capacidades de negociação do par de participantes aumentam se esse par conseguiu trocar e decrescem caso contrário. No caso da regra a) as capacidade de negociação

dos dois participantes convergem para um de dois valores possíveis enquanto que no caso da regra b) as capacidade de negociação dos dois participantes convergem para um único valor intermédio.

**Modelos de resposta imunitária** As consequências da inibição da secreção da interleucina 2 pelas células T reguladoras (Treg) são examinadas por modelação matemática. Determinamos a fórmula que descreve o balanço fino entre as células T reguladoras e as células T em equilíbrios correspondentes a estados controlados e de resposta imunitária. Demonstramos que a proliferação dependente de citocinas exhibe um quórum limiar da população de células T que determina se após activação será desenvolvida uma resposta imunitária. Também determinamos as fórmulas analíticas dos limiares de proliferação de células T que permitem estudar a sensibilidade dos quórums limiares de crescimento que controlam as respostas imunitárias. Introduzimos uma assimetria para reflectir que a diferença entre a taxa de crescimento e de mortalidade pode ser maior para as células T e Tregs activas do que para as inactivas. Esta assimetria pode dever-se à existência de células T de memória e explica a razão pela qual aumentos lentos dos estímulos antigénicos não levam a uma resposta imunitária, mas aumentos rápidos provocam uma resposta imunitária. Finalmente, estudamos a proliferação de células espectadoras no modelo de resposta imunitária com assimetria. A exposição a um patógeno resulta num aumento da taxa de proliferação das células T espectadoras. Se a população destas células T espectadoras se tornar suficientemente grande, pode surgir autoimunidade eventualmente após um longo período transiente.



# Contents

<b>Acknowledgments</b>	<b>iii</b>
<b>Abstract</b>	<b>v</b>
<b>Resumo</b>	<b>ix</b>
<b>1 Introduction</b>	<b>19</b>
<b>2 Cournot competition Models</b>	<b>31</b>
2.1 Introduction . . . . .	31
2.2 R&D investments on costs . . . . .	32
2.2.1 The R&D cost reduction investment programs . . . . .	33
2.2.2 Optimal output levels . . . . .	36
2.2.3 New Production costs . . . . .	38
2.2.4 Best R&D investment response functions . . . . .	42
2.3 Nash investment equilibria . . . . .	59
2.4 FOP-Model boundary characterization . . . . .	70
2.4.1 Single Nash investment region . . . . .	70
2.4.2 Nil Nash investment region . . . . .	86
2.4.3 Competitive Nash investment region . . . . .	94
2.5 FOP-Model regions with multiple Nash equilibria . . . . .	96
2.6 FOP-Model R&D deterministic dynamics . . . . .	99

---

2.7	Conclusions . . . . .	103
<b>3</b>	<b>Edgeworthian Economies Models</b>	<b>107</b>
3.1	Introduction . . . . .	107
3.2	The Edgeworth model and some necessary results . . . . .	108
3.3	The main result . . . . .	111
3.4	Beyond the p-statistical duality . . . . .	114
3.5	Proof of Theorem 3.3.1 . . . . .	115
3.6	An extension to Arrow-Debreu economies . . . . .	118
3.7	Trade deviating from the bilateral Walras equilibrium . . . . .	120
3.8	Evolution of the bargaining skills . . . . .	122
3.9	Conclusions . . . . .	124
<b>4</b>	<b>Immune Response Models</b>	<b>125</b>
4.1	Introduction . . . . .	125
4.1.1	Immune response model . . . . .	126
4.1.2	Dynamics of the model . . . . .	129
4.1.3	Bifurcation diagrams . . . . .	131
4.1.4	Dynamics of cross-reactive proliferation . . . . .	134
4.2	Analysis of the model . . . . .	136
4.3	Asymmetry in the immune response model . . . . .	148
4.3.1	The model . . . . .	150
4.3.2	Bifurcation diagrams . . . . .	152
4.3.3	Fast and slow variation of antigenic stimulation . . . . .	154
4.3.4	Dynamics of bystander proliferation . . . . .	156
4.4	Conclusions . . . . .	161

# List of Figures

- 2.1 New production costs as a function of the investment (when  $\theta_1 = \theta_2 = 0$ ). **(A)** The maximum reduction in the production costs is  $\Delta_i$ , obtained for an infinite investment  $v_i = +\infty$ . **(B)** (zoom of the left part of **(A)**) When the investment is  $v_i = \lambda_i$  the reduction in the production costs is  $\Delta_i/2$ . **(C)** Figure **(A)** with both axes in the Logarithmic scale. . . . . 35
- 2.2 **(A)** R&D cost reduction investment functions: FOP-Model cost reduction investment function,  $a_i$ , green line, and AJ-Model cost reduction investment function,  $a_i^A$ , black line; **(B)** Figure **(A)** with both axes in the Logarithmic scale. . . . . 36
- 2.3 We exhibit the duopoly region  $D$  and the monopoly regions  $M_1$  and  $M_2$  for Firms  $F_1$  and  $F_2$ , respectively, in terms of their new production costs  $(a_1, a_2)$ ;  $l_{M_i}$  with  $i \in \{1, 2\}$  are the boundaries between  $M_i$  and  $D$ . . . . . 40



- 
- 2.4 Full characterization, for the FOP-Model, of the Nash investment regions in terms of the Firms' initial production costs  $(c_1, c_2)$ . The monopoly lines  $l_{M_i}$  are colored black. The nil Nash investment region  $N$  is colored grey. The single Nash investment regions  $S_1$  and  $S_2$  are colored blue and red, respectively. The competitive Nash investment region  $C$  is colored green. The region where  $S_1$  and  $S_2$  intersect are colored pink, the region where  $S_1$  and  $C$  intersect are colored lighter blue and the region where  $S_2$  and  $C$  intersect are colored yellow. The region where the regions  $S_1$ ,  $S_2$  and  $C$  intersect are colored lighter grey. . . . . 62
- 2.5 Full characterization, for the AJ-Model, of the Nash investment regions in terms of the Firms' initial production costs  $(c_1, c_2)$ . The monopoly lines  $l_{M_i}$  are colored black. The single Nash investment regions  $S_1$  and  $S_2$  are colored blue and red, respectively. The competitive Nash investment region  $C$  is colored green. . . . . 63
- 2.6 Firms' Nash investments in terms of their initial production costs  $(c_1, c_2)$ . The Nash investment for Firm  $F_1$  in the competitive Nash investment region  $C$  are colored blue and the Nash investment for Firm  $F_2$  in the competitive Nash investment region  $C$  are colored green. The Nash investments in the single Nash investment region  $S_1$  (respectively  $S_2$ ) are colored lighter blue (respectively yellow). (A) FOP-Model; (B) AJ-Model. . . . . 64

- 2.7 Firms' profits in terms of their initial production costs  $(c_1, c_2)$ . The Nash investment for Firm  $F_1$  in the competitive Nash investment region  $C$  are colored blue and the Nash investment for Firm  $F_2$  in the competitive Nash investment region  $C$  are colored green. The Firms' profits in the single Nash investment region  $S_1$  (respectively  $S_2$ ) are colored lighter blue (respectively yellow). (A) FOP-Model; (B) AJ-Model. . . . 65
- 2.8 Firms' new production costs in terms of their initial production costs  $(c_1, c_2)$ . The Nash investment for Firm  $F_1$  in the competitive Nash investment region  $C$  are colored blue and the Nash investment for Firm  $F_2$  in the competitive Nash investment region  $C$  are colored green. The Firms' new production costs in the single Nash investment region  $S_1$  (respectively  $S_2$ ) are colored lighter blue (respectively yellow). (A) FOP-Model; (B) AJ-Model. . . . . 65
- 2.9 Percentage of the Firms' total profit invested in R&D in terms of their initial production costs  $(c_1, c_2)$ . The Nash investment for Firm  $F_1$  in the competitive Nash investment region  $C$  are colored blue and the Nash investment for Firm  $F_2$  in the competitive Nash investment region  $C$  are colored green. The Firms' new production costs in the single Nash investment region  $S_1$  (respectively  $S_2$ ) are colored lighter blue (respectively yellow). (A) FOP-Model; (B) AJ-Model. . . . 66

2.10 Full characterization of the Nash investment regions in terms of the Firms' initial production costs  $(c_1, c_2)$ . The monopoly lines  $l_{M_i}$  are colored black. The nil Nash investment region  $N$  is colored grey. The single Nash investment regions  $S_1$  and  $S_2$  are colored blue and red, respectively. The competitive Nash investment region  $C$  is colored green. The region where  $S_1$  and  $S_2$  intersect are colored pink, the region where  $S_1$  and  $C$  intersect are colored lighter blue and the region where  $S_2$  and  $C$  intersect are colored yellow. The region where the regions  $S_1, S_2$  and  $C$  intersect are colored lighter grey. **(A)** FOP-Model; **(B)** AJ-Model; **(C)** Zoom of **(B)**; **(D)** Zoom of **(B)**. . . . . 67

2.11 Firms' Nash investments in terms of their initial production costs  $(c_1, c_2)$ . The Nash investment for Firm  $F_1$  in the competitive Nash investment region  $C$  are colored blue and the Nash investment for Firm  $F_2$  in the competitive Nash investment region  $C$  are colored green. The Nash investments in the single Nash investment region  $S_1$  (respectively  $S_2$ ) are colored lighter blue (respectively yellow). **(A)** FOP-Model; **(B)** AJ-Model. . . . . 68

- 2.12 Firms' profits in terms of their initial production costs  $(c_1, c_2)$ . The Nash investment for Firm  $F_1$  in the competitive Nash investment region  $C$  are colored blue and the Nash investment for Firm  $F_2$  in the competitive Nash investment region  $C$  are colored green. The Firms' profits in the single Nash investment region  $S_1$  (respectively  $S_2$ ) are colored lighter blue (respectively yellow). (A) FOP-Model; (B) AJ-Model. . . . 68
- 2.13 Firms' new production costs in terms of their initial production costs  $(c_1, c_2)$ . The Nash investment for Firm  $F_1$  in the competitive Nash investment region  $C$  are colored blue and the Nash investment for Firm  $F_2$  in the competitive Nash investment region  $C$  are colored green. The Firms' new production costs in the single Nash investment region  $S_1$  (respectively  $S_2$ ) are colored lighter blue (respectively yellow). (A) FOP-Model; (B) AJ-Model. . . . . 69
- 2.14 Percentage of the Firms' total profit invested in R&D in terms of their initial production costs  $(c_1, c_2)$ . The Nash investment for Firm  $F_1$  in the competitive Nash investment region  $C$  are colored blue and the Nash investment for Firm  $F_2$  in the competitive Nash investment region  $C$  are colored green. The Firms' new production costs in the single Nash investment region  $S_1$  (respectively  $S_2$ ) are colored lighter blue (respectively yellow). (A) FOP-Model; (B) AJ-Model. . . . 69

- 2.15 Full characterization of the single Nash investment region  $S_1$  and of the nil Nash investment region  $N$  in terms of the Firms' initial production costs  $(c_1, c_2)$ . The subregions  $N_{LL}$ ,  $N_{LH}$ ,  $N_{HL}$  and  $N_{HH}$  of the nil Nash investment region  $N$  are colored yellow. The subregion  $S_1^R$  of the single Nash investment region  $S_1$  is colored lighter blue. The subregion  $S_1^F$  of the single Nash investment region  $S_1$  is decomposed in three subregions: the *single Duopoly region*  $S_i^D$  colored blue, the *single Monopoly region*  $S_i^M$  colored green and the *single Monopoly boundary region*  $S_i^B$  colored red. . . . . 70
- 2.16 **(A)** Full characterization of the boundaries of the single monopoly region  $S_1^M$ : the upper boundary  $U_{S_1}^C$  is the union of a vertical segment line  $U_{S_1}^l$  with a curve  $U_{S_1}^c$ ; the lower boundary  $L_{S_1}^M$ ; and the left boundary  $Le_{S_1}^M$ ; **(B)** Zoom of the upper part of figure **(A)** where the boundaries  $U_{S_1}^C$  and  $U_{S_1}^l$  can be seen in more detail. . . . . 72
- 2.17 Each of the plots corresponds to the profit  $\pi_1$  of Firm  $F_1$  when Firm  $F_2$  decides not to invest, i.e.  $\pi_1(v_1, 0; c_1, c_2)$ . The plot in red (II) corresponds to a pair of production costs  $(c_1, c_2) \in U_{S_1}^l$ , the plot in blue (I) corresponds to a pair of production costs  $(c_1, c_2)$  that are in the single monopoly region  $S_1^M$  and the plot in green (III) corresponds to a pair of production costs  $(c_1, c_2)$  that are in the nil Nash investment region  $N_{HH}$ . 75

2.18 Each of the plots corresponds to the profit  $\pi_1$  of Firm  $F_1$  when Firm  $F_2$  decides not to invest, i.e.  $\pi_1(v_1, 0; c_1, c_2)$ . The plot in red (II) corresponds to a pair of production costs  $(c_1, c_2) \in U_{S_1}^c$ , the plot in blue (I) corresponds to a pair of production costs  $(c_1, c_2)$  that are in the single monopoly region  $S_1^M$  and the plot in green (III) corresponds to a pair of production costs  $(c_1, c_2)$  that are in the nil Nash investment region  $N_{HH}$ . 76

2.19 Each of the plots corresponds to the Profit  $\pi_2$  of Firm  $F_2$  when Firm  $F_1$  decides to invest  $v_1$  and Firm  $F_2$  has two possible best responses  $V_2(v_1) = \{v_2; 0\}$  with  $v_2 > 0$ , i.e.  $\pi_2(V_1(0), v_2; c_1, c_2)$ . The plot in red (II) corresponds to a pair of production costs  $(c_1, c_2) \in I_{S_1}^M$ , the plot in blue (I) corresponds to a pair of production costs  $(c_1, c_2)$  that are in the single monopoly region  $S_1^M$  and the plot in green (III) corresponds to a pair of production costs  $(c_1, c_2)$  that are in the single monopoly region  $S_2^M$ . . . . . 79

2.20 Full characterization of the boundaries of the single monopoly boundary region  $S_1^B$ : the upper boundary  $U_{S_1}^B$  and the lower boundary  $L_{S_1}^B$ . . . . . 81

2.21 (A) Full characterization of the boundaries of the single duopoly region  $S_1^D$ : the upper boundary  $U_{S_1}^D$ ; the lower boundary  $L_{S_1}^D$ ; and the left boundary  $Le_{S_1}^D$ ; (B) Zoom of the lower part of  $Le_{S_1}^D$ . . . . . 82

- 2.22 Each of the plots corresponds to the Profit  $\pi_2$  of Firm  $F_2$  when Firm  $F_1$  decides not to invest. The plot in red (II) corresponds to a pair of production costs  $(c_1, c_2) \in L_{S_1}^D$ , the plot in blue (I) corresponds to a pair of production costs  $(c_1, c_2)$  that are in the competitive Nash investment region  $C$  and the plot in green (III) corresponds to a pair of production costs  $(c_1, c_2)$  that are in the single duopoly region  $S_2^D$ . . . . 84
- 2.23 Full characterization of the boundaries of the single recovery region  $S_1^R$ : the upper boundary  $U_{S_1}^R$ ; the right boundary  $R_{S_1}^R$ ; and the left boundary  $Le_{S_1}^R$ . In green the competitive Nash investment region  $C$ , in grey the nil Nash investment region  $N$ , in red the single Nash investment region  $S_2$  for Firm  $F_2$  and in blue the single recovery region  $S_1^R$  for Firm  $F_1$ . . . . 85
- 2.24 Each of the plots corresponds to the profit  $\pi_2$  of Firm  $F_2$  when Firm  $F_1$  decides not to invest, i.e.  $\pi_{2,D}(V_1(0), v_2; c_1, c_2)$ . The plot in red (II) corresponds to a pair of production costs  $(c_1, c_2) \in U_{S_1}^R$ , the plot in blue (I) corresponds to a pair of production costs  $(c_1, c_2)$  that are in the nil Nash investment region  $N_{HL}$  and the plot in green (III) corresponds to a pair of production costs  $(c_1, c_2)$  that are in the single recovery region  $S_1^R$ . . . . . 86

- 2.25 Full characterization of the nil Nash investment region  $N$  in terms of the Firms' initial production costs  $(c_1, c_2)$ : **(A)** The subregion  $N_{LL}$  of the nil Nash investment region  $N$  is colored grey corresponding to initial production cost such that the Firms do not invest and do not produce; **(B)** The subregion  $N_{LH}$  of the nil Nash investment region  $N$  is colored grey corresponding to initial production cost such that the Firms do not invest and do not produce and dark blue corresponding to cases where the Firms do not invest but Firm  $F_1$  produces a certain amount  $q_1$  greater than zero; **(C)** The subregion  $N_{HH}$  of the nil Nash investment region  $N$  is colored grey corresponding to initial production cost such that the Firms do not invest and do not produce; dark blue corresponding to cases where the Firms do not invest but Firm  $F_1$  produces a certain amount  $q_1$  greater than zero and dark red corresponding to cases where the Firms do not invest but Firm  $F_2$  produces a certain amount  $q_2$  greater than zero. . . . . 87
- 2.26 Each of the plots corresponds to the profit  $\pi_1$  of Firm  $F_1$  when Firm  $F_2$  decides not to invest, i.e.  $\pi_{1,D}(V_1(0), 0; c_1, c_2)$ . The plot in red (II) corresponds to a pair of production costs  $(c_1, c_2) \in R_{N_{LL}}$ , the plot in blue (I) corresponds to a pair of production costs  $(c_1, c_2)$  that are in the nil Nash investment region  $N_{LL}$  and the plot in green (III) corresponds to a pair of production costs  $(c_1, c_2)$  that are in the single recovery region  $S_1^R$ . . . . . 91



- 2.27 Each of the plots corresponds to the profit  $\pi_2$  of Firm  $F_2$  when Firm  $F_1$  decides not to invest, i.e.  $\pi_{2,M_2}(0, V_2(0); c_1, c_2)$ . The plot in red (II) corresponds to a pair of production costs  $(c_1, c_2) \in U_{N_{LL}}$ , the plot in blue (I) corresponds to a pair of production costs  $(c_1, c_2)$  that are in the nil Nash investment region  $N_{LL}$  and the plot in green (III) corresponds to a pair of production costs  $(c_1, c_2)$  that are in the single recovery region  $S_2^R$ . . . . . 92
- 2.28 Each of the plots corresponds to the profit  $\pi_1$  of Firm  $F_1$  when Firm  $F_2$  decides not to invest, i.e.  $\pi_1(V_1(0), 0; c_1, c_2)$ . The plot in red (II) corresponds to a pair of production costs  $(c_1, c_2) \in d_1$ , the plot in blue (I) corresponds to a pair of production costs  $(c_1, c_2)$  that are in the nil Nash investment region  $N_{LH}$  and the plot in green (III) corresponds to a pair of production costs  $(c_1, c_2)$  that are in the single favorable region  $S_1^F$ . . . . . 93
- 2.29 Each of the plots corresponds to the profit  $\pi_1$  of Firm  $F_1$  when Firm  $F_2$  decides not to invest, i.e.  $\pi_{1,D}(V_1(0), 0; c_1, c_2)$ . The plot in red (II) corresponds to a pair of production costs  $(c_1, c_2) \in d_3$ , the plot in blue (I) corresponds to a pair of production costs  $(c_1, c_2)$  that are in the nil Nash investment region  $N_{LH}$  and the plot in green (III) corresponds to a pair of production costs  $(c_1, c_2)$  that are in the single favorable region  $S_1^F$ . . . . . 93

2.30 Each of the plots corresponds to the profit  $\pi_2$  of Firm  $F_2$  when Firm  $F_1$  decides not to invest, i.e.  $\pi_{2,D}(0, V_2(0); c_1, c_2)$ . The plot in red (II) corresponds to a pair of production costs  $(c_1, c_2) \in d_4$ , the plot in blue (I) corresponds to a pair of production costs  $(c_1, c_2)$  that are in the single recovery region  $S_2^R$  and the plot in green (III) corresponds to a pair of production costs  $(c_1, c_2)$  that are in the nil Nash investment region  $N_{LH}$ . . . . . 94

2.31 Firms' investments in the competitive Nash investment region. The competitive Nash investment region is colored green, the single Nash investment region  $S_1$  (respectively  $S_2$ ) is colored blue (respectively red) and the nil Nash investment region  $N$  is colored grey. . . . . 95

2.32 (A) Nash investment regions in the high production costs region,  $c_i \in [9, 10]$ , with  $i \neq j$ ; (B) Zoom of (A) in the region where there are three Nash investment equilibria; (C) Dynamics on the production costs in the high production costs region,  $c_i \in [9, 10]$ , with  $i \neq j$ : in blue, the dynamics in the single Nash investment region for Firm  $F_1$ ,  $S_1$  where only Firm  $F_1$  invests; in red the dynamics in the single Nash investment region for Firm  $F_2$ ,  $S_2$  where only Firm  $F_2$  invests; and in green the dynamics in the competitive Nash investment region  $C$  where both Firms invest. . . . . 96

- 2.33 We fix the initial production cost of Firm  $F_1$ ,  $c_1 = 9.7$  and plot (A) the Nash investment equilibria (NIE) of Firm  $F_1$  and the Nash investment equilibria of Firm  $F_2$ ; (B) the profit of Firm  $F_1$  and the profit of Firm  $F_2$  where green means that the pair  $(c_1, c_2)$  belongs to the single Nash investment region  $S_1$  and red means that the pair  $(c_1, c_2)$  belongs to the single Nash investment region  $S_2$ . . . . . 97
- 2.34 We fix the initial production cost of Firm  $F_1$ ,  $c_1 = 9.2$  and plot (A) the Nash investment equilibria (NIE) of Firm  $F_1$  and the Nash investment equilibria of Firm  $F_2$ ; (B) the profit of Firm  $F_1$  and the profit of Firm  $F_2$  where green means that the pair  $(c_1, c_2)$  belongs to the single Nash investment region  $S_1$ , red means that the pair  $(c_1, c_2)$  belongs to the single Nash investment region  $S_2$  and blue means that the pair  $(c_1, c_2)$  belongs to the competitive Nash investment region  $C$ . . . . . 98
- 2.35 We fix the initial production cost of Firm  $F_1$ ,  $c_1 = 9.35$  and plot (A) the Nash investment equilibria (NIE) of Firm  $F_1$  and the Nash investment equilibria of Firm  $F_2$ ; (B) the profit of Firm  $F_1$  and the profit of Firm  $F_2$  where green means that the pair  $(c_1, c_2)$  belongs to the single Nash investment region  $S_1$ , red means that the pair  $(c_1, c_2)$  belongs to the single Nash investment region  $S_2$  and blue means that the pair  $(c_1, c_2)$  belongs to the competitive Nash investment region  $C$ . . . . . 98

---

2.36	Dynamics on the production costs in terms of the initial production costs $(c_1, c_2)$ : in blue, the dynamics in the single Nash investment region for Firm $F_1$ , $S_1$ where only Firm $F_1$ invests; in red the dynamics in the single Nash investment region for Firm $F_2$ , $S_2$ where only Firm $F_2$ invests; and in green the dynamics in the competitive Nash investment region $C$ where both Firms invest. . . . .	99
2.37	Plot of the New production cost (NPC) of Firm $F_1$ and the New production cost of Firm $F_2$ with the initial production cost of Firm $F_1$ $c_1 = 9.7$ fixed where green means that the pair $(c_1, c_2)$ belongs to the single Nash investment region $S_1$ and red means that the pair $(c_1, c_2)$ belongs to the single Nash investment region $S_2$ . . . . .	102
2.38	Plot of the New production cost (NPC) of Firm $F_1$ and the New production cost of Firm $F_2$ with the initial production cost of Firm $F_1$ $c_1 = 9.2$ fixed where green means that the pair $(c_1, c_2)$ belongs to the single Nash investment region $S_1$ , red means that the pair $(c_1, c_2)$ belongs to the single Nash investment region $S_2$ and blue means that the pair $(c_1, c_2)$ belongs to the competitive Nash investment region $C$ . . . . .	102

- 2.39 Plot of the New production cost (NPC) of Firm  $F_1$  and the New production cost of Firm  $F_2$  with the initial production cost of Firm  $F_1$   $c_1 = 9.35$  fixed where green means that the pair  $(c_1, c_2)$  belongs to the single Nash investment region  $S_1$ , red means that the pair  $(c_1, c_2)$  belongs to the single Nash investment region  $S_2$  and blue means that the pair  $(c_1, c_2)$  belongs to the competitive Nash investment region  $C$ . . . . 103
- 3.1 The horizontal line, in red, corresponds to  $d = 0$ . **(A)** The error bar is, as usual, centered in the mean and the upper (resp. lower) limit is the mean plus (resp. minus) the standard deviation; **(B)** The error bar is centered in the mean and the upper (resp. lower) limit is the mean plus (resp. minus) the standard deviation over the square root of the number of runs (100). . . . . 115
- 3.2 Edgeworth Box with the indifference curves for the more skilled participant  $i$  (blue curve) and for the less skilled participant  $j$  (green curve). The red curve is the core and the red dots represent the contract curve. The slope of the pink segment line is the bilateral Walras equilibrium price. The slope of the black segment line is a price that gives advantage to the more skilled participant. The interception point  $D$  of the black line with the core indicates the final allocations from the trade deviating from the bilateral Walras equilibrium. The point  $E$  indicates the initial endowments. 121

- 
- 3.3 Cumulative distribution function of the variation of the utility (defined as  $u_f - u_0$ ) for the less skilled participants (black) and for the more skilled participants (red). **(A)** Simulation with 20% of highly skilled participants and 80% of less skilled participants; **(B)** Simulation with 80% of highly skilled participants and 20% of less skilled participants. . . . . 122
- 3.4 Variation of the bargaining skills with time. **(A)** The bargaining skills decrease when trade is allowed and increase otherwise; **(B)** The bargaining skills increase when trade is allowed and decrease otherwise. . . . . 124
- 4.1 Model schematic showing growth, death and phenotype transitions of the Treg populations  $R, R^*$ , and autoimmune T cell  $T, T^*$  populations. Cytokine dynamics are not shown: IL-2 is secreted by activated T cells  $T^*$  and adsorbed by all the T cell populations equally. . . . . 126
- 4.2 Time series plots for T cell populations on exposure to antigen with various antigenicities  $b$  and  $T_{input} = 0$ . Two initial conditions are shown, low initial  $T$  cell load (solid), and high initial T cell load (dashed). **(A)** Regulation, low  $b = 5 \times 10^{-2}$ ; **(B)** Escape and control, intermediate  $b = 0.5$ ; **(C)** Escape, high  $b = 5000$ . Total Treg (red), immune T cells (black). Reproduced from [11]. . . . . 131

- 4.3 Bifurcation plots with respect to the antigenic stimulation  $b$  of T cells. Shown are two cases: Tregs present with  $R + R^*$  red,  $T + T^*$  black, and no Tregs with  $T + T^*$  blue. Stable steady states are shown as solid lines, unstable as dashed. Reproduced from [11]. . . . . 133
- 4.4 T cell cross reactivity between a pathogen and self. **(A)** Cross reactive autoimmune T cells on pathogen infection can return to a controlled state if antigenic stimulation from self ( $b = 0.1$ ) is low; **(B)** For high  $b = 0.5$  stimulation from self, an initially controlled autoimmune T cell clone escapes when infection occurs with a cross reacting pathogen; **(C)** Identical to **(B)** except infection interval is 7 days. A pathogen infection is modelled as a step increase in  $b$  to 5000 for day 0-10 (**(A)** and **(B)**), 0-7 (**(C)**) to model both the increase in antigen (cross reactive) and costimulation. Key: Red solid  $R + R^*$ , Black dashed  $T + T^*$ . Reproduced from [11]. . . . . 135
- 4.5 **(A)** The equilibria manifold for Thymic inputs  $T_{input} \in [1, 10000]$ . Low values of  $b$  are darker and higher values are lighter; **(B)** Cross section of the equilibria manifold for  $T_{input} = 100$ . It illustrates Theorem 4.2.1, showing the total concentration of Tregs  $y(x) = R + R^*$  as a function of the total concentration of T cells  $x = T + T^*$ . The parameters are at their default values. . . . . 137

- 4.6 The hysteresis of the equilibria manifold for Thymic inputs  $T_{input} \in [1, 10000]$ , with the other parameters at their default values. These figures show the relation between the antigenic stimulation level  $b$ , the concentration of T cells  $x = T + T^*$ , and the concentration of Tregs  $y = R + R^*$ . The hysteresis unfolds for high values of the parameter  $T_{input}$ . **(A)** Low values of  $y = R + R^*$  are darker and higher values are lighter; **(B)** Low values of  $x = T + T^*$  are darker and higher values are lighter; **(C)** Cross section of the equilibria manifold for  $T_{input} = 100$ , illustrating Theorem 4.2.2, with the concentration of T cells  $x$  (black solid line) and the concentration of Tregs  $y$  (redred dashes); **(D)** Cross section of the equilibria manifold for  $T_{input} = 100$ , illustrating Theorem 4.2.3, with the concentration of T cells  $x$  (blueblue dashes) for the simplified model without Tregs. We also show the concentration of T cells  $x$  (black solid line) from Theorem 4.2.2. . . . . 143

- 4.7 Dependence of the thresholds with parameter  $T_{input}$  . . . . . 149



- 4.8 Equilibria for different tunings  $a = a_0 + mb$  of the antigenic stimulations, with  $a_0 = 1/2.4$ . From A to F the slope  $m$  increases. Black lines: concentration of T cells, Red lines: concentration of Tregs. Solid lines indicate stable equilibria and dashed lines indicate unstable equilibria. **(A)** ( $m = 0$ ) we see the hysteresis similar to the one observed in [11]; **(B)** ( $m = 0.164428$ ) we see the appearance of a saddle node point; **(C)** ( $m = 0.165$ ) the point increases to a loop limited by two folds; **(D)** ( $m = 1$ ) the loop is bigger; **(E)** ( $m = 1.64298$ ) the loop touches the hysteresis threshold  $b_H$  in a transcritical bifurcation; **(F)** ( $m = 2$ ) the loop has merged with the hysteresis. Further increases of the slope will not make qualitative differences in the figure. . . . . 153

4.9 Effect of different rates of increase of  $b$ . The level of antigenic stimulation  $b$  of T cells varies between 0.01 and 10 in a log-sigmoid function of time with steepness factor  $\tau$ . The antigenic stimulation  $a$  of Tregs is  $a(b) = 1/2.4 + 2b$ . Black dashes: total concentration of T cells ( $T + T^*$ ) Red line: total concentration of Tregs ( $R + R^*$ ). Blue dash-dots: antigenic stimulation  $b$  of T cells (presented as  $b/100$  to fit in the window). Vertical grey dots: median time of the variation (100 days). **(A)** Fast variations of the antigenic stimulation ( $\tau = 10$  days) give an immune response; **(B)** For slow variations of the antigenic stimulation ( $\tau = 100$  days) the T cells remain controlled. For intermediate rates of variation either there is an immune response (**(C)**  $\tau = 28$  days) or a controlled state (**(D)**  $\tau = 29$  days). . . . . 155

- 
- 4.10 Bystander proliferation for different models. (A) The symmetric case: the T cells not responding to the pathogen have equal concentration to the T cells responding to the pathogen; (B) Only the secreting T cells  $T^*$  die slower: the T cells not responding to the pathogen have lower concentration than the T cells responding to the pathogen; (C) The asymmetric case: the T cells not responding to the pathogen have lower concentration than the T cells responding to the pathogen and take more time than in case B to achieve an immune response. Black dots: concentration of T cells responding to the pathogen ( $T_b + T_b^*$ ); Green dashes: concentration of T cells not responding to the pathogen ( $T_c + T_c^*$ ); Red line: concentration of Tregs ( $R + R_*$ ). . . . . 159

# List of Tables

4.1	Model parameters. Reproduced from [11]. . . . .	130
-----	---	-----



# Chapter 1

## Introduction

This PhD Thesis is the result of three different research projects I have been involved in. Different areas of knowledge in Mathematics were applied to Economical and Biomedical Sciences.

In Chapter 2, together with B. Oliveira and A.A. Pinto, we study a Cournot competition model with R&D investments on the reduction of the production costs. This chapter is mostly based on the research articles [29] and [30], in the conference proceedings [21], [22], [23], [54], [55], [57] and [58] and in the book chapters [31] and [59]. In Chapter 3, jointly with B.F. Finkenstädt, B. Oliveira, A.A. Pinto and A.N. Yannacopoulos, we study random matching Edgeworthian economies. This chapter is mostly based on the research article [27], in the conference proceedings [24], [25], [26], [33] and [56] and in the book chapter [28]. In Chapter 4, a problem in Immunology is studied. This Chapter is joint work with N.J. Burroughs, B. Oliveira and A.A. Pinto. This Chapter is mostly based on the work developed in three research articles, namely [13], [14] and [15] and in the

book chapter [32].

In Chapter 2 we consider a Cournot competition model where two Firms invest in R&D projects to reduce their production costs. This competition is modeled, as usual, by a two-stage game (see d'Aspremont and A. Jacquemin [4]). In the first subgame, two Firms choose, simultaneously, their R&D investment strategy to reduce their initial production costs. In the second subgame, the two Firms are involved in a Cournot competition with production costs equal to the reduced cost determined by the R&D cost reduction investment program. We introduce a new R&D cost reduction investment function inspired by the logistic equation (see Equation (2.2)) whose properties are different from the ones exhibited by the usual R&D cost reduction investment function (see Equation (2.3)). The main differences between our cost reduction investment function and the standard d'Aspremont and A. Jacquemin's cost reduction investment function are: (i) the cost reduction obtained by the Firms using d'Aspremont and A. Jacquemin's R&D cost reduction investment function tends to infinity with the investment whereas the cost reduction obtained by the Firms using our R&D cost reduction investment function tends to a capacity that is proportional to the difference between the current production cost of Firm  $F_i$  and the minimum attainable production cost  $c_L$ ; (ii) the derivative at zero investment using d'Aspremont and A. Jacquemin's R&D cost reduction investment function [4] is infinity whereas using the cost reduction investment function that we propose is a finite value. Thus, two different cost reduction investment functions are considered: the standard R&D cost reduction investment function,  $a_i^A$ , introduced in the literature by d'Aspremont and A. Jacquemin [4]; and an

---

R&D cost reduction investment function, inspired by the logistic equation,  $a_i$ , that was introduced by Ferreira et al [29]. We compare both cost reduction investment functions and analyze, in terms of equilibria outcome, both cases. We will refer to the model where d'Aspremont and A. Jacquemin's cost reduction investment function is used as *AJ-Model* and to the model where our cost reduction investment function is used as the *FOP-Model*. We find the Perfect Nash equilibria of the Cournot competition model with R&D cost reduction investment programs two stage-game and study the economical effects of these distinct Perfect Nash equilibria. The second subgame, consisting of a Cournot competition, has a unique perfect Nash equilibrium. For the first subgame, consisting of an R&D cost reduction investment program, we find, for the FOP-Model, four different regions of Nash investment equilibria that we characterize as follows: a competitive Nash investment region  $C$  where both Firms invest, a single Nash investment region  $S_1$  for Firm  $F_1$ , where only Firm  $F_1$  invests, a single Nash investment region  $S_2$  for Firm  $F_2$ , where only Firm  $F_2$  invests, and a nil Nash investment region  $N$ , where neither of the Firms invest. In the AJ-Model, for the first subgame, we only find three different Nash investment equilibria regions: the competitive Nash investment region  $C$  and the single Nash investment regions  $S_1$  and  $S_2$ . This difference in behavior is due to the shape of the R&D cost reduction investment function considered for this model bringing an higher incentive to invest reflected in the disappearance of the nil Nash investment region found for the FOP-Model.

For the FOP-Model, the nil Nash investment region  $N$  consists of four nil Nash investment subregions,  $N_{LL}$ ,  $N_{LH}$ ,  $N_{HL}$  and  $N_{HH}$  where neither of



the Firms invest and so have constant production costs. In the nil Nash investment region  $N_{LL}$  both Firms have low production costs; in the nil Nash investment region  $N_{LH}$  Firm  $F_1$  has low production cost and Firm  $F_2$  has high production cost; in the nil Nash investment region  $N_{HL}$  Firm  $F_2$  has low production cost and Firm  $F_1$  has high production cost; and in the nil Nash investment region  $N_{HH}$  both Firms have high production costs. The economical reasons for both Firms to choose not to invest in the nil Nash investment regions  $N_{LL}$ ,  $N_{HL}$ ,  $N_{LH}$  and  $N_{HH}$  are quite different. In the region  $N_{LL}$ , neither of the Firms invest because the Firms already have so low costs that the investment is not recovered by the increase in the profit associated to the decrease of their production costs. In the region  $N_{LH}$  (respectively  $N_{HL}$ ), neither of the Firms invest because Firm  $F_1$  (respectively  $F_2$ ) has so low production costs and Firm  $F_2$  (respectively  $F_1$ ) has so high production costs that if one Firm invests and decreases its production costs, then it is not able to recover its investment with the corresponding increase in the profit associated to the new production costs. In the region  $N_{HH}$  neither of the Firms invest because the Firms already have so high production costs that the investment is not recovered by the increase in the profit associated to the decrease of their production costs. The single Nash investment region  $S_i$  can be decomposed into two disjoint regions: a *single favorable Nash investment region*  $S_i^F$  where the production costs, after investment, are favorable to Firm  $F_i$ ; and a *single recovery Nash investment region*  $S_i^R$  where the production costs, after investment are, still, favorable to Firm  $F_j$  but Firm  $F_i$  recovers, slightly, from its initial disadvantage. The economical reasons for Firm  $F_j$  deciding not to invest in the single favora-

ble Nash investment region  $S_i^F$  and in the single recovery Nash investment region  $S_i^R$  are opposite. In the single favorable Nash investment region  $S_i^F$ , the production costs of Firm  $F_j$  are too high for the Firm  $F_j$  to recover its investment by increasing its profit due to decreasing its production costs. In the single recovery Nash investment region  $S_i^R$ , the production costs of Firm  $F_j$  are too low for the Firm  $F_j$  to be willing to invest to decrease, even more, its production costs and, so, Firm  $F_i$  is able to decrease its production costs by investing. The single favorable Nash investment region  $S_i^F$  can also be decomposed into three regions: the *single duopoly region*  $S_i^D$ , the *single monopoly region*  $S_i^M$  and the *single monopoly boundary region*  $S_i^B$ . The single monopoly region  $S_i^M$  consists of all production costs such that, after Firm  $F_i$ 's investment, the new production costs are in the monopoly region of Firm  $F_i$ . The single monopoly boundary region  $S_i^B$  consists of all production costs such that, after Firm  $F_i$ 's investment, the new production costs are in the boundary between the monopoly region and the duopoly region of Firm  $F_i$ . The single duopoly region  $S_i^D$  consists of all production costs such that, after the Firm  $F_i$ 's investment, the new production costs are still in the duopoly region of Firm  $F_i$ .

The Nash investment equilibria are not necessarily unique leading to an economical complexity in the choice of the best R&D investment strategies by the Firms. In the AJ-Model, the Nash investment equilibria are unique (at least when the Firms do not decide to go on a Joint Venture program together) but, for the FOP-Model, the intersections between the single Nash investment region  $S_1$ , the single Nash investment region  $S_2$  and the competitive Nash investment region  $C$  are not always empty.

We also compute the best Nash investment response functions when the Firms go on a Joint Venture program together and exhibit how the Nash investment regions change. We note that for the AJ-Model and in opposition with what was observed in the pure competition case, there are regions with multiple Nash investment equilibria.

In Section 2.6 we introduce, for the FOP-Model, the R&D deterministic dynamics on the production costs of the Cournot competition, based on the R&D investment strategies of the Firms, as follows: at every period of time, the Firms choose the investment corresponding to one of the Nash investment equilibria that determines the new production costs of the Firms. Hence, the implicit equations determining the R&D deterministic dynamics are distinct in the competitive Nash investment region  $C$  and in the single Nash investment regions  $S_1$  and  $S_2$ . The nil Nash investment region  $N$  determines the set of all production costs that are fixed by the dynamics. The competitive Nash investment region  $C$  determines the region where the production costs of both Firms evolve along the time. The single Nash investment region  $S_1$  determines the set of production costs where the production cost of Firm  $F_2$  is constant and only the production cost of Firm  $F_1$  evolves. Similarly, the single Nash investment region  $S_2$  determines the set of production costs where the production cost of Firm  $F_1$  is constant and only the production cost of Firm  $F_2$  evolves. Depending upon the initial production costs of both Firms and upon their R&D investment strategies, the nil Nash investment region  $N$  is the set of equilibria for the R&D deterministic dynamics. It is unusual in dynamical systems to have a non-isolated set of equilibrium points. This is due to the complex

investment structure that we have to deal in this problem. The nil Nash investment region  $N$  is the union of four disjoint compact sets with non empty interior  $N_{LL}, N_{HL}, N_{LH}, N_{HH}$ . The nil Nash investment regions  $N_{LL}, N_{HL}$  and  $N_{LH}$  correspond to their asymptotic production costs. The R&D deterministic dynamics in the single Nash investment region  $S_1 = S_1^F \cup S_1^R$  are implicitly determined by Theorems 2.2.1 and 2.2.2. In the single Nash investment region  $S_1$ , only Firm  $F_1$  invests along the time. If  $(c_1, c_2)$  belongs to the single favorable Nash investment region  $S_1^F$ , then, under the R&D deterministic dynamics, the production costs approach, along the time, the region  $N_{LH}$ . Hence, the production costs of Firm  $F_1$  approach low costs of production, but the production costs of Firm  $F_2$  are always fixed at high values. Furthermore, at some period of time, the pair of new production costs can fall in the monopoly region and, so, Firm  $F_2$  can be driven out of the market by Firm  $F_1$ . If  $(c_1, c_2)$  belongs to the single recovery Nash investment region  $S_1^R$  then the production costs approach, under the R&D deterministic dynamics, the region  $N_{LL}$ . Hence, Firm  $F_1$  is able to recover, along the time, from its disadvantage approaching the region where both Firms have low production costs  $N_{LL}$ . In the competitive Nash investment region  $C$  both Firms invest and their new production costs, under the R&D deterministic dynamics, belong to the duopoly region  $D$ . The R&D deterministic dynamics in the competitive Nash investment region  $C$  lead both Firms, along the time, to approach the nil Nash investment region  $N_{LL}$  corresponding to both Firms having low production costs. As described above, the economical effects observed are quite distinct depending upon the initial production costs of both Firms belonging to the single recovery

Nash investment region  $S_i^R$ , single favorable Nash investment region  $S_i^F$ , and competitive Nash investment region  $C$ . For high production costs, that can correspond to the production of new technologies, there are subregions of production costs where there are multiple Nash investment equilibria. Hence, the production costs evolve, along the time, to the distinct economic regions  $N_{HL}$ ,  $N_{LH}$  and  $N_{LL}$ . In the region  $R_{S_1 \cap S_2}$ , where there are, simultaneously, two single Nash investment equilibria, if one Firm decides to invest in the first period, then the Firm that invests drives the other Firm out of the Market, and its production costs will decrease, along the time, to low production costs. Hence, the short and long term economical outcome for both Firms depends only upon the  $R\&D$  investment decision of both Firms at period one. This shows the high relevance of the Firms rapidly implementing their  $R\&D$  cost reduction investment programs in the case of high initial production costs. In the region  $R_{S_1 \cap C}$  (respectively  $R_{S_2 \cap C}$ ) if both Firms decide to implement their  $R\&D$  cost reduction investment programs according to the Nash investment strategy in region  $C$  both Firms will stay in the market and their production costs will approach, along the time, low production costs. However, if one of the Firms decides not to invest in period one, this Firm is driven out of the Market and the production costs of the other Firm will approach, along the time, low production costs in the region  $N_{LH}$  (respectively  $N_{HL}$ ). For further information on  $R\&D$  cost reduction investment programs in Cournot competitions see the works of Amir et al[2], Kamien et al[39].

The problem of providing strategic foundations of general equilibrium theory, has been a long standing problem of crucial importance in economic

theory. The main objective of this strand of thought is to provide a market game, realistic enough to describe the behavior of agents in real market situations, such that the equilibrium of this game approaches under certain conditions the competitive equilibrium for the same market. A particularly fruitful and popular way of pursuing this line of research is through the use of dynamic matching games, in which agents meet randomly, and exchange rationally, according to local rules. Such attempts started with the seminal work *Mathematical Pshycics* of Francis Ysidro Edgeworth in 1881, [20], and were further advanced by a number of researchers, including Shubik [71], Aumann and Shapley [5],[6], Aliprantis, Brown and Burkinshaw [1], Mas Colell [47] etc. More specifically, the approach through random matching games was promoted by researchers such as Rubinstein and Wolinsky [66], Binmore and Herrero [7], Gale [36] and references therein, McLennan and Schonnenschein [49] etc. In Chapter 3 this problem is approached and we wish to contribute to this literature, by studying conditions under which the equilibrium of a market game, defined by a random matching game, approaches the equilibrium of a fully competitive Walrasian model. We study models of Edgeworthian exchange economies, without production nor consumption of the two goods traded in the market place. The random matching game, consists of agents, paired at random, who exchange goods at the bilateral Walras equilibrium price, which is the price at the core, such that the market locally clears. The choice for this scenario, is inspired by the work of Binmore and Herrero [7]. Under some symmetry conditions, on the initial endowments and the agents preferences, it is showed that for the special case of Cobb-Douglas utility functions, the expectation of the

logarithm of the equilibrium price, obtained as a limit for the repeated game as the number of trades tends to infinity, is equal to the expectation of the logarithm of the Walrasian equilibrium price. We also consider a modification to the model, where we associate to each participant either a low or high bargaining skill factor which brings up a game alike the prisoner's dilemma into the usual Edgeworthian exchange economy. In this model, the participants trade at a price different from the bilateral Walras equilibrium price, with advantage to the more skilled bargainer. However, if both participants are highly skilled bargainers, they will not be allowed to trade, as a penalization. If the pair elected to trade is formed by two low skilled bargainers, they will trade according to the usual bilateral Walras equilibrium price. For this modified model we consider that the market has a group of low skilled bargainers and a group of high skilled bargainers, with different sizes. We study, in this market, the variations on the utility values of the participants. Our observations indicate that the group with higher median increase in the utilities is the one in minority, meaning that is better to be in minority. Finally, we let the bargaining skills of the participants be a continuous variable that evolves, along the trades, according to one of the following rules: a) the bargaining skills of the participants decrease if they were able to trade and increases otherwise; b) the bargaining skills of the participants increases if they were able to trade and decreases otherwise. We observe that for rule a) the bargaining skills of the participants approach either a high bargaining skill or a low bargaining skill, and that for rule b) the bargaining skills of all participants converge to an intermediate bargaining skill.

The primary function of the immune system is the protection of the host from pathogen invasion. During such an invasion, T cells specific to the antigen proliferate and under most circumstances successfully remove the pathogen. However, the immune system can also target self antigens (autoimmunity) and cause tissue damage and death. Regulatory T cells, or Tregs, have emerged as a fundamental component of the T cell repertoire, being generated in the thymus under positive selection by self peptides [38]. The Treg repertoire is as diverse as conventional T cells [38] and perform vital immune suppressive functions. Removal of Tregs, eg by (cell sorted) adoptive transfer experiments cause a variety of autoimmune disorders in rodents, whilst many autoimmune diseases can be associated with a misregulation of Tregs, eg IPEX [68]. Under exposure to their specific antigen, conventional T cells are activated leading to secretion of growth cytokines (predominantly interleukine 2, denoted IL2), and expression of the interleukine 2 receptor which triggers cytokine driven proliferation. However, in the presence of active Tregs the growth of conventional T cells is inhibited. Part of this growth inhibition is the inhibition of IL2 secretion by T cells [74, 69]. Significantly, addition of IL2 abrogates inhibition, whilst IL2 appears to be a key intermediary of the dynamics between Tregs and conventional T cells [35, 65, 76]. The process of Treg signalling to conventional T cells is still a matter of debate, evidence exists for both cell:cell mediated inhibition and soluble mediators such as  $\text{TNF}\beta$  and IL10 [68]. It is likely that multiple methods of regulation are involved. Further, most studies indicate that regulation is not T cell specific, i.e. Tregs inhibit all conventional T cells independent of their antigen specificity [75], although a different



report suggests the contrary [73]. Tregs clearly function to limit such autoimmune responses with a delicate balance between appropriate immune activation and immune response suppression being achieved. How such a balance is established and controlled is the central focus of the papers [11], [13]. The motivation is the observation that T cell proliferation through cytokines already has such a control structure; cytokine driven growth exhibits a quorum population size threshold [18]. In [11] it is proposed that Tregs locally adjust these thresholds by inhibiting IL2 secretion. The immune response-suppression axis is then a balance between the local numbers of activated T cells (eg from a pathogen encounter) and activated Tregs. This balance can be altered by cross reactivity [11] or through bystander proliferation [15]. In Subsection 4.1.1 we present an immune response model as a set of six ordinary differential equations. The analysis of the model is discussed in Section 4.2, where is shown that this model has a bistability region bounded by two thresholds of antigenic stimulation of T cells and we discuss the immune responses when there is cross reactivity between a pathogen and a self antigen. An asymmetry in the immune response model is presented in Section 4.3. This asymmetry takes into account that T cells in different states have distinct death rates. We observe that this model has a better behavior than the model with symmetric death rates in the simulations of a bystander immune response. The model with the asymmetry has a transcritical bifurcation for some tuning between the antigenic stimulation of T cells and the antigenic stimulation of Tregs. Thus, the rate of increase of antigenic stimulation of T cells may determine, for parameter values near the transcritical bifurcation, if an immune response arises or not.

# Chapter 2

## Cournot competition Models

### 2.1 Introduction

The work presented in this Chapter is joint work with B. Oliveira and A.A. Pinto and most of it is contained in the research articles [29] and [30], in the conference proceedings [21], [22], [23], [54], [55], [57] and [58] and in the book chapters [31] and [59].

We present a new R&D cost reduction investment function in a Cournot competition model inspired by the logistic equation. We do a full characterization of the associated game and study the short and long term economical effects derived from using this new R&D cost reduction investment function. In particular, we find the existence of regions with multiple Nash investment equilibria. We present an exhaustive characterization of the boundaries of the different economical regions that are found. For low production costs, that can correspond to the production of old technologies, the long term economical effects are not very sensitive to small changes in the efficiency of

the R&D programs neither to small changes in the market structure. However, for high production costs, that can correspond to the production of new technologies, the long term economical effects are very sensitive to small changes in the efficiency of the R&D programs and also to small changes in the market structure. We compare the results obtained for the model using our cost reduction investment function with the ones obtained using d'Aspremont and A. Jacquemin's cost reduction investment function.

## 2.2 R&D investments on costs

The Cournot competition with R&D cost reduction investment programs consists of two subgames in one period of time. The first subgame is an R&D cost reduction investment program, where both Firms have initial production costs and choose, simultaneously, their R&D investment strategies to obtain new production costs. The second subgame is a Cournot competition with production costs equal to the reduced cost determined by the R&D cost reduction investment function. As it is well known, the second subgame has a unique perfect Nash equilibrium. For the first subgame two different cost reduction investment functions are considered: the standard R&D cost reduction function,  $a_i^A$ , introduced in the literature by d'Aspremont and A. Jacquemin [4]; and an R&D cost reduction investment function, inspired by the logistic equation,  $a_i$ , that was introduced by Ferreira et al [29]. Throughout this Section we will describe and compare both cost reduction investment functions and analyze, in terms of equilibria outcome, both cases. We will refer to the model where d'Aspremont and A.

Jacquemin's cost reduction investment function is used as *AJ-Model* and to the model where our cost reduction investment function is used as the *FOP-Model*.

### 2.2.1 The R&D cost reduction investment programs

Let us consider an economy with a monopolistic sector with two Firms,  $F_1$  and  $F_2$ , each one producing a differentiated good. Following Singh and Vives [72], we assume that the representative consumer preferences are described by the following utility function

$$U(q_1, q_2) = \alpha_1 q_1 + \alpha_2 q_2 - (\beta_1 q_1^2 + 2\gamma q_1 q_2 + \beta_2 q_2^2) / 2, \quad (2.1)$$

where  $q_i$  is the quantity produced by the Firm  $F_i$ , and  $\alpha_i, \beta_i > 0$ . The inverse demands are linear and, letting  $p_i$  be the price of the good produced by the Firm  $F_i$ , they are given, in the region of quantity space where prices are positive, by

$$p_i = \alpha_i - \beta_i q_i - \gamma q_j.$$

The goods can be substitutes  $\gamma > 0$ , independent  $\gamma = 0$ , or complements  $\gamma < 0$ .

Demand for good  $i$  is always downward sloping in its own price and increases (decreases) the price of the competitor, if the goods are substitutes (complements). The ratio  $\gamma^2/\beta_i^2$  expresses the degree of product differentiation ranging from zero, when the goods are independent, to one, when the goods are perfect substitutes. When  $\gamma > 0$  and  $\gamma^2/\beta_i^2$  approaches one, we

are close to a homogeneous market. We consider two different cost reduction investment functions:  $a_i$ , inspired by the logistic equation, that was introduced by Ferreira et al [29] and is used in the FOP-Model; and  $a_i^A$  that was introduced by d'Aspremont and A. Jacquemin [4] and is used in the AJ-Model.

In the FOP-Model, the Firm  $F_i$  invests an amount  $v_i$  in an R&D cost reduction investment program  $a_i : \mathbb{R}_0^+ \rightarrow [b_i, c_i]$  that reduces its production cost to

$$a_i(v_i) = c_i - \frac{\epsilon_i(c_i - c_L)(v_i + \theta_i v_j)}{\lambda_i + v_i + \theta_i v_j}. \quad (2.2)$$

where (i) the parameter  $\theta_i$  is the spillover parameter determining how the investment  $v_j$  made by Firm  $F_j$  affects Firm  $F_i$ 's new production cost (bigger  $\theta_i$ , means bigger advantage taken by Firm  $F_i$  from Firm  $F_j$ 's investment on R&D); (ii) the parameter  $c_i$  is the unitary production cost of Firm  $F_i$  at the beginning of the period satisfying  $c_L \leq c_i \leq \alpha_i$ ; (iii) the parameter  $c_L$  is the minimum attainable production cost; (iv) the parameter  $0 < \epsilon_i < 1$  as the following meaning: since  $b_i = a_i(+\infty) = c_i - \epsilon_i(c_i - c_L)$ , the maximum reduction  $\Delta_i = \epsilon_i(c_i - c_L)$  of the production cost is a percentage  $0 < \epsilon_i < 1$  of the difference between the current cost  $c_i$  and the lowest possible production cost  $c_L$ ; (v) the parameter  $\lambda_i > 0$  can be seen as a measure of the inverse of the quality of the R&D cost reduction investment program for Firm  $F_i$ , because a smaller  $\lambda_i$  will result in a bigger reduction of the production costs for the same investment. Note that, in particular, when there are no spillovers, i.e.  $\theta_1 = \theta_2 = 0$ ,  $c_i - a_i(\lambda_i)$  gives half  $\Delta_i/2$  of the maximum possible reduction  $\Delta_i$  of the production cost for Firm  $F_i$  (see Figure 2.1).

Let us define, for simplicity of notation,  $\eta_i = \epsilon_i(c_i - c_L)$ .

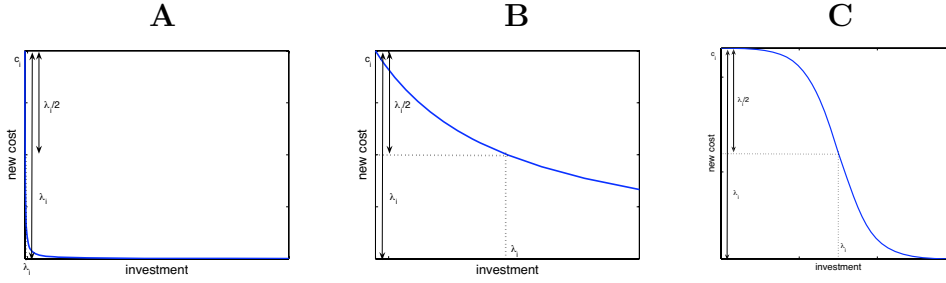


Figure 2.1: New production costs as a function of the investment (when  $\theta_1 = \theta_2 = 0$ ). **(A)** The maximum reduction in the production costs is  $\Delta_i$ , obtained for an infinite investment  $v_i = +\infty$ . **(B)** (zoom of the left part of **(A)**) When the investment is  $v_i = \lambda_i$  the reduction in the production costs is  $\Delta_i/2$ . **(C)** Figure **(A)** with both axes in the Logarithmic scale.

In the AJ-Model, a different R&D cost reduction investment function is used (see [4] for more details),  $a_i^A : [0, (\lambda_i c_i / \eta_i)^2] \rightarrow [0, c_i]$ , given by

$$a_i^A(v_i) = c_i - \frac{\epsilon_i(c_i - c_L)}{\lambda_i} \sqrt{v_i + \theta_i v_j}, \quad (2.3)$$

with  $\epsilon_i, \lambda_i > 0$ . The main differences between both R&D cost reduction investment programs are in the shape of the underlying cost reduction investment functions (see Figure 2.2) determining that (when there are no spillovers  $\theta_i = \theta_j = 0$ ): (a) the derivative at zero investment using d'Aspremont and A. Jacquemin's R&D cost reduction investment program [4] is infinity whereas using ours is a finite value, i.e.

$$\partial a_i^A / \partial v_i = \infty \text{ and } \partial a_i / \partial v_i \neq \infty$$

(b) the cost reduction obtained by the Firms using d'Aspremont and A.

Jacquemin's R&D cost reduction investment program tends to infinity with the investment whereas the cost reduction obtained by the Firms using our R&D cost reduction investment program tends to a capacity that is proportional to the difference between the current production cost of Firm  $F_i$  and the minimum attainable production cost  $c_L$  i.e.

$$\lim_{v_i \rightarrow \infty} a_i^A = c_i - \infty \text{ and } \lim_{v_i \rightarrow \infty} a_i = c_i - \eta_i = c_i - \epsilon(c_i - c_L)$$

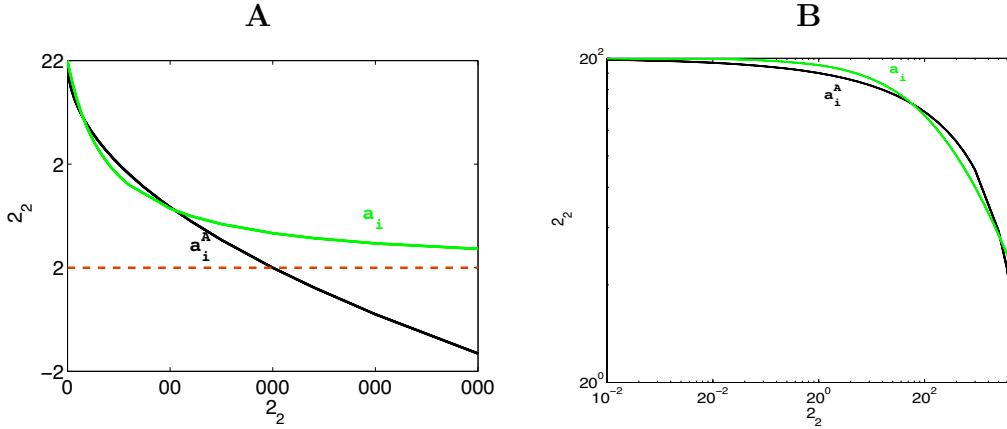


Figure 2.2: (A) R&D cost reduction investment functions: FOP-Model cost reduction investment function,  $a_i$ , green line, and AJ-Model cost reduction investment function,  $a_i^A$ , black line; (B) Figure (A) with both axes in the Logarithmic scale.

## 2.2.2 Optimal output levels

The profit  $\pi_i(q_i, q_j)$  of Firm  $F_i$  is given by

$$\pi_i(q_i, q_j) = q_i (\alpha_i - \beta_i q_i - \gamma q_j - a_i) - v_i, \quad (2.4)$$

for  $i, j \in \{1, 2\}$  and  $i \neq j$ .

The Nash equilibrium output  $(q_1^*, q_2^*)$  is given by

$$q_i^* = \begin{cases} 0, & \text{if } R_i \leq 0 \\ R_i, & \text{if } 0 < R_i < \frac{\alpha_j - a_j}{\gamma} \\ \frac{\alpha_i - a_i}{2\beta_i}, & \text{if } R_i \geq \frac{\alpha_j - a_j}{\gamma} \end{cases}, \quad (2.5)$$

where

$$R_i = \frac{2\beta_j\alpha_i - \gamma\alpha_j - 2\beta_j a_i + \gamma a_j}{4\beta_i\beta_j - \gamma^2},$$

with  $i, j \in \{1, 2\}$  and  $i \neq j$ . Hence if  $R_i \leq 0$ , the Firm  $F_j$  is at monopoly output level and, conversely, if  $R_i \geq (\alpha_j - a_j)/\gamma$  the Firm  $F_i$  is at monopoly output level and for intermediate values,  $0 < R_i < (\alpha_j - a_j)/\gamma$ , both Firms have positive optimal output levels and so we are in the presence of duopoly competition. From now on, we assume that both Firms choose their Nash equilibrium outputs  $(q_1^*, q_2^*)$ . Thus, Firm  $F_i$  has profit  $\pi_i^*(q_1^*, q_2^*)$  given by

$$\pi_i^*(q_1^*, q_2^*) = \begin{cases} -v_i, & \text{if } R_i \leq 0 \\ \beta_i R_i^2 - v_i, & \text{if } 0 < R_i < \frac{\alpha_j - a_j}{\gamma} \\ \frac{(\alpha_i - a_i)^2}{4\beta_i} - v_i, & \text{if } R_i \geq \frac{\alpha_j - a_j}{\gamma} \end{cases}. \quad (2.6)$$



### 2.2.3 New Production costs

The sets of possible new production costs for Firms  $F_1$  and  $F_2$ , given initial production costs  $c_1$  and  $c_2$ , are  $A_i$  for the FOP-Model and  $A_i^A$  for the AJ-Model. These sets are given, respectively, by

$$A_i = A_i(c_1, c_2) = [b_i, c_i] \quad \text{and} \quad A_i^A = A_i^A(c_1, c_2) = [0, c_i],$$

where  $b_i = c_i - \epsilon_i(c_i - c_L)$ , for  $i \in \{1, 2\}$ .

The R&D cost reduction investment programs  $a_1$  and  $a_2$  of the Firms determine a bijection between the *investment region*  $\mathbb{R}_0^+ \times \mathbb{R}_0^+$  of both Firms and the *new production costs region*  $A_1 \times A_2$ , given by the map

$$\begin{aligned} \mathbf{a} = (a_1, a_2) : \mathbb{R}_0^+ \times \mathbb{R}_0^+ &\longrightarrow A_1 \times A_2 \\ (v_1, v_2) &\longmapsto (a_1(v_1, v_2), a_2(v_1, v_2)) \end{aligned}$$

where

$$a_i(v_i) = c_i - \frac{\eta_i(v_i + \theta_i v_j)}{\lambda_i + v_i + \theta_i v_j}.$$

We denote the inverse map of  $\mathbf{a}$  by  $W = (W_1, W_2) : \mathbf{a}(\mathbb{R}_0^+ \times \mathbb{R}_0^+) \rightarrow \mathbb{R}_0^+ \times \mathbb{R}_0^+$

$$W_i(a_i, a_j) = \frac{\lambda_i(a_i - c_i)(c_j - a_j - \eta_j) + \theta_i(a_i - c_i)(a_j - c_j) + \eta_i \theta_i \lambda_j(a_j - c_j)}{h_i h_j + \theta_i \theta_j (c_i - a_i)(a_j - c_j) + \theta_i \theta_j \eta_j (c_i - a_i) + \eta_i \theta_i \theta_j (c_j - a_j) - \eta_i \eta_j \theta_i \theta_j}$$

where  $h_i = (c_i - a_i - \eta_i)$ .

The R&D cost reduction investment programs  $a_1^A$  and  $a_2^A$  of the Firms determine a bijection between the *investment region*  $\mathbb{R}_0^+ \times \mathbb{R}_0^+$  of both Firms

and the *new production costs region*  $A_1^A \times A_2^A$ , given by the map

$$\begin{aligned} \mathbf{a}^A = (a_1^A, a_2^A) : \mathbb{R}_0^+ \times \mathbb{R}_0^+ &\longrightarrow A_1^A \times A_2^A \\ (v_1, v_2) &\longmapsto (a_1^A(v_1, v_2), a_2^A(v_1, v_2)) \end{aligned}$$

where

$$a_i(v_i) = c_i - \frac{\eta_i}{\lambda_i} \sqrt{v_i + \theta_i v_j}.$$

We denote the inverse map of  $\mathbf{a}^A$  by  $W^A = (W_1^A, W_2^A) : \mathbf{a}^A(\mathbb{R}_0^+ \times \mathbb{R}_0^+) \rightarrow \mathbb{R}_0^+ \times \mathbb{R}_0^+$

$$W_i^A(a_i^A, a_j^A) = \left( \left( \frac{\lambda_i(c_i - a_i^A)}{\eta_i} \right)^2 - \theta_i \left( \frac{\lambda_j(c_j - a_j^A)}{\eta_j} \right)^2 \right) / (1 - \theta_i \theta_j).$$

The new production costs region can be decomposed, at most, into three disconnected economical regions characterized by the optimal output level of the Firms (see Figure 2.3):

$M_1$  the *monopoly region*  $M_1$  of Firm  $F_1$  that is characterized by the optimal output level of Firm  $F_1$  being the monopoly output, hence the optimal output level of Firm  $F_2$  is zero;

$D$  the *duopoly region*  $D$  that is characterized by the optimal output levels of both Firms being non-zero and, hence, below their monopoly output levels;

$M_2$  the *monopoly region*  $M_2$  of Firm  $F_2$  that is characterized by the optimal output level of Firm  $F_2$  being the monopoly output and, hence the optimal output level of Firm  $F_1$  is zero.

The boundary between the duopoly region  $D$  and the monopoly region  $M_i$  is  $l_{M_i}$  with  $i \in \{1, 2\}$

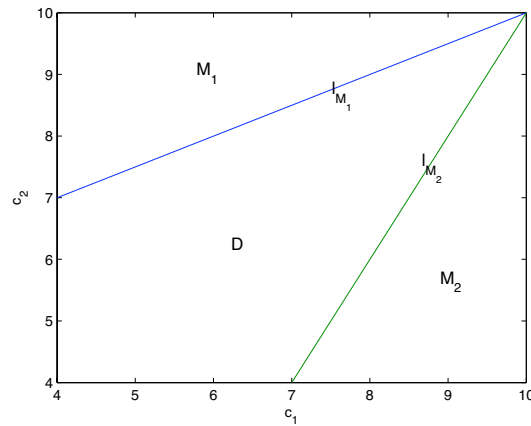


Figure 2.3: We exhibit the duopoly region  $D$  and the monopoly regions  $M_1$  and  $M_2$  for Firms  $F_1$  and  $F_2$ , respectively, in terms of their new production costs  $(a_1, a_2)$ ;  $l_{M_i}$  with  $i \in \{1, 2\}$  are the boundaries between  $M_i$  and  $D$ .

**Lemma 2.2.1** *The boundary between the monopoly region  $M_2$  and the duopoly region  $D$  is the segment line  $l_{M_2}$  given by*

$$a_2 = \frac{2\beta_2}{\gamma}(a_1 - \alpha_1) + \alpha_2.$$

**Proof:** By equation (2.5), we have that

$$q_1^* = (2\beta_2\alpha_1 - \gamma\alpha_2 - 2\beta_2a_1 + \gamma a_2)/(4\beta_1\beta_2 - \gamma^2).$$

Hence,  $q_1^*$  becomes zero if, and only if,

$$2\beta_2\alpha_1 - \gamma\alpha_2 - 2\beta_2a_1 + \gamma a_2 = 0.$$

□

**Lemma 2.2.2** *The boundary between the monopoly region  $M_1$  and the duopoly region  $D$  is the segment line  $l_{M_1}$  given by*

$$a_2 = \frac{\gamma}{2\beta_1}(a_1 - \alpha_1) + \alpha_2.$$

**Proof:** Analogous to the previous proof.

□

In equilibrium, i.e. when both Firms choose their optimal output levels, the profit function  $\pi_i : A_i \times A_j \rightarrow \mathbb{R}$  of Firm  $F_i$ , in terms of its new production costs  $(a_1, a_2)$ , is a piecewise smooth continuous function given by

$$\pi_i(a_1, a_2) = \begin{cases} \pi_{i,M_i}, & \text{if } (a_1, a_2) \in M_i \\ \pi_{i,D}, & \text{if } (a_1, a_2) \in D \\ -W_i(a_1, a_2), & \text{if } (a_1, a_2) \in M_j \end{cases},$$

where

$$\begin{aligned}\pi_{i,M_i} &= \pi_{i,M_i}(a_1, a_2; c_1, c_2) = \frac{(\alpha_i - a_i)^2}{4\beta_i} - W_i(a_1, a_2) \\ \pi_{i,D} &= \pi_{i,D}(a_1, a_2; c_1, c_2) = \frac{\beta_i (2\beta_j(\alpha_i - a_i) - \gamma(\alpha_j - a_j))^2}{(4\beta_i\beta_j - \gamma^2)^2} - W_i(a_1, a_2)\end{aligned}$$

### 2.2.4 Best R&D investment response functions

We can now derive the *best investment response function*  $V_1(v_2)$  of Firm  $F_1$  to a given investment  $v_2$  of Firm  $F_2$ :

$$V_1(v_2) = \arg \max_{v_1} \pi_1(a_1(v_1, v_2), a_2(v_1, v_2)).$$

We will study separately the cases where the new production costs belong to (i) the monopoly region  $M_1$ ; (ii) the duopoly region  $D$ ; (iii) the monopoly region  $M_2$ . First, we compute the best investment response function for the FOP-Model when the Firms are in pure competition. Afterwards we do the same computations when the Firms decide to go on a Joint Venture together. Finally, we determine the best investment response function for the AJ-Model when Firms are in pure competition and when the Firms decide to go on a Joint Venture together.

#### FOP-Model

Here, we compute the best investment response functions for the FOP-Model. If there is  $v_1 \in \mathbb{R}_0^+$  such that  $(a_1(v_1, v_2), a_2(v_1, v_2)) \in M_1$ , we select the best response  $v_1$  of Firm  $F_1$ , restricted to  $(a_1(v_1, v_2), a_2(v_1, v_2)) \in M_1$ ,

to the investment  $v_2$  of Firm  $F_2$  as follows: Let  $Z_{M_1}$  be the set of solutions  $v_1$  of the following equation

$$\frac{\partial \pi_{1,M_1}}{\partial v_1} = 0,$$

such that  $(a_1(v_1, v_2), a_2(v_1, v_2)) \in M_1$ . Let  $F_{M_1}$  be the set of  $v_1$  such that  $(a_1(v_1, v_2), a_2(v_1, v_2)) \in l_{M_1}$ . The best response  $v_1$  of Firm  $F_1$  in  $M_1$  is given by

$$v_1 = \arg \max_{v_1 \in Z_{M_1} \cup F_{M_1}} \pi_{1,M_1}(a_1(v_1, v_2), a_2(v_1, v_2)).$$

Since the investment  $v_2$  is fixed, let us characterize the set  $Z_{M_i}$ .

Let  $L_i = 6\beta_i\lambda_i^2 - \eta_i^2\lambda_i + \eta_i\lambda_i(c_i - \alpha_i)$  and  $N_i = 2\beta_i\lambda_i^3 + \eta_i\lambda_i^2(c_i - \alpha_i)$ .

**Theorem 2.2.1** *Let  $v_i$  be such that  $(a_1(v_1, v_2), a_2(v_1, v_2)) \in M_i$ . The set  $Z_{M_i}$  is the set of zeros of the following polynomial:*

$$2\beta_i v_i^3 + 6\beta_i \lambda_i v_i^2 + L_i v_i + N_i = 0 \quad (2.7)$$

**Proof:** Let us compute

$$\frac{d\pi_{i,M}}{dv_i} = \frac{\partial \pi_{i,M}}{\partial a_i} \frac{\partial a_i}{\partial v_i} + \frac{\partial \pi_{i,M}}{\partial v_i}$$

Hence  $d\pi_{i,M}/dv_i = 0$ , if and only if

$$\frac{\eta_i \lambda_i (\alpha_i - a_i)}{2\beta_i (\lambda_i + v_i)^2} = 1$$

Since  $a_i = c_i - (\eta_i v_i)/(\lambda_i + v_i)$ , the previous expression can be written as

$$\eta_i \lambda_i (\alpha_i - c_i) + \frac{\lambda_i \eta_i^2 v_i}{\lambda_i + v_i} = 2\beta_i (\lambda_i^2 + 2\lambda_i v_i + v_i^2)$$

That is equivalent to

$$\begin{aligned} \eta_i \lambda_i (\alpha_i - c_i) v_i + \eta_i \lambda_i^2 (\alpha_i - c_i) + \eta_i^2 \lambda_i v_i &= 2\beta_i \lambda_i^3 + 2\beta_i \lambda_i^2 v_i + \\ &+ 4\beta_i \lambda_i^2 v_i + 4\beta_i \lambda_i v_i^2 + 2\beta_i \lambda_i v_i^2 + 2\beta_i v_i^3. \end{aligned}$$

The above equality is equivalent to (2.7). □

If there is  $v_1 \in \mathbb{R}_0^+$  such that  $(a_1(v_1, v_2), a_2(v_1, v_2)) \in D$ , we select the best response  $v_1$  of Firm  $F_1$ , restricted to  $(a_1(v_1, v_2), a_2(v_1, v_2)) \in D$ , to the new production cost  $a_2$  of Firm  $F_2$  as follows: Let  $Z_D$  be the set of zeros  $v_1$  of the following polynomial

$$\frac{\partial \pi_{1,D}}{\partial v_1} = 0,$$

such that  $(a_1(v_1, v_2), a_2(v_1, v_2)) \in D$ . The best response  $v_1$  of Firm  $F_1$  in  $D$  is given by

$$v_1 = \arg \max_{v_1 \in Z_D \cup F_{M_1}} \pi_{1,D}(a_1(v_1, v_2), a_2(v_1, v_2)).$$

Let us characterize the set  $Z_D$ .

Let  $A_i = 4\beta_i \beta_j \eta_i \lambda_i$ ,  $B_i = 2\beta_i \gamma \eta_j \lambda_j$ ,  $C = (4\beta_i \beta_j - \gamma^2)^2$ ,  $E_i = \alpha_i - c_i + \eta_i$ ,  $F_i = 2\beta_j E_i - \gamma E_j$ ,  $G_i = -2\beta_j \eta_i \lambda_i$  and  $H_i = \gamma \eta_i \lambda_i$ .

**Theorem 2.2.2** *Let  $(v_1, v_2)$  be such that  $(a_1(v_1, v_2), a_2(v_1, v_2)) \in D$ . The*

set  $Z_D$  is the set of zeros of the following polynomial:

$$f_1(\theta_i, \theta_j, W_i, W_j) - \theta_j f_2(\theta_i, \theta_j, W_i, W_j) = 0 \quad (2.8)$$

where

$$\begin{aligned} f_1(\theta_i, \theta_j, W_i, W_j) &= -CW_i^3W_j^3 + A_iF_iW_iW_j^3 + A_iG_iW_j^3 + A_iH_jW_j^2W_i, \\ f_2(\theta_i, \theta_j, W_i, W_j) &= B_iF_iW_jW_i^3 + B_iG_iW_i^2W_j + B_iH_jW_i^3, \end{aligned}$$

and  $W_i = \lambda_i + v_i + \theta_i v_j$ .

**Proof:** Since  $W_i = \lambda_i + v_i + \theta_i v_j$ , we get  $\alpha_i - a_i = E_i - \eta_i \lambda_i / W_i$  and  $a_j - \alpha_j = -E_j + \eta_j \lambda_j / W_j$ .

Let us compute

$$\frac{d\pi_{i,D}}{dv_i} = \frac{\partial \pi_{i,D}}{\partial a_i} \frac{\partial a_i}{\partial v_i} + \frac{\partial \pi_{i,D}}{\partial a_j} \frac{\partial a_j}{\partial v_i} + \frac{\partial \pi_{i,D}}{\partial v_i}. \quad (2.9)$$

We have that

$$\begin{aligned} \frac{\partial \pi_{i,D}}{\partial a_i} &= -\frac{4\beta_i\beta_j(2\beta_j(\alpha_i - a_i) + \gamma(a_j - \alpha_j))}{(4\beta_i\beta_j - \gamma^2)^2} = \frac{-4\beta_i\beta_j(F_i + G_i/W_i + H_j/W_j)}{C}, \\ \frac{\partial a_i}{\partial v_i} &= -\frac{\eta_i \lambda_i}{(\lambda_i + v_i + \theta_i v_j)^2} = \frac{-\eta_i \lambda_i}{W_i^2}, \\ \frac{\partial \pi_{i,D}}{\partial a_j} &= \frac{2\beta_i\gamma(2\beta_j(\alpha_i - a_i) + \gamma(a_j - \alpha_j))}{(4\beta_i\beta_j - \gamma^2)^2} = \frac{2\beta_i\gamma(F_i + G_i/W_i + H_j/W_j)}{C}, \\ \frac{\partial a_j}{\partial v_i} &= -\frac{\theta_j \eta_j \lambda_j}{(\lambda_j + v_j + \theta_j v_i)^2} = \frac{-\eta_j \theta_j \lambda_j}{W_j^2}, \\ \frac{\partial \pi_{i,D}}{\partial v_i} &= -1. \end{aligned}$$



Using the previous equalities in equation (2.9), we get

$$\begin{aligned} \frac{d\pi_{i,D}}{dv_i} &= \frac{-4\beta_i\beta_j(F_i + G_i/W_i + H_j/W_j) - \eta_i\lambda_i}{C} \frac{1}{W_i^2} + \\ &+ \frac{2\beta_i\gamma(F_i + G_i/W_i + H_j/W_j) - \eta_j\theta_j\lambda_j}{C} \frac{1}{W_j^2} - 1 \end{aligned}$$

Hence,  $d\pi_{i,D}/dv_i = 0$  if, and only if

$$\begin{aligned} -CW_i^3W_j^3 + A_iF_iW_iW_j^3 &+ A_iG_iW_j^3 + A_iH_jW_j^2W_i - \\ &- \theta_j (B_iF_iW_jW_i^3 + B_iG_iW_i^2W_j + B_iH_jW_i^3) = 0 \end{aligned}$$

□

Let  $I_i = -A_iF_i/C$ ,  $J_i = -A_iH_i/C$  and  $K_i = -A_iG_i/C$ .

**Corollary 2.2.1** *Suppose that Firms use patents (i.e. without spillovers,  $\theta_i = \theta_j = 0$ ). Let  $(v_1, v_2)$  be such that  $(a_1(v_1), a_2(v_2)) \in D$ . The set  $Z_D$  is the set of zeros of the following polynomial:*

$$V_i^3V_j + I_iV_iV_j + J_iV_i + K_iV_j = 0, \quad (2.10)$$

where  $V_i = \lambda_i + v_i$ .

**Proof:** From (2.8), making  $\theta_i = \theta_j = 0$  we get

$$CV_j^3V_i^3 - A_iF_iV_j^3V_i - A_iG_iV_j^3 - A_iH_iV_iV_j^2 = 0.$$

Since  $V_j \neq 0$ , the previous equation can be written as (2.10).

□

If there is  $v_1 \in \mathbb{R}_0^+$  such that  $(a_1(v_1, v_2), a_2(v_1, v_2)) \in M_2$ , the best response  $v_2$  of Firm  $F_1$ , restricted to  $(a_1(v_1, v_2), a_2(v_1, v_2)) \in M_2$ , is given by Firm  $F_1$  investing zero, i.e. not investing. Hence,  $V_1(v_2)$  is given by

$$V_1(v_2) = \arg \max_{v_1 \in F} \pi_1(a_1(v_1, v_2), a_2(v_1, v_2)),$$

where  $V_1 \in F = Z_{M_1} \cup F_{M_1} \cup Z_D \cup \{0\}$ .

We note that, the best investment response function  $V_i : \mathbb{R}_0^+ \rightarrow \mathbb{R}_0^+$  can be a multi-valued function.

**Theorem 2.2.3** *The best investment response function  $V_i : \mathbb{R}_0^+ \rightarrow \mathbb{R}_0^+$  of Firm  $F_i$  is explicitly computed.*

**Proof:** Using  $l_{M_1}$  and  $l_{M_2}$  we know, explicitly, the domains  $Z_D$  and  $Z_M$ . Applying Theorem 2.2.2, we find the investment critical points and we check, using  $l_{M_1}$  and  $l_{M_2}$ , if they belong to  $Z_D$ . If so, we keep them, otherwise we discard them. We apply Theorem 2.2.1, to find the investment critical points and we check, using  $l_{M_1}$  and  $l_{M_2}$ , if they belong to  $Z_M$ . If so, we keep them, otherwise we discard them. Finally, we compare the profit values along the boundaries of  $Z_D$  and  $Z_M$  with the profit values attained at the critical points kept in  $Z_D$  and  $Z_M$  to determine the best investment  $v_i$  for Firm  $F_i$ .

□

## FOP-Model with Joint Venture

Here, we compute the best investment response functions when both Firms decide to go on a Joint Venture program together. Thus, the equivalents to Theorems

2.2.1 and 2.2.2 are computed for this case. Since they go on a Joint Venture program, each Firm maximizes the sum of both Firms profits when taking their decisions. Thus,  $\pi = \pi_1 + \pi_2$ .

**Theorem 2.2.4** *Let  $v_i$  be such that  $(a_1(v_1, v_2), a_2(v_1, v_2)) \in M_i$ . The set  $Z_{M_i}$  is the set of zeros of the following polynomial:*

$$2\beta_i v_i^3 + 6\beta_i \lambda_i v_i^2 + L_i v_i + N_i = 0.$$

**Proof:** If  $(a_i, c_j) \in M_i$ , then  $\pi = \pi_i + \pi_j = \pi_i$ . Thus Theorem 2.2.1 still holds in the case of Joint venture. □

**Theorem 2.2.5** *Let  $(v_1, v_2)$  be such that  $(a_1(v_1, v_2), a_2(v_1, v_2)) \in D$ . The set  $Z_D$  is the set of zeros of the following polynomial:*

$$f_1(\theta_i, \theta_j, W_i, W_j) + \theta_j f_2(\theta_i, \theta_j, W_i, W_j) = 0 \quad (2.11)$$

where

$$\begin{aligned} f_1(\theta_i, \theta_j, W_i, W_j) &= CW_i^3 W_j^3 + (A_i - B_j F_j) W_i W_j^3 + (A_i - B_j G_j) W_j^2 W_i + \\ &\quad + (A_i G_i - B_j H_i) W_j^3, \\ f_2(\theta_i, \theta_j, W_i, W_j) &= (A_j - B_i F_i) W_i^3 W_j + (A_j + B_i G_i) W_i^2 W_j + (A_j - B_i H_j) W_i^3, \end{aligned}$$

and  $W_i = \lambda_i + v_i + \theta_i v_j$ .

**Proof:** Since  $W_i = \lambda_i + v_i + \theta_i v_j$ , we get  $\alpha_i - a_i = E_i - \eta_i \lambda_i / W_i$  and  $a_j - \alpha_j = -E_j + \eta_j \lambda_j / W_j$ . Since we are in the case where Firms cooperate via Joint Venture, the profit both Firms want to optimize is given by  $\pi = \pi_i + \pi_j$ .

Let us compute

$$\frac{d\pi_D}{dv_i} = \frac{\partial\pi_{i,D}}{\partial a_i} \frac{\partial a_i}{\partial v_i} + \frac{\partial\pi_{i,D}}{\partial a_j} \frac{\partial a_j}{\partial v_i} + \frac{\partial\pi_{i,D}}{\partial v_i} + \frac{\partial\pi_{j,D}}{\partial a_i} \frac{\partial a_i}{\partial v_i} + \frac{\partial\pi_{j,D}}{\partial a_j} \frac{\partial a_j}{\partial v_i} + \frac{\partial\pi_{j,D}}{\partial v_i} \quad (2.12)$$

We have that

$$\begin{aligned} \frac{\partial\pi_{i,D}}{\partial a_i} &= -\frac{4\beta_i\beta_j(2\beta_j(\alpha_i - a_i) + \gamma(a_j - \alpha_j))}{(4\beta_i\beta_j - \gamma^2)^2} = \frac{-4\beta_i\beta_j(F_i + G_i/W_i + H_j/W_j)}{C}, \\ \frac{\partial a_i}{\partial v_i} &= -\frac{\eta_i\lambda_i}{(\lambda_i + v_i + \theta_i v_j)^2} = \frac{-\eta_i\lambda_i}{W_i^2}, \\ \frac{\partial\pi_{i,D}}{\partial a_j} &= \frac{2\beta_i\gamma(2\beta_j(\alpha_i - a_i) + \gamma(a_j - \alpha_j))}{(4\beta_i\beta_j - \gamma^2)^2} = \frac{2\beta_i\gamma(F_i + G_i/W_i + H_j/W_j)}{C}, \\ \frac{\partial a_j}{\partial v_i} &= -\frac{\theta_j\eta_j\lambda_j}{(\lambda_j + v_j + \theta_j v_i)^2} = \frac{-\eta_j\theta_j\lambda_j}{W_j^2}, \\ \frac{\partial\pi_{j,D}}{\partial a_i} &= -\frac{2\gamma\beta_j(2\beta_i(\alpha_j - a_j) + \gamma(a_i - \alpha_i))}{(4\beta_i\beta_j - \gamma^2)^2} = \frac{2\gamma\beta_j(F_j + G_j/W_j + H_i/W_i)}{C}, \\ \frac{\partial\pi_{j,D}}{\partial a_j} &= \frac{-4\beta_i\beta_j(F_j + G_j/W_j + H_i/W_i)}{C}, \\ \frac{\partial\pi_{i,D}}{\partial v_i} &= -1. \end{aligned}$$

Using the previous equalities in equation (2.12), we get

$$\begin{aligned} \frac{d\pi_{i,D}}{dv_i} &= \frac{2\beta_i\gamma(F_j + G_j/W_j + H_i/W_i)}{C} \frac{-\eta_i\lambda_i}{W_i^2} + \\ &+ \frac{-4\beta_i\beta_j(F_j + G_j/W_j + H_i/W_i)}{C} \frac{-\eta_j\lambda_j\theta_j}{W_j^2} + \\ &+ \frac{-4\beta_i\beta_j(F_i + G_i/W_i + H_j/W_j)}{C} \frac{-\eta_i\lambda_i}{W_i^2} + \\ &+ \frac{2\beta_i\gamma(F_i + G_i/W_i + H_j/W_j)}{C} \frac{-\eta_j\lambda_j\theta_j}{W_j^2} - 1 \end{aligned}$$

Hence,  $d\pi_{i,D}/dv_i = 0$  if, and only if

$$\begin{aligned} & - CW_i^3W_j^3 + (A_i - B_jF_j)W_iW_j^3 + (A_i - B_jG_j)W_j^2W_i + (A_iG_i - B_jH_i)W_j^3 + \\ & + \theta_j((A_j - B_iF_i)W_i^3W_j + (A_j + B_iG_i)W_i^2W_j + (A_j - B_iH_j)W_i^3) = 0 \end{aligned}$$

□

**Corollary 2.2.2** *Suppose that Firms use patents (i.e. without spillovers,  $\theta_i = \theta_j = 0$ ). Let  $(v_1, v_2)$  be such that  $(a_1(v_1, v_2), a_2(v_1, v_2)) \in D$ . The set  $Z_D$  is the set of zeros of the following polynomial:*

$$\begin{aligned} CW_i^3W_j^3 & + (A_i - B_jF_j)W_iW_j^3 + (A_i - B_jG_j)W_j^2W_i + \\ & + (A_iG_i - B_jH_i)W_j^3 = 0 \end{aligned} \quad (2.13)$$

where  $W_i = \lambda_i + v_i$ .

**Proof:** From (2.11), making  $\theta_i = \theta_j = 0$  we get (2.13).

□

### AJ-Model

Here, we compute the best investment response functions for the AJ-Model. If there is  $v_1 \in \mathbb{R}_0^+$  such that  $(a_1(v_1, v_2), a_2(v_1, v_2)) \in M_1$ , we select the best response  $v_1$  of Firm  $F_1$ , restricted to  $(a_1(v_1, v_2), a_2(v_1, v_2)) \in M_1$ , to the investment  $v_2$  of Firm  $F_2$  as follows: Let  $Z_{M_1}$  be the set of solutions  $v_1$  of the following equation

$$\frac{\partial \pi_{1,M_1}}{\partial v_1} = 0,$$

such that  $(a_1(v_1, v_2), a_2(v_1, v_2)) \in M_1$ . Let  $F_{M_1}$  be the set of  $v_1$  such that  $(a_1(v_1, v_2), a_2(v_1, v_2)) \in l_{M_1}$ . The best response  $v_1$  of Firm  $F_1$  in  $M_1$  is given by

$$v_1 = \arg \max_{v_1 \in Z_{M_1} \cup F_{M_1}} \pi_{1, M_1}(a_1(v_1, v_2), a_2(v_1, v_2)).$$

Since the investment  $v_2$  is fixed, let us characterize the set  $Z_{M_i}$ .

**Theorem 2.2.6** *Let  $v_i$  be such that  $(a_1(v_1, v_2), a_2(v_1, v_2)) \in M_i$ . The set  $Z_{M_i}$  is given by:*

$$v_i = \left( \frac{\eta_i \lambda_i (\alpha_i - c_i)}{4\beta_i \lambda_i^2 - \epsilon_i^2 (c_i - c_L)^2} \right)^2.$$

**Proof:** We have that

$$\begin{aligned} \frac{\partial \pi_{i, M}}{\partial a_i} &= \frac{(a_i - \alpha_i)}{2\beta_i}, \\ \frac{\partial a_i}{\partial v_i} &= -\frac{\eta_i}{2\lambda_i \sqrt{v_i}}, \\ \frac{\partial \pi_i}{\partial v_i} &= -1. \end{aligned}$$

Thus,

$$\begin{aligned} \frac{d\pi_{i, M}}{dv_i} &= \frac{(\alpha_i - a_i)}{2\beta_i} \frac{\eta_i}{2\lambda_i \sqrt{v_i}} - 1 \\ &= \frac{\eta_i (\alpha_i - a_i)}{4\beta_i \lambda_i \sqrt{v_i}} - 1 \end{aligned}$$

Hence,  $d\pi_{i, M}/dv_i = 0$  if, and only if

$$v_i = \left( \frac{\eta_i \lambda_i (\alpha_i - c_i)}{4\beta_i \lambda_i^2 - \epsilon_i^2 (c_i - c_L)^2} \right)^2$$

□

If there is  $v_1 \in \mathbb{R}_0^+$  such that  $(a_1(v_1, v_2), a_2(v_1, v_2)) \in D$ , we select the best response  $v_1$  of Firm  $F_1$ , restricted to  $(a_1(v_1, v_2), a_2(v_1, v_2)) \in D$ , to the new production cost  $a_2$  of Firm  $F_2$  as follows: Let  $Z_D$  be the set of zeros  $v_1$  of the following polynomial

$$\frac{\partial \pi_{1,D}}{\partial v_1} = 0,$$

such that  $(a_1(v_1, v_2), a_2(v_1, v_2)) \in D$ . The best response  $v_1$  of Firm  $F_1$  in  $D$  is given by

$$v_1 = \arg \max_{v_1 \in Z_D \cup F_{M_1}} \pi_{1,D}(a_1(v_1, v_2), a_2(v_1, v_2)).$$

Let us characterize the set  $Z_D$ .

Let  $O_i = -4\beta_i \beta_j / (4\beta_i \beta_j - \gamma^2)^2$ .

**Theorem 2.2.7** *Let  $(v_1, v_2)$  be such that  $(a_1(v_1, v_2), a_2(v_1, v_2)) \in D$ . The set  $Z_D$  is the set of zeros of the following polynomial:*

$$f_1(\theta_i, \theta_j, W_i, W_j) + \theta_j f_2(\theta_i, \theta_j, W_i, W_j) = 0 \quad (2.14)$$

where

$$\begin{aligned} f_1(\theta_i, \theta_j, W_i, W_j) &= W_j^2 (2\lambda_i \lambda_j \beta_j \gamma O_i \eta_i \eta_j) + W_i W_j (-4\beta_j^2 \lambda_j^2 \eta_i^2 O_i - 4\beta_j \lambda_i^2 \lambda_j^2) + \\ &+ W_j (-4O_i \beta_j^2 \eta_i \lambda_i \lambda_j^2 (\alpha_i - c_i) + 2\lambda_i \lambda_j^2 \beta_j \gamma \eta_i O_i (\alpha_j - c_j)) \end{aligned}$$

$$\begin{aligned} f_2(\theta_i, \theta_j, W_i, W_j) &= W_i^2 (2\beta_j \lambda_i \lambda_j O_i \gamma \eta_i \eta_j) + W_i W_j (-O_i \gamma^2 \eta_j^2 \lambda_i^2) + \\ &+ W_i (2\beta_j \lambda_i^2 \lambda_j O_i \gamma \eta_j (\alpha_i - c_i) - O_i \lambda_j \lambda_i^2 \gamma^2 \eta_j (\alpha_j - c_j)) \end{aligned}$$

and  $W_i = \sqrt{v_i + \theta_i v_j}$ .

**Proof:** Note that  $W_i = \sqrt{v_i + \theta_i v_j}$ . Thus, Let us compute

$$\frac{d\pi_{i,D}}{dv_i} = \frac{\partial\pi_{i,D}}{\partial a_i} \frac{\partial a_i}{\partial v_i} + \frac{\partial\pi_{i,D}}{\partial a_j} \frac{\partial a_j}{\partial v_i} + \frac{\partial\pi_{i,D}}{\partial v_i}. \quad (2.15)$$

We have that

$$\begin{aligned} \frac{\partial\pi_{i,D}}{\partial a_i} &= -\frac{4\beta_i\beta_j(2\beta_j(\alpha_i - a_i) + \gamma(a_j - \alpha_j))}{(4\beta_i\beta_j - \gamma^2)^2} = 2O_i\beta_j(\alpha_i - c_i) + \frac{2\beta_j\eta_i O_i}{\lambda_i} W_i - \\ &\quad - \gamma O_i(\alpha_j - c_j) - \frac{\gamma\eta_j O_i}{\lambda_j} W_j, \\ \frac{\partial a_i}{\partial v_i} &= -\frac{\eta_i(c_i - c_L)}{2\lambda_i W_i} = -\frac{\eta_i}{2\lambda_i W_i}, \\ \frac{\partial\pi_{i,D}}{\partial a_j} &= \frac{2\beta_i\gamma(2\beta_j(\alpha_i - a_i) + \gamma(a_j - \alpha_j))}{(4\beta_i\beta_j - \gamma^2)^2} = -O_i\gamma(\alpha_i - c_i) - \frac{O_i\gamma\eta_i}{\lambda_i} W_i + \\ &\quad + \frac{O_i\gamma^2}{2\beta_j}(\alpha_j - c_j) + \frac{O_i\gamma^2\eta_j}{2\beta_j\lambda_j} W_j, \\ \frac{\partial a_j}{\partial v_i} &= -\frac{\theta_j\eta_j(c_j - c_L)}{2\lambda_j W_j} = -\frac{\eta_j\theta_j}{2\lambda_j W_j}, \\ \frac{\partial\pi_{i,D}}{\partial v_i} &= -1. \end{aligned}$$

Using the previous equalities in equation (2.15), we get

$$\begin{aligned} \frac{d\pi_{i,D}}{dv_i} &= \left(2O_i\beta_j(\alpha_i - c_i) + \frac{2\beta_j\eta_i O_i}{\lambda_i} W_i - \gamma O_i(\alpha_j - c_j) - \frac{\gamma\eta_j O_i}{\lambda_j} W_j\right) \left(-\frac{\eta_i}{2\lambda_i W_i}\right) + \\ &\quad + \left(-O_i\gamma(\alpha_i - c_i) - \frac{O_i\gamma\eta_i}{\lambda_i} W_i + \frac{O_i\gamma^2}{2\beta_j}(\alpha_j - c_j) + \frac{O_i\gamma^2\eta_j}{2\beta_j\lambda_j} W_j\right) \left(-\frac{\eta_j\theta_j}{2\lambda_j W_j}\right) - 1 \end{aligned}$$



Hence,  $d\pi_{i,D}/dv_i = 0$  if, and only if

$$\begin{aligned}
& W_j^2 (2\lambda_i \lambda_j \beta_j \gamma O_i \eta_i \eta_j) + W_i W_j (-4\beta_j^2 \lambda_j^2 \eta_i^2 O_i - 4\beta_j \lambda_i^2 \lambda_j^2) + \\
& + W_j (-4O_i \beta_j^2 \eta_i \lambda_i \lambda_j^2 (\alpha_i - c_i) + 2\lambda_i \lambda_j^2 \beta_j \gamma \eta_i O_i (\alpha_j - c_j)) + \\
& + \theta_j (W_i^2 (2\beta_j \lambda_i \lambda_j O_i \gamma \eta_i \eta_j) + W_i W_j (-O_i \gamma^2 \eta_j^2 \lambda_i^2) + \\
& + W_i (2\beta_j \lambda_i^2 \lambda_j O_i \gamma \eta_j (\alpha_i - c_i) - O_i \lambda_j \lambda_i^2 \gamma^2 \eta_j (\alpha_j - c_j))) = 0
\end{aligned}$$

□

**Corollary 2.2.3** *Suppose that Firms use patents (i.e. without spillovers,  $\theta_i = \theta_j = 0$ ). Let  $(v_1, v_2)$  be such that  $(a_1(v_1, v_2), a_2(v_1, v_2)) \in D$ . The set  $Z_D$  is the set of zeros of the following polynomial:*

$$\begin{aligned}
& W_j^2 (2\lambda_i \lambda_j \beta_j \gamma O_i \eta_i \eta_j) + W_i W_j (-4\beta_j^2 \lambda_j^2 \eta_i^2 O_i - 4\beta_j \lambda_i^2 \lambda_j^2) + \\
& + W_j (-4O_i \beta_j^2 \eta_i \lambda_i \lambda_j^2 (\alpha_i - c_i) + 2\lambda_i \lambda_j^2 \beta_j \gamma \eta_i O_i (\alpha_j - c_j)) = 0 \quad (2.16)
\end{aligned}$$

where  $W_i = \sqrt{v_i}$ .

**Proof:** From (2.14), making  $\theta_i = \theta_j = 0$  we get (2.16).

□

If there is  $v_1 \in \mathbb{R}_0^+$  such that  $(a_1(v_1, v_2), a_2(v_1, v_2)) \in M_2$ , the best response  $v_1$  of Firm  $F_1$ , restricted to  $(a_1(v_1, v_2), a_2(v_1, v_2)) \in M_2$ , is given by Firm  $F_1$  investing zero, i.e. not investing. Hence,  $V_1(v_2)$  is given by

$$V_1(v_2) = \arg \max_{v_1 \in F} \pi_1(a_1(v_1, v_2), a_2(v_1, v_2)),$$

where  $V_1 \in F = Z_{M_1} \cup F_{M_1} \cup Z_D \cup \{0\}$ .

**Theorem 2.2.8** *The best investment response function  $V_i : \mathbb{R}_0^+ \rightarrow \mathbb{R}_0^+$  of Firm  $F_i$  is explicitly computed.*

**Proof:** Analogous to Theorem 2.2.3.

□

### AJ-Model with Joint Venture

Here, we compute the best investment response functions when both Firms decide to go on a Joint Venture program together. Thus, the equivalents to Theorems 2.2.6 and 2.2.7 are computed for this case. Since they go on a Joint Venture program, each Firm maximizes the sum of both Firms profits when taking their decisions. Thus,  $\pi = \pi_1 + \pi_2$ .

**Theorem 2.2.9** *Let  $v_i$  be such that  $(a_1(v_1, v_2), a_2(v_1, v_2)) \in M_i$ . The set  $Z_{M_i}$  is given by:*

$$v_i = \left( \frac{\eta_i \lambda_i (\alpha_i - c_i)}{4\beta_i \lambda_i^2 - \epsilon_i^2 (c_i - c_L)^2} \right)^2.$$

**Proof:** If  $(a_i, c_j) \in M_i$ , then  $\pi = \pi_i + \pi_j = \pi_i$ . Thus Theorem 2.2.6 still holds in the case of Joint venture.

□

If there is  $v_1 \in \mathbb{R}_0^+$  such that  $(a_1(v_1, v_2), a_2(v_1, v_2)) \in D$ , we select the best response  $v_1$  of Firm  $F_1$ , restricted to  $(a_1(v_1, v_2), a_2(v_1, v_2)) \in D$ , to the new production cost  $a_2$  of Firm  $F_2$  as follows: Let  $Z_D$  be the set of zeros  $v_1$  of the following polynomial

$$\frac{\partial \pi}{\partial v_1} = 0,$$

such that  $(a_1(v_1, v_2), a_2(v_1, v_2)) \in D$ . The best response  $v_1$  of Firm  $F_1$  in  $D$  is given by

$$v_1 = \arg \max_{v_1 \in Z_D \cup F_{M_1}} \pi(a_1(v_1, v_2), a_2(v_1, v_2)).$$

Let us characterize the set  $Z_D$ .

**Theorem 2.2.10** *Let  $(v_1, v_2)$  be such that  $(a_1(v_1, v_2), a_2(v_1, v_2)) \in D$ . The set  $Z_D$  is the set of zeros of the following polynomial:*

$$f_1(\theta_i, \theta_j, W_i, W_j) + \theta_j f_2(\theta_i, \theta_j, W_i, W_j) = 0 \quad (2.17)$$

where

$$\begin{aligned} f_1(\theta_i, \theta_j, W_i, W_j) &= W_j^2 (2\lambda_i \lambda_j \beta_i \beta_j \gamma O_i \eta_i \eta_j + 2O_i \gamma \eta_i \eta_j \beta_i \beta_j) + \\ &+ W_i W_j (-4\beta_j^2 \beta_i \lambda_j^2 \eta_i^2 O_i - 4\beta_i \beta_j \lambda_i^2 \lambda_j^2 - 2O_i \gamma^2 \eta_i^2 \beta_i \beta_j \lambda_j^2) + \\ &+ W_j (-4O_i \beta_i \beta_j^2 \eta_i \lambda_i \lambda_j^2 (\alpha_i - c_i) + 2\lambda_i \lambda_j^2 \beta_i \beta_j \gamma \eta_i O_i (\alpha_j - c_j) + \\ &+ 2O_i \gamma \eta_i \beta_i \beta_j \lambda_i \lambda_j^2 (\alpha_j - c_j) - O_i \eta_i \gamma^2 \lambda_i \lambda_j^2 \beta_i (\alpha_i - c_i)) \\ f_2(\theta_i, \theta_j, W_i, W_j) &= W_i^2 (2\beta_i \beta_j \lambda_i \lambda_j O_i \gamma \eta_i \eta_j + 2O_i \gamma \eta_i \eta_j \lambda_i \lambda_j \beta_i \beta_j) + \\ &+ W_i W_j (-O_i \gamma^2 \eta_j^2 \lambda_i^2 \beta_i - 4\beta_i^2 O_i \eta_j^2 \lambda_i^2 \beta_j) + \\ &+ W_i (2\beta_i \beta_j \lambda_i^2 \lambda_j O_i \gamma \eta_j (\alpha_i - c_i) - O_i \beta_i \lambda_i^2 \gamma^2 \eta_j (\alpha_j - c_j) - \\ &- 4O_i \beta_i^2 \beta_j \eta_j \lambda_j \lambda_i^2 (\alpha_j - c_j) + 2O_i \gamma \eta_j \lambda_j \lambda_i^2 \beta_i \beta_j (\alpha_i - c_i)) \end{aligned}$$

and  $W_i = \sqrt{v_i + \theta_i v_j}$ .

**Proof:** Note that  $W_i = \sqrt{v_i + \theta_i v_j}$ . Since we are in the case where Firms cooperate via Joint Venture, the profit both Firms want to optimize is given by  $\pi = \pi_i + \pi_j$ .

Let us compute

$$\frac{d\pi_D}{dv_i} = \frac{\partial\pi_{i,D}}{\partial a_i} \frac{\partial a_i}{\partial v_i} + \frac{\partial\pi_{i,D}}{\partial a_j} \frac{\partial a_j}{\partial v_i} + \frac{\partial\pi_{i,D}}{\partial v_i} + \frac{\partial\pi_{j,D}}{\partial a_i} \frac{\partial a_i}{\partial v_i} + \frac{\partial\pi_{j,D}}{\partial a_j} \frac{\partial a_j}{\partial v_i} + \frac{\partial\pi_{j,D}}{\partial v_i}. \quad (2.18)$$

We have that

$$\begin{aligned} \frac{\partial\pi_{i,D}}{\partial a_i} &= -\frac{4\beta_i\beta_j(2\beta_j(\alpha_i - a_i) + \gamma(a_j - \alpha_j))}{(4\beta_i\beta_j - \gamma^2)^2} = 2O_i\beta_j(\alpha_i - c_i) + \frac{2\beta_j\eta_i O_i}{\lambda_i} W_i - \\ &\quad - \gamma O_i(\alpha_j - c_j) - \frac{\gamma\eta_j O_i}{\lambda_j} W_j, \\ \frac{\partial a_i}{\partial v_i} &= -\frac{\eta_i(c_i - c_L)}{2\lambda_i W_i} = -\frac{\eta_i}{2\lambda_i W_i}, \\ \frac{\partial\pi_{i,D}}{\partial a_j} &= \frac{2\beta_i\gamma(2\beta_j(\alpha_i - a_i) + \gamma(a_j - \alpha_j))}{(4\beta_i\beta_j - \gamma^2)^2} = -O_i\gamma(\alpha_i - c_i) - \frac{O_i\gamma\eta_i}{\lambda_i} W_i + \\ &\quad + \frac{O_i\gamma^2}{2\beta_j}(\alpha_j - c_j) + \frac{O_i\gamma^2\eta_j}{2\beta_j\lambda_j} W_j, \\ \frac{\partial a_j}{\partial v_i} &= -\frac{\theta_j\eta_j(c_j - c_L)}{2\lambda_j W_j} = -\frac{\eta_j\theta_j}{2\lambda_j W_j}, \\ \frac{\partial\pi_{j,D}}{\partial a_i} &= -\frac{2\gamma\beta_j(2\beta_i(\alpha_j - a_j) + \gamma(a_i - \alpha_i))}{(4\beta_i\beta_j - \gamma^2)^2} = -O_i\gamma(\alpha_j - c_j) - \frac{O_i\gamma\eta_j}{\lambda_j} W_j + \\ &\quad + \frac{O_i\gamma^2}{2\beta_i}(\alpha_i - c_i) + \frac{O_i\gamma^2\eta_i}{\lambda_i} W_i, \\ \frac{\partial\pi_{j,D}}{\partial a_j} &= 2O_i\beta_i(\alpha_j - c_j) + \frac{2\beta_i O_i\eta_j}{\lambda_j} W_j - O_i\gamma(\alpha_i - c_i) - \frac{O_i\gamma\eta_i}{\lambda_i} W_i, \\ \frac{\partial\pi_{i,D}}{\partial v_i} &= -1, \\ \frac{\partial\pi_{j,D}}{\partial v_i} &= 0. \end{aligned}$$

Using the previous equalities in equation (2.18), we get

$$\begin{aligned} \frac{d\pi_D}{dv_i} &= \left( 2O_i\beta_j(\alpha_i - c_i) + \frac{2\beta_j\eta_i O_i}{\lambda_i} W_i - \gamma O_i(\alpha_j - c_j) - \frac{\gamma\eta_j O_i}{\lambda_j} W_j \right) \left( -\frac{\eta_i}{2\lambda_i W_i} \right) + \\ &\quad + \left( -O_i\gamma(\alpha_i - c_i) - \frac{O_i\gamma\eta_i}{\lambda_i} W_i + \frac{O_i\gamma^2}{2\beta_j}(\alpha_j - c_j) + \frac{O_i\gamma^2\eta_j}{2\beta_j\lambda_j} W_j \right) \left( -\frac{\eta_j\theta_j}{2\lambda_j W_j} \right) - 1 + \end{aligned}$$

$$\begin{aligned}
& + \left( -O_i\gamma(\alpha_j - c_j) - \frac{O_i\gamma\eta_j}{\lambda_j}W_j + \frac{O_i\gamma^2}{2\beta_i}(\alpha_i - c_i) + \frac{O_i\gamma^2\eta_i}{\lambda_i}W_i \right) \left( -\frac{\eta_i}{2\lambda_i W_i} \right) + \\
& + \left( 2O_i\beta_i(\alpha_j - c_j) + \frac{2\beta_i O_i\eta_j}{\lambda_j}W_j - O_i\gamma(\alpha_i - c_i) - \frac{O_i\gamma\eta_i}{\lambda_i}W_i \right) \left( -\frac{\eta_j\theta_j}{2\lambda_j W_j} \right)
\end{aligned}$$

Hence,  $d\pi_{i,D}/dv_i = 0$  if, and only if

$$\begin{aligned}
& W_j^2 (2\lambda_i\lambda_j\beta_i\beta_j\gamma O_i\eta_i\eta_j + 2O_i\gamma\eta_i\eta_j\beta_i\beta_j) + \\
& + W_iW_j (-4\beta_j^2\beta_i\lambda_j^2\eta_i^2 O_i - 4\beta_i\beta_j\lambda_i^2\lambda_j^2 - 2O_i\gamma^2\eta_i^2\beta_i\beta_j\lambda_j^2) + \\
& + W_j(-4O_i\beta_i\beta_j^2\eta_i\lambda_i\lambda_j^2(\alpha_i - c_i) + 2\lambda_i\lambda_j^2\beta_i\beta_j\gamma\eta_i O_i(\alpha_j - c_j) + \\
& + 2O_i\gamma\eta_i\beta_i\beta_j\lambda_i\lambda_j^2(\alpha_j - c_j) - O_i\eta_i\gamma^2\lambda_i\lambda_j^2\beta_i(\alpha_i - c_i)) + \\
& + \theta_j(W_i^2(2\beta_i\beta_j\lambda_i\lambda_j O_i\gamma\eta_i\eta_j + 2O_i\gamma\eta_i\eta_j\lambda_i\lambda_j\beta_i\beta_j) + \\
& + W_iW_j(-O_i\gamma^2\eta_j^2\lambda_i^2\beta_i - 4\beta_i^2 O_i\eta_j^2\lambda_i^2\beta_j) + \\
& + W_i(2\beta_i\beta_j\lambda_i^2\lambda_j O_i\gamma\eta_j(\alpha_i - c_i) - O_i\beta_i\lambda_i^2\gamma^2\eta_j(\alpha_j - c_j) - \\
& - 4O_i\beta_i^2\beta_j\eta_j\lambda_j\lambda_i^2(\alpha_j - c_j) + 2O_i\gamma\eta_j\lambda_j\lambda_i^2\beta_i\beta_j(\alpha_i - c_i)) = 0
\end{aligned}$$

□

**Corollary 2.2.4** *Suppose that Firms use patents (i.e. without spillovers,  $\theta_i = \theta_j = 0$ ). Let  $(v_1, v_2)$  be such that  $(a_1(v_1, v_2), a_2(v_1, v_2)) \in D$ . The set  $Z_D$  is the set of zeros of the following polynomial:*

$$\begin{aligned}
& W_j^2 (2\lambda_i\lambda_j\beta_i\beta_j\gamma O_i\eta_i\eta_j + 2O_i\gamma\eta_i\eta_j\beta_i\beta_j) + \\
& + W_iW_j (-4\beta_j^2\beta_i\lambda_j^2\eta_i^2 O_i - 4\beta_i\beta_j\lambda_i^2\lambda_j^2 - 2O_i\gamma^2\eta_i^2\beta_i\beta_j\lambda_j^2) + \\
& + W_j(-4O_i\beta_i\beta_j^2\eta_i\lambda_i\lambda_j^2(\alpha_i - c_i) + 2\lambda_i\lambda_j^2\beta_i\beta_j\gamma\eta_i O_i(\alpha_j - c_j) + \\
& + 2O_i\gamma\eta_i\beta_i\beta_j\lambda_i\lambda_j^2(\alpha_j - c_j) - O_i\eta_i\gamma^2\lambda_i\lambda_j^2\beta_i(\alpha_i - c_i)) = 0 \quad (2.19)
\end{aligned}$$

where  $W_i = \sqrt{v_i}$ .

**Proof:** From (2.17), making  $\theta_i = \theta_j = 0$  we get (2.19).

□

## 2.3 Nash investment equilibria

Let  $c_L$  be the minimum attainable production cost and  $\alpha$  the market saturation. Given production costs  $(c_1, c_2) \in [c_L, \alpha] \times [c_L, \alpha]$ , the *Nash investment equilibria*  $(v_1, v_2) \in \mathbb{R}_0^+ \times \mathbb{R}_0^+$  are the solutions of the system

$$\begin{cases} v_1 = V_1(v_2) \\ v_2 = V_2(v_1) \end{cases}$$

where  $V_1$  and  $V_2$  are the best investment response functions computed in the previous sections. All the results presented hold in an open region of parameters  $(c_L, \epsilon_i, \alpha_i, \lambda_i, \beta_i, \gamma_i, \theta_i, \theta_j)$  containing the point  $(4, 0.2, 10, 10, 0.013, 0.013, 0, 0)$ .

For the FOP-Model, we find four different regions of Nash investment equilibria namely, a competitive Nash investment region  $C$  where both Firms invest, a single Nash investment region  $S_1$  for Firm  $F_1$ , where only Firm  $F_1$  invests, a single Nash investment region  $S_2$  for Firm  $F_2$ , where only Firm  $F_2$  invests, and a nil Nash investment region  $N$ , where neither of the Firms invest (see Figure 2.4). The single Nash investment region  $S_i$  can be decomposed into two disjoint regions: a *single favorable Nash investment region*  $S_i^F$  where the production costs, after investment, are favorable to Firm  $F_i$ ; and a *single recovery Nash investment region*  $S_i^R$  where the production costs, after investment are, still, favorable to Firm  $F_j$  but Firm  $F_i$  recovers, slightly, from its initial disadvantage. The economical reasons for Firm  $F_j$  deciding not to invest in the single favorable Nash investment region  $S_i^F$  and in the single recovery Nash investment region  $S_i^R$  are

opposite. In the single favorable Nash investment region  $S_i^F$ , the production costs of Firm  $F_j$  are too high for the Firm  $F_j$  to recover its investment by increasing its profit due to decreasing its production costs. In the single recovery Nash investment region  $S_i^R$ , the production costs of Firm  $F_j$  are too low for the Firm  $F_j$  to be willing to invest to decrease, even more, its production costs and, so, Firm  $F_i$  is able to decrease its production costs by investing. The single favorable Nash investment region  $S_i^F$  can also be decomposed into three regions: the *single duopoly region*  $S_i^D$ , the *single monopoly region*  $S_i^M$  and the *single monopoly boundary region*  $S_i^B$ . The single monopoly region  $S_i^M$  consists of all production costs such that, after Firm  $F_i$ 's investment, the new production costs are in the monopoly region of Firm  $F_i$ . The single monopoly boundary region  $S_i^B$  consists of all production costs such that, after Firm  $F_i$ 's investment, the new production costs are in the boundary between the monopoly region and the duopoly region of Firm  $F_i$ . The single duopoly region  $S_i^D$  consists of all production costs such that, after the Firm  $F_i$ 's investment, the new production costs are still in the duopoly region of Firm  $F_i$ . The economical reasons for both Firms choosing not to invest in the nil Nash investment regions  $N_{LL}$ ,  $N_{HL}$ ,  $N_{LH}$  and  $N_{HH}$  are quite different. In the region  $N_{LL}$ , neither of the Firms invest because the Firms already have so low costs that the investment is not recovered by the increase in the profit associated to the decrease of their production costs. In the region  $N_{LH}$  (respectively  $N_{HL}$ ), neither of the Firms invest because Firm  $F_1$  (respectively  $F_2$ ) has so low production costs and Firm  $F_2$  (respectively  $F_1$ ) has so high production costs that if one Firm invests and decreases its production costs, then it is not able to recover its investment with the corresponding increase in the profit associated to the new production costs. In the region  $N_{HH}$  neither of the Firms invest because the Firms already have so high production costs that the invest-

ment is not recovered by the increase in the profit associated to the decrease of their production costs. In the AJ-Model we only find three different Nash investment equilibria regions, i.e., the competitive Nash investment region  $C$  and the single Nash investment regions  $S_1$  and  $S_2$ . This different behavior is due to the shape of d'Aspremont and A. Jacquemin's R&D cost reduction investment function traducing an higher incentive to invest reflected in the disappearance of the nil Nash investment region. We also find that, for the FOP-Model, the Nash investment equilibria consists of a unique, or two, or three points depending upon the pair of initial production costs, as we will explain throughout this Section. The set of all Nash investment equilibria form the *Nash investment equilibrium set*. We now present the Nash investment equilibria by considering the following three regions of production costs:

$C$  the *competitive Nash investment region*  $C$  that is characterized by both Firms investing;

$S_i$  the *single Nash investment region*  $S_i$  that is characterized by only one of the Firms investing;

$N$  the *nil Nash investment region*  $N$  that is characterized by neither of the Firms investing.

Denote by  $R = [c_L, \alpha_1] \times [c_L, \alpha_2]$  the region of all possible pairs of productions costs  $(c_1, c_2)$ . Let  $A^c = R - A$  be the complementary of  $A$  in  $R$ . As shown in Figure 2.4 where we exhibit the Nash investment regions for the FOP-Model, (i) the intersection  $R_{S_1 \cap S_2} = (S_1^M \cup S_1^B) \cap (S_2^M \cup S_2^B) \cap C^c$  between the *single Nash investment regions*  $S_1$  and  $S_2$  is non empty; (ii) the intersection  $R_{C \cap S_i} = C \cap (S_i^M \cup S_i^B) \cap S_j^c$  with  $i \neq j$  between the *competitive Nash investment region*  $C$  and the *single Nash investment region*  $S_i$  is non empty; (iii) for high enough



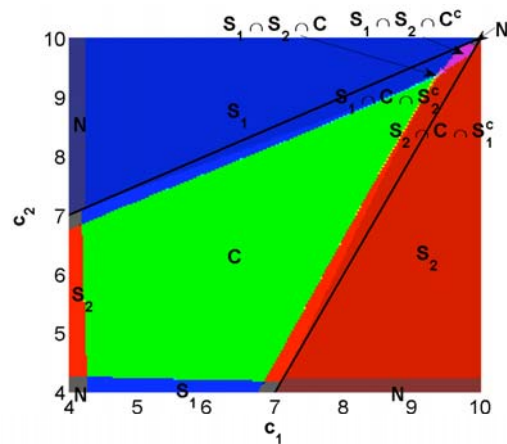


Figure 2.4: Full characterization, for the FOP-Model, of the Nash investment regions in terms of the Firms' initial production costs  $(c_1, c_2)$ . The monopoly lines  $l_{M_i}$  are colored black. The nil Nash investment region  $N$  is colored grey. The single Nash investment regions  $S_1$  and  $S_2$  are colored blue and red, respectively. The competitive Nash investment region  $C$  is colored green. The region where  $S_1$  and  $S_2$  intersect are colored pink, the region where  $S_1$  and  $C$  intersect are colored lighter blue and the region where  $S_2$  and  $C$  intersect are colored yellow. The region where the regions  $S_1$ ,  $S_2$  and  $C$  intersect are colored lighter grey.

initial production costs, unexpectedly, the intersection  $R_{S_1 \cap C \cap S_2} = (S_1^M \cup S_1^B) \cap C \cap (S_2^M \cup S_2^B)$  between the *competitive Nash investment region*  $C$  and the *single Nash investment regions*  $S_1$  and  $S_2$  is non empty.

In Figure 2.5, we illustrate the Nash investment regions for the AJ-Model. We observe that there are only three different Nash investment equilibria regions: a competitive Nash investment region  $C$ , a single Nash investment region  $S_1$  for Firm  $F_1$  and a single Nash investment region  $S_2$  for Firm  $F_2$ . Moreover, the regions with multiple Nash investment equilibria,  $R_{S_1 \cap S_2}$ ,  $R_{C \cap S_i}$  and  $R_{S_1 \cap C \cap S_2}$ , that appear in the FOP-Model, no longer exist.

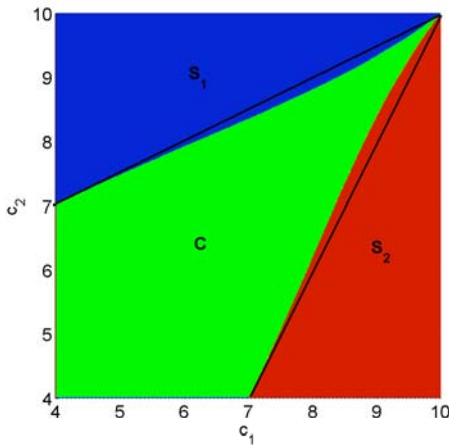


Figure 2.5: Full characterization, for the AJ-Model, of the Nash investment regions in terms of the Firms' initial production costs  $(c_1, c_2)$ . The monopoly lines  $l_{M_i}$  are colored black. The single Nash investment regions  $S_1$  and  $S_2$  are colored blue and red, respectively. The competitive Nash investment region  $C$  is colored green.

In the next Figures, we exhibit both for the FOP-Model and the AJ-Model: the Firms' Nash investment equilibria (see Figure 2.6), the Firms' Profits (see Figure 2.7), the Firms' new production costs (see Figure 2.8), the ratio between the Firms' investment on R&D and their total income (see Figure 2.9). We ob-

serve that the Firms choose higher values of investment when the production costs take intermediate values. Moreover, there is a discontinuity in the production costs between the monopoly and the duopoly regions. We also observe that each Firm has higher profits when its own production cost is low and the other Firm's production cost is high. For the Firms' profits, we notice a discontinuity in the derivative, when the production costs change from the monopoly to the duopoly region. For the percentage of the Firms' total profit invested in R&D, we observe that, the higher the production costs, the higher the ratio is. In particular, for the FOP-Model, when the production costs are really high, the Firms' investment in R&D is almost all their entire profit.

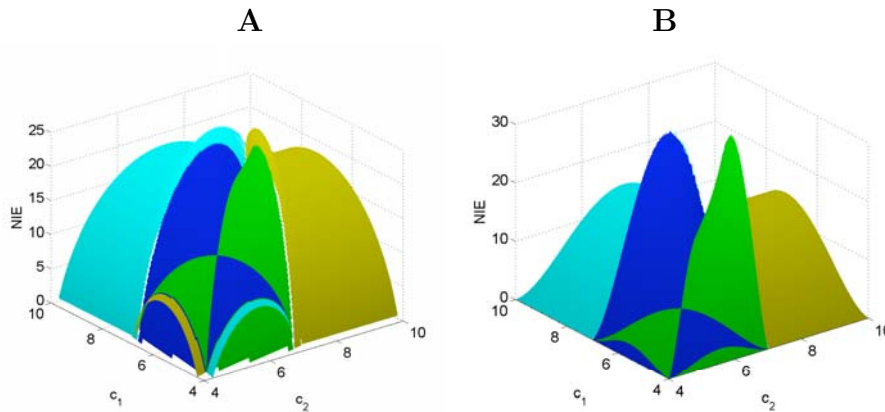


Figure 2.6: Firms' Nash investments in terms of their initial production costs  $(c_1, c_2)$ . The Nash investment for Firm  $F_1$  in the competitive Nash investment region  $C$  are colored blue and the Nash investment for Firm  $F_2$  in the competitive Nash investment region  $C$  are colored green. The Nash investments in the single Nash investment region  $S_1$  (respectively  $S_2$ ) are colored lighter blue (respectively yellow). (A) FOP-Model; (B) AJ-Model.

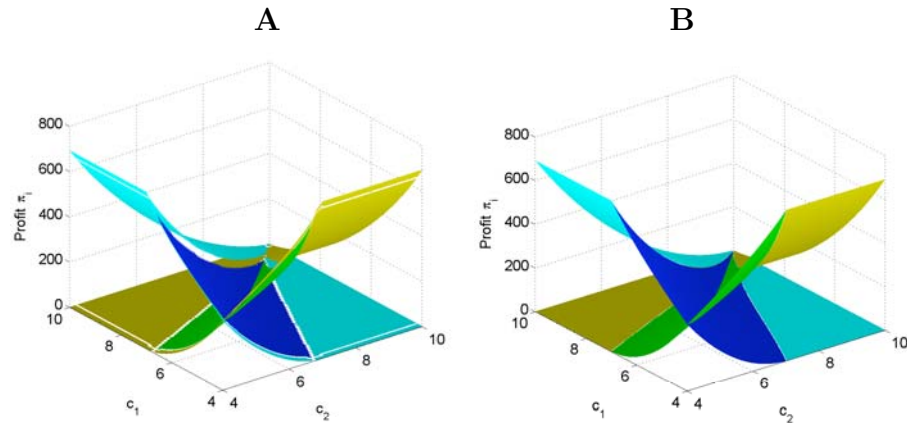


Figure 2.7: Firms' profits in terms of their initial production costs  $(c_1, c_2)$ . The Nash investment for Firm  $F_1$  in the competitive Nash investment region  $C$  are colored blue and the Nash investment for Firm  $F_2$  in the competitive Nash investment region  $C$  are colored green. The Firms' profits in the single Nash investment region  $S_1$  (respectively  $S_2$ ) are colored lighter blue (respectively yellow). (A) FOP-Model; (B) AJ-Model.

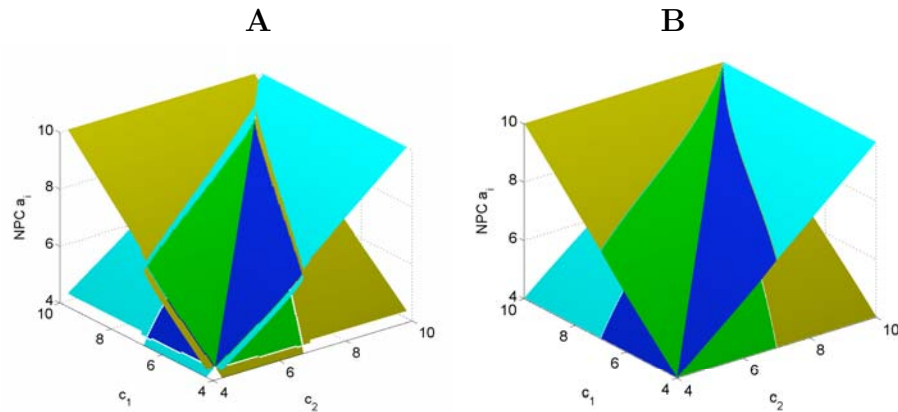


Figure 2.8: Firms' new production costs in terms of their initial production costs  $(c_1, c_2)$ . The Nash investment for Firm  $F_1$  in the competitive Nash investment region  $C$  are colored blue and the Nash investment for Firm  $F_2$  in the competitive Nash investment region  $C$  are colored green. The Firms' new production costs in the single Nash investment region  $S_1$  (respectively  $S_2$ ) are colored lighter blue (respectively yellow). (A) FOP-Model; (B) AJ-Model.

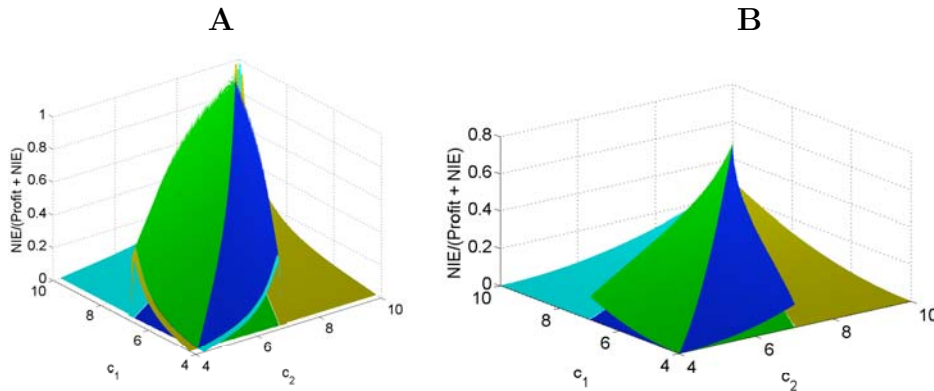


Figure 2.9: Percentage of the Firms' total profit invested in R&D in terms of their initial production costs  $(c_1, c_2)$ . The Nash investment for Firm  $F_1$  in the competitive Nash investment region  $C$  are colored blue and the Nash investment for Firm  $F_2$  in the competitive Nash investment region  $C$  are colored green. The Firms' new production costs in the single Nash investment region  $S_1$  (respectively  $S_2$ ) are colored lighter blue (respectively yellow). (A) FOP-Model; (B) AJ-Model.

In Figure 2.10, we exhibit how the Nash investment regions change when the Firms go on a Joint Venture program. Note that for the AJ-Model, we observe the appearance of two regions with multiple equilibria: a region with a single Nash investment equilibrium  $S_1$  and a competitive Nash investment equilibrium  $C$  and a region with a single Nash investment equilibrium  $S_2$  and a competitive Nash investment equilibrium  $C$ . Next, we show how the Firms' Nash investment equilibria (see Figure 2.11), the Firms' Profits (see Figure 2.12), the Firms' new production costs (see Figure 2.13), the ratio between the Firms' investment on R&D and their total income (see Figure 2.14) change when the Firms decide to go on a Joint Venture program. Notice that the competitive region is much smaller for both Firms when they go on a joint venture together.

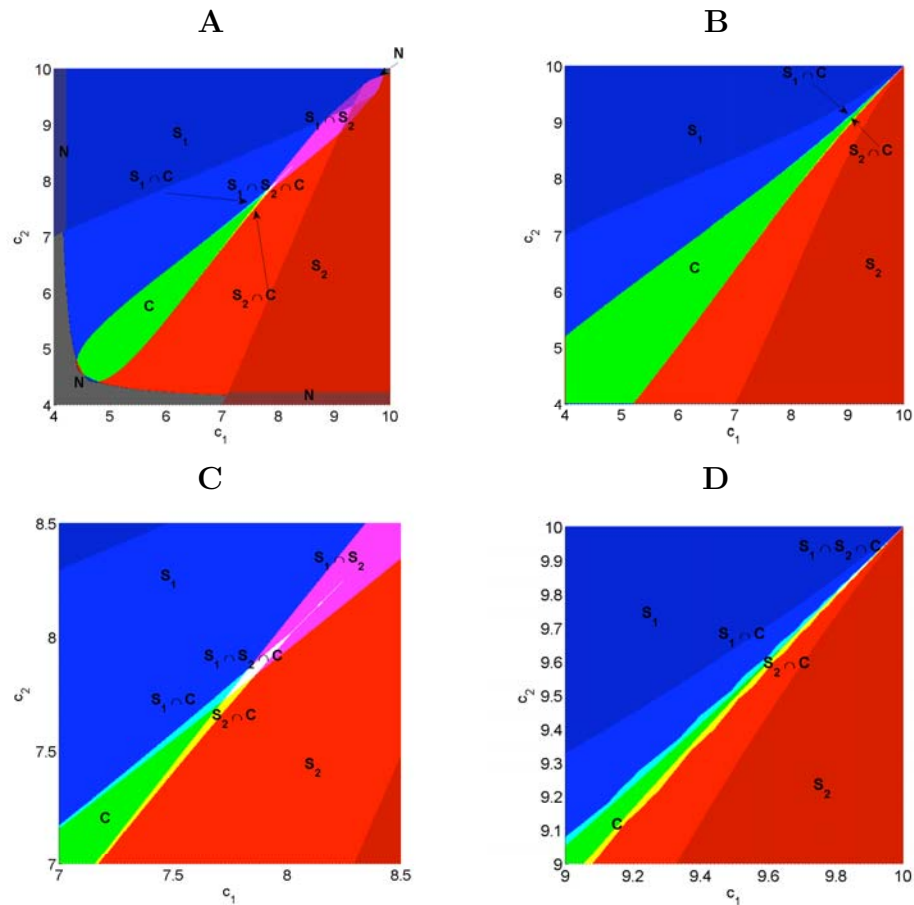


Figure 2.10: Full characterization of the Nash investment regions in terms of the Firms' initial production costs  $(c_1, c_2)$ . The monopoly lines  $l_{M_i}$  are colored black. The nil Nash investment region  $N$  is colored grey. The single Nash investment regions  $S_1$  and  $S_2$  are colored blue and red, respectively. The competitive Nash investment region  $C$  is colored green. The region where  $S_1$  and  $S_2$  intersect are colored pink, the region where  $S_1$  and  $C$  intersect are colored lighter blue and the region where  $S_2$  and  $C$  intersect are colored yellow. The region where the regions  $S_1$ ,  $S_2$  and  $C$  intersect are colored lighter grey. (A) FOP-Model; (B) AJ-Model; (C) Zoom of (B); (D) Zoom of (B).

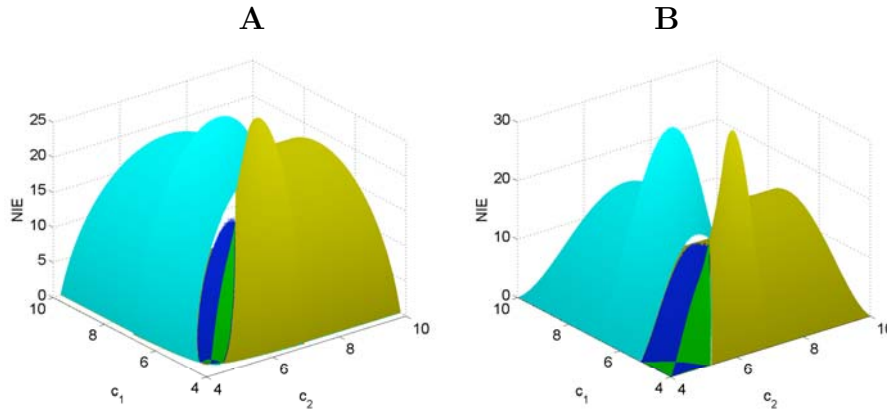


Figure 2.11: Firms' Nash investments in terms of their initial production costs  $(c_1, c_2)$ . The Nash investment for Firm  $F_1$  in the competitive Nash investment region  $C$  are colored blue and the Nash investment for Firm  $F_2$  in the competitive Nash investment region  $C$  are colored green. The Nash investments in the single Nash investment region  $S_1$  (respectively  $S_2$ ) are colored lighter blue (respectively yellow). (A) FOP-Model; (B) AJ-Model.

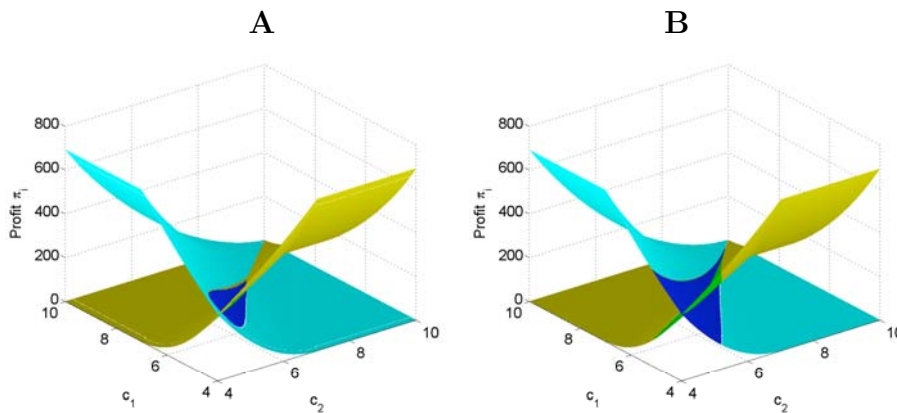


Figure 2.12: Firms' profits in terms of their initial production costs  $(c_1, c_2)$ . The Nash investment for Firm  $F_1$  in the competitive Nash investment region  $C$  are colored blue and the Nash investment for Firm  $F_2$  in the competitive Nash investment region  $C$  are colored green. The Firms' profits in the single Nash investment region  $S_1$  (respectively  $S_2$ ) are colored lighter blue (respectively yellow). (A) FOP-Model; (B) AJ-Model.

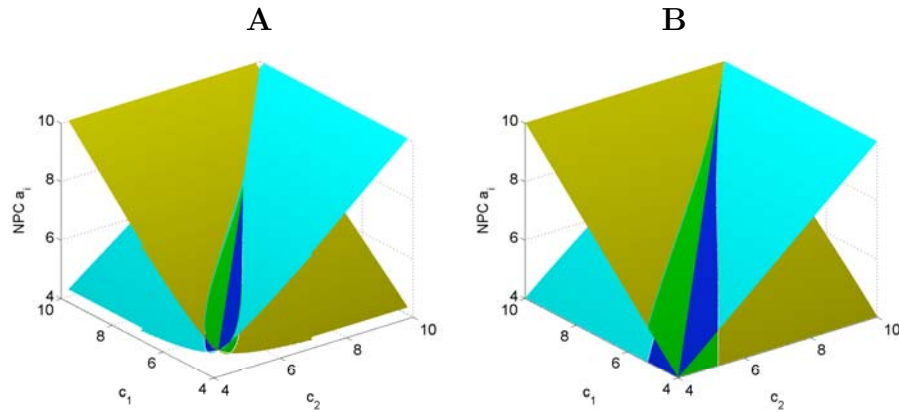


Figure 2.13: Firms' new production costs in terms of their initial production costs  $(c_1, c_2)$ . The Nash investment for Firm  $F_1$  in the competitive Nash investment region  $C$  are colored blue and the Nash investment for Firm  $F_2$  in the competitive Nash investment region  $C$  are colored green. The Firms' new production costs in the single Nash investment region  $S_1$  (respectively  $S_2$ ) are colored lighter blue (respectively yellow). (A) FOP-Model; (B) AJ-Model.

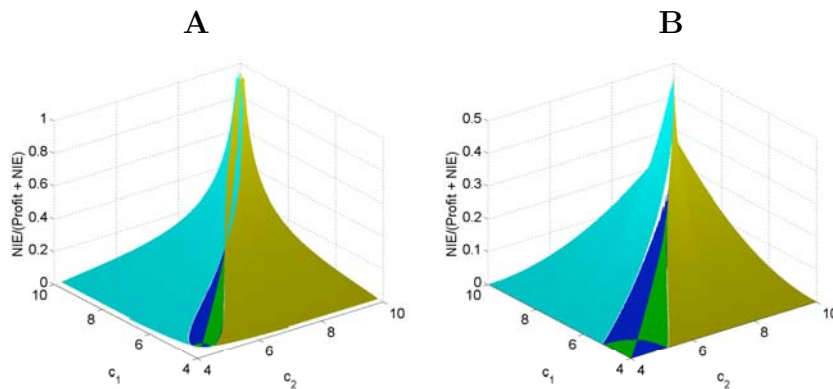


Figure 2.14: Percentage of the Firms' total profit invested in R&D in terms of their initial production costs  $(c_1, c_2)$ . The Nash investment for Firm  $F_1$  in the competitive Nash investment region  $C$  are colored blue and the Nash investment for Firm  $F_2$  in the competitive Nash investment region  $C$  are colored green. The Firms' new production costs in the single Nash investment region  $S_1$  (respectively  $S_2$ ) are colored lighter blue (respectively yellow). (A) FOP-Model; (B) AJ-Model.



## 2.4 FOP-Model boundary characterization

In this Section we present, for the FOP-Model, a full characterization of the boundaries of the Nash investment regions described previously. We study separately the boundaries of the single Nash investment region (see Subsection 2.4.1), the nil Nash investment region (see Subsection 2.4.2) and the competitive Nash investment region (see Subsection 2.4.3).

### 2.4.1 Single Nash investment region

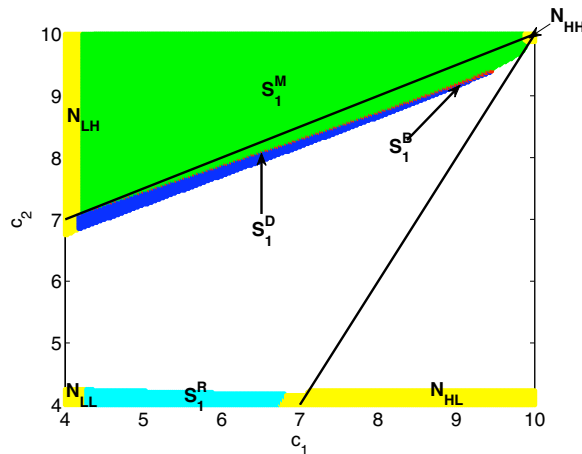


Figure 2.15: Full characterization of the single Nash investment region  $S_1$  and of the nil Nash investment region  $N$  in terms of the Firms' initial production costs  $(c_1, c_2)$ . The subregions  $N_{LL}$ ,  $N_{LH}$ ,  $N_{HL}$  and  $N_{HH}$  of the nil Nash investment region  $N$  are colored yellow. The subregion  $S_1^R$  of the single Nash investment region  $S_1$  is colored lighter blue. The subregion  $S_1^F$  of the single Nash investment region  $S_1$  is decomposed in three subregions: the *single Duopoly region*  $S_i^D$  colored blue, the *single Monopoly region*  $S_i^M$  colored green and the *single Monopoly boundary region*  $S_i^B$  colored red.

The *single Nash investment region*  $S_i$  consists of the set of production costs  $(c_1, c_2)$  with the property that the Nash investment equilibrium set contains a

pair  $(v_1, v_2)$  with the Nash investment  $v_i = V_i(0) > 0$  and the Nash investment  $v_j = V_j(v_i) = 0$ , for  $j \neq i$ .

The single Nash investment region  $S_i$  can be decomposed into two disjoint regions: a *single favorable Nash investment region*  $S_i^F$  where the production costs, after investment, are favorable to Firm  $F_i$ , and in a *single recovery Nash investment region*  $S_i^R$  where the production costs, after investment are, still, favorable to Firm  $F_j$  but Firm  $F_i$  recovers a little from its disadvantageous (see Figure 2.15).

The single favorable Nash investment region  $S_i^F$  can be decomposed into three regions: the *single Duopoly region*  $S_i^D$ , the *single Monopoly region*  $S_i^M$  and the *single Monopoly boundary region*  $S_i^B$  (see Figure 2.15). For every cost  $(c_1, c_2) \in S_i^F$ , let  $(a_1(v_1), a_2(v_2))$  be the new production costs obtained by the Firms  $F_1$  and  $F_2$  choosing the Nash investment equilibrium  $(v_1, v_2)$  with  $v_j = 0$ . The single duopoly region  $S_i^D$  consists of all production costs  $(c_1, c_2)$  such that for the Nash new investment costs  $(a_1(v_1), a_2(v_2))$  the Firms are in the duopoly region  $D$  (see Figure 2.15). The single monopoly region  $S_i^M$  consists of all production costs  $(c_1, c_2)$  such that for the new production costs  $(a_1(v_1), a_2(v_2))$  Firm  $F_i$  is in the interior of the Monopoly region  $M_i$ . The single monopoly boundary region  $S_i^B$  consists of all production costs  $(c_1, c_2)$  such that the new production costs  $(a_1(v_1), a_2(v_2))$  are in the boundary of the Monopoly region  $l_{M_i}$ .

We now characterize the boundaries of the single favorable Nash investment region  $S_1^F$  (due to the symmetry, a similar characterization holds for  $S_2^F$ ). We study the boundaries of  $S_1^M$  by separating it into four distinct boundaries: the *upper boundary*  $U_{S_1}^M$ , that is the union of a vertical segment line  $U_{S_1}^l$  and a curve  $U_{S_1}^c$ , the *intermediate boundary*  $I_{S_1}^M$ , the *lower boundary*  $L_{S_1}^M$  and the *left boundary*  $Le_{S_1}^M$  (see Figure 2.16). The left boundary of the single monopoly region  $Le_{S_1}^M$

is the right boundary  $d_1$  of the nil Nash investment region  $N_{LH}$  that will be characterized in Subsection 2.4.2.

The boundary of the single monopoly boundary region  $S_1^B$  is the union of a *upper boundary*  $U_{S_1}^B$  and a *lower boundary*  $L_{S_1}^B$  (see Figure 2.20).

The boundary of the single duopoly region  $S_1^D$  is the union of a *upper boundary*  $U_{S_1}^D$ , a *lower boundary*  $L_{S_1}^D$  and a *left boundary*  $Le_{S_1}^D$  (see Figure 2.21). The left boundary of the single duopoly region  $Le_{S_1}^D$  is the right boundary  $d_3$  of the nil Nash investment region  $N_{LH}$  that will be characterized in Subsection 2.4.2.

The single recovery Nash investment region  $S_1^R$  has three boundaries: the *upper boundary*  $U_{S_1}^R$ , the *left boundary*  $Le_{S_1}^R$ , and the *right boundary*  $R_{S_1}^R$  (see Figure 2.23).

### Boundary of the single monopoly region $S_1^M$

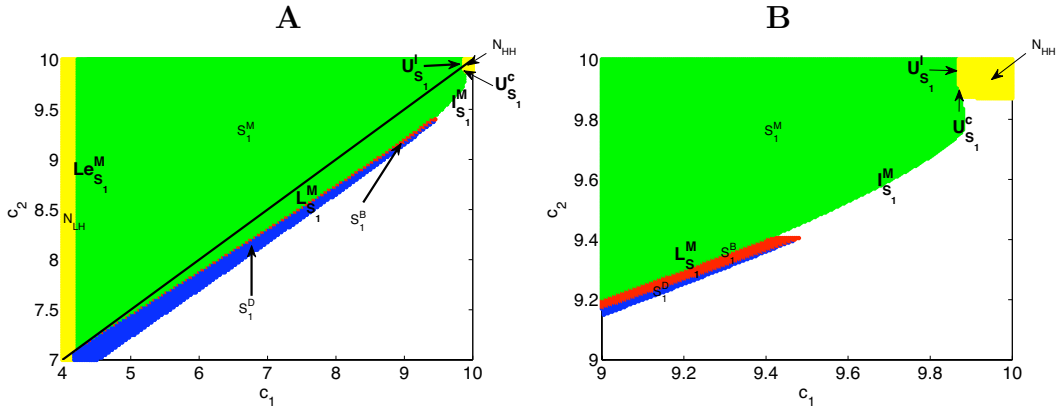


Figure 2.16: (A) Full characterization of the boundaries of the single monopoly region  $S_1^M$ : the upper boundary  $U_{S_1}^M$  is the union of a vertical segment line  $U_{S_1}^l$  with a curve  $U_{S_1}^c$ ; the lower boundary  $L_{S_1}^M$ ; and the left boundary  $Le_{S_1}^M$ ; (B) Zoom of the upper part of figure (A) where the boundaries  $U_{S_1}^c$  and  $U_{S_1}^l$  can be seen in more detail.

In the following Lemmas we characterize, separately, the boundaries of the

single monopoly region  $S_1^M$ . Let us characterize the boundary  $U_{S_1}^l$  between the single monopoly region  $S_1^M$  and the nil Nash investment region  $N_{HH}$  with initial production costs  $(c_1, c_2)$  in the Monopoly region  $M_1$ . The boundary  $U_{S_1}^l$  is a vertical segment line corresponding to initial production costs  $(c_1, c_2)$  such that the profit  $\pi_{1,M_1}(0, 0; c_1, c_2) = \pi_{1,M_1}(v_1, 0; c_1, c_2)$  where  $v_1 = V_1(0)$  is the best investment response of Firm  $F_1$  to a zero investment of Firm  $F_2$  (see Figure 2.17). In Lemma 2.4.1, we give the algebraic characterization of  $U_{S_1}^l = \{c_1^M\} \times [l_{S_1}^M(c_1^M), \alpha_1]$  by determining the value  $c_1^M$ . The value  $l_{S_1}^M(c_1^M)$  such that  $(c_1^M, l_{S_1}^M(c_1^M)) \in l_{M_1}$  is computed using Lemma 2.2.2. Let

- $K_1 = -(8\beta_1\lambda_1 - \epsilon_1^2(c_1 - c_L)^2 - 2\epsilon_1(\alpha_1 - c_1)(c_1 - c_L))/(8\beta_1)$ ;
- $K_2 = (4\beta_1\lambda_1^2 - 2\epsilon_1\lambda_1(\alpha_1 - c_1)(c_1 - c_L))/(64\beta_1)$ ;
- $K_3 = -(4\beta_1\lambda_1^2 - 2\epsilon_1\lambda_1(\alpha_1 - c_1)(c_1 - c_L))/(4\beta_1)$ .

**Lemma 2.4.1** *The initial production costs  $c_1 = c_1^M$  of Firm  $F_1$ , such that  $(c_1^M, c_2) \in U_{S_1}^l$  and the best investment response  $v_1 = V_1(0)$  of Firm  $F_1$  to a zero investment of Firm  $F_2$  are implicitly determined as solutions of the following polynomial equations:*

$$2\beta_1 v_1^3 + 6\beta_1 \lambda_1 v_1^2 + L_1 v_1 + N_1 = 0 \quad (2.20)$$

$$K_2^2 - K_1^2 + K_3 + 2V_1 K_1 - V_1^2 = 0 \quad (2.21)$$

**Proof:** By Theorem 2.2.1,  $\partial\pi_{1,M_1}(v_1, 0; c_1, c_2)/\partial v_1 = 0$  can be written as equality

(2.20). From  $\pi_{1,M_1}(0, 0; c_1, c_2) = \pi_{1,M_1}(v_1, 0; c_1, c_2)$ , we get

$$(\alpha_1 - c_1)^2 = \left( \alpha_1 - c_1 + \frac{\epsilon_1(c_1 - c_L)v_1}{\lambda_1 + v_1} \right)^2 - 4\beta_1 v_1$$

that leads to

$$4\beta_1 v_1^2 + (8\beta_1 \lambda_1 - \epsilon_1^2)(c_1 - c_L)^2 - 2\epsilon_1(\alpha_1 - c_1)(c_1 - c_L)v_1 + (4\beta_1 \lambda_1^2 - 2\epsilon_1 \lambda_1(\alpha_1 - c_1)(c_1 - c_L)) = 0.$$

Choosing the positive solution of the above equality, we get

$$v_1 = K_1 + \sqrt{K_2^2 + K_3}$$

that is equivalent to equality (2.21). By Theorem 2.2.1,  $\partial\pi_{1,M_1}(v_1, 0; c_1^M(c_2), c_2)/\partial v_1 = 0$  can be written as equality (2.20).

□

Let us characterize the boundary  $U_{S_1}^c$  between the single monopoly region  $S_1^M$  and the nil Nash investment region  $N_{HH}$  with initial production costs  $(c_1, c_2)$  in the Monopoly region  $M_1$ . The boundary  $U_{S_1}^c$  is a curve corresponding to initial production costs  $(c_1, c_2)$  such that the profit  $\pi_{1,M_1}(0, 0; c_1, c_2) = \pi_{1,M_1}(v_1, 0; c_1, c_2)$  where  $v_1 = V_1(0)$  is the best investment response of Firm  $F_1$  to a zero investment of Firm  $F_2$  (see Figure 2.18). In Lemma 2.4.2 we give the algebraic characterization of the curve  $U_{S_1}^c = \{c_1(c_2) : c_2 \in [B(U_{S_1}^C; I_{S_1}^M), l_{S_1}^M(c_1^M)]\}$ . The value  $l_{S_1}^M(c_1^M)$  is such that  $(c_1^M, l_{S_1}^M(c_1^M)) \in l_{M_1}$  is computed and, as before, using Lemma 2.2.2. Let  $B(U_{S_1}^C; I_{S_1}^M)$  be the common boundary  $U_{S_1}^C \cap I_{S_1}^M$  between the boundaries of the single monopoly region  $U_{S_1}^C$  and  $I_{S_1}^M$ . The point  $B(U_{S_1}^C; I_{S_1}^M)$  is determined as a solution of the polynomial equations presented in Lemma 2.4.1 and Lemma 2.4.2.

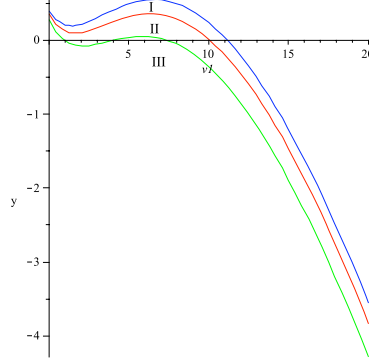


Figure 2.17: Each of the plots corresponds to the profit  $\pi_1$  of Firm  $F_1$  when Firm  $F_2$  decides not to invest, i.e.  $\pi_1(v_1, 0; c_1, c_2)$ . The plot in red (II) corresponds to a pair of production costs  $(c_1, c_2) \in U_{S_1}^l$ , the plot in blue (I) corresponds to a pair of production costs  $(c_1, c_2)$  that are in the single monopoly region  $S_1^M$  and the plot in green (III) corresponds to a pair of production costs  $(c_1, c_2)$  that are in the nil Nash investment region  $N_{HH}$ .

Let

- $K_4 = (\beta_1(2\beta_2(\alpha_1 - c_1) - \gamma(\alpha_2 - c_2))^2)/((4\beta_1\beta_2 - \gamma^2)^2)$ ;
- $K_5 = K_4 - (\alpha_1 - c_1)^2 - \epsilon_1^2(c_1 - c_L)^2 - 2\epsilon_1(c_1 - c_L)(\alpha_1 - c_1) + 8\beta_1\alpha_1$ ;
- $K_6 = 2\lambda_1 K_4 - 2\lambda_1(\alpha_1 - c_1)^2 - 2\epsilon_1\lambda_1(c_1 - c_L)(\alpha_1 - c_1) + 4\beta_1\lambda_1^2$ .

**Lemma 2.4.2** *The initial production costs  $c_1 = c_1^M(c_2)$  of Firm  $F_1$  such that  $(c_1^M(c_2), c_2) \in U_{S_1}^c$ , and the best investment response  $v_1 = V_1(0)$  of Firm  $F_1$  to a zero investment of Firm  $F_2$  are implicitly determined as solutions of the following polynomial equations:*

$$2\beta v_1^3 + 6\beta\lambda v_1^2 + L_1 v_1 + N_1 = 0 \quad (2.22)$$

and

$$4\beta_1 v_1^3 + K_5 v_1^2 + K_6 v_1 + K_4 \lambda_1^2 - (\alpha_1 - c_1)^2 \lambda_1^2 = 0 \quad (2.23)$$

**Proof:** From  $\pi_{1,D}(0, 0; c_1, c_2) = \pi_{1,M_1}(v_1, 0; c_1, c_2)$  we get

$$\frac{\beta_1(2\beta_2(\alpha_1 - c_1) - \gamma(\alpha_2 - c_2))^2}{(4\beta_1\beta_2 - \gamma^2)^2} = \left( \alpha_1 - c_1 + \frac{\epsilon_1(c_1 - c_L)v_1}{\lambda_1 + v_1} \right)^2 - 4\beta_1 v_1$$

that leads to equation (2.23). By Theorem 2.2.1,  $\partial\pi_{1,M_1}(v_1, 0; c_1^M(c_2), c_2)/\partial v_1 = 0$  can be written as equality (2.22).

□

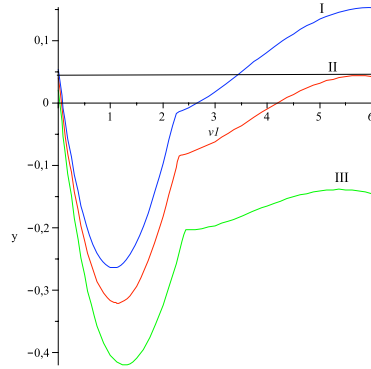


Figure 2.18: Each of the plots corresponds to the profit  $\pi_1$  of Firm  $F_1$  when Firm  $F_2$  decides not to invest, i.e.  $\pi_1(v_1, 0; c_1, c_2)$ . The plot in red (II) corresponds to a pair of production costs  $(c_1, c_2) \in U_{S_1}^c$ , the plot in blue (I) corresponds to a pair of production costs  $(c_1, c_2)$  that are in the single monopoly region  $S_1^M$  and the plot in green (III) corresponds to a pair of production costs  $(c_1, c_2)$  that are in the nil Nash investment region  $N_{HH}$ .

Let us characterize the boundary  $I_{S_1}^M$  between the single monopoly region  $S_1^M$  and the single Nash investment region  $S_2^M$  with initial production costs  $(c_1, c_2)$

in the Monopoly region  $M_1$  (see Figure 2.19). The intermediate boundary  $I_{S_1}^M$  of the single monopoly region  $S_1^M$  is characterized by the best investment response  $V_2(V_1(0))$  of Firm  $F_2$  to the best investment response  $V_1(0)$  of Firm  $F_1$  to zero, to be a set with two elements. One of the elements  $V_2^-$  of  $V_2(V_1(0))$  is zero and the other element  $V_2^+$  is greater than zero. In Lemma 2.4.3 we give the algebraic characterization of the curve  $I_{S_1}^M = \{c_1(c_2) : c_2 \in [B(I_{S_1}^M; L_{S_1}^M), B(U_{S_1}^C; I_{S_1}^M)]\}$ . The point  $B(I_{S_1}^M; L_{S_1}^M)$  is implicitly determined as a solution of the polynomial equations presented in Lemma 2.4.3 and Lemma 2.4.2. The point  $B(U_{S_1}^C; I_{S_1}^M)$  is determined, as before, as a solution of the polynomial equations presented in Lemma 2.4.1 and Lemma 2.4.2.

Let  $L_1$  and  $N_1$  be as in Theorem 2.2.1. Let  $C$ ,  $A_2$ ,  $B_2$  and  $H_2$  be as in Theorem 2.2.2. Let

- $K_7 = -4\beta_1\gamma(c_1 - \epsilon_1(c_1 - c_L))(c_2 - \epsilon_2(c_2 - c_L))$ ;
- $K_8 = -4\beta_1\gamma\epsilon_1\lambda_1(c_2 - c_L)(c_1 - \epsilon_1(c_1 - c_L))$ ;
- $K_9 = -4\beta_1\gamma\epsilon_1\lambda_1(c_1 - c_L)(c_2 - \epsilon_2(c_2 - c_L))$ ;
- $K_{10} = -4\beta_1\gamma\epsilon_1\epsilon_2\lambda_1\lambda_2(c_1 - c_L)(c_2 - c_L)$ ;
- $K_{11} = 4\beta_1^2c_1^2 + \epsilon_1^2(c_1 - c_L) - 2\epsilon_1c_1(c_1 - c_L) + \gamma c_2^2 + \epsilon_2^2(c_2 - c_L) - 2\epsilon_2c_2(c_2 - c_L) + c_1(8\beta_1^2\alpha_1 + 4\beta_1\alpha_1\gamma) - \epsilon_1(c_1 - c_L)(8\beta_1^2\alpha_1 + 4\beta_1\alpha_1\gamma) + c_2(-2\alpha_2\gamma^2 + 4\beta_1\gamma\alpha_2) - \epsilon_2(c_2 - c_L)(-2\alpha_2\gamma^2 + 4\beta_1\gamma\alpha_2) + 4\beta_1^2\alpha_1^2 + \gamma^2\alpha_2^2 - 4\beta_1\gamma\alpha_2^2 + (\lambda_1(4\beta_1\beta_2 - \gamma^2))^2/\beta_2$ ;
- $K_{12} = -2\lambda_1\epsilon_1^2(c_1 - c_L) + 2\epsilon_1\lambda_1c_1(c_1 - c_L) + \lambda_1\epsilon_1(c_1 - c_L)$ ;
- $W_1 = v_1 + \lambda_1$ ;  $W_2 = v_2 + \lambda_2$ .

**Lemma 2.4.3** *The initial production costs  $c_1 = c_1^M(c_2)$  of Firm  $F_1$  such that  $(c_1^M(c_2), c_2) \in I_{S_1}^M$ , the best investment  $v_1 = V_1(0)$  of Firm  $F_1$  to a zero investment*



of Firm  $F_2$  and the best investment of Firm  $F_2$   $V_2^+ \in V_2(V_1(0))$  are implicitly determined as solutions of the following polynomial equations:

$$\begin{aligned} K_7 W_1^4 W_2^4 &+ K_8 W_1^4 W_2^3 + K_9 W_1^3 W_2^4 + K_{10} W_1^3 W_2^3 - ((4\beta_1\beta_2 - \gamma^2)^2/\beta_2) W_2^3 W_1^2 + \\ &+ K_{11} W_1^2 W_2^2 + K_{12} W_1 W_2^2 + K_{13} W_2 W_1^2 + \\ &+ \lambda_2^2 \epsilon_2^2 (c_2 - c_L) W_1^2 + \lambda_1^2 \epsilon_1^2 (c_1 - c_L) W_2^2 = 0 \end{aligned} \quad (2.24)$$

and

$$C W_2^3 W_1 + A_2 W_2 W_1 + B_2 W_1 - (B_2/\lambda_2) H_2 W_2 = 0 \quad (2.25)$$

and

$$2\beta_1 (W_1 - \lambda_1)^3 + 6\beta_1 \lambda_1 (W_1 - \lambda_1)^2 + L_1 (W_1 - \lambda_1) + N_1 = 0 \quad (2.26)$$

**Proof:** From  $\pi_{2,D}(v_1, v_2; c_1, c_2) = 0$ , we get

$$\frac{\beta_2 (2\beta_1 (\alpha_1 - a_1) - \gamma (\alpha_2 - a_2))^2}{(4\beta_1\beta_2 - \gamma^2)^2} - v_2 = 0.$$

The equality above can be written as

$$\begin{aligned} 4\beta_1^2 a_1^2 &+ \gamma a_2^2 + (-8\beta_1^2 \alpha_1 + 4\beta_1 \alpha_1 \gamma) a_1 + (-2\alpha_2 \gamma^2 + 4\beta_1 \gamma \alpha_2) a_2 - 4\beta_1 \gamma a_1 a_2 + \\ &+ (4\beta_1^2 \alpha_1^2 + \gamma^2 \alpha_2^2 - 4\beta_1 \gamma \alpha_2^2) - ((4\beta_1\beta_2 - \gamma^2)^2/\beta_2) v_2 = 0. \end{aligned}$$

Substituting  $a_i = c_i - (\eta_i v_i)/(\lambda_i + v_i)$  and doing some algebraic manipulations we get equality (2.24). By Theorem 2.2.2, we have that  $\partial \pi_{2,D}(v_1, v_2; c_1^M(c_2), c_2)/\partial v_2 = 0$  can be written as equality (2.25).

By Theorem 2.2.1, we have that  $\partial\pi_{1,M_1}(v_1, 0; c_1^M(c_2), c_2)/\partial v_1 = 0$  can be written as equality (2.26).

□

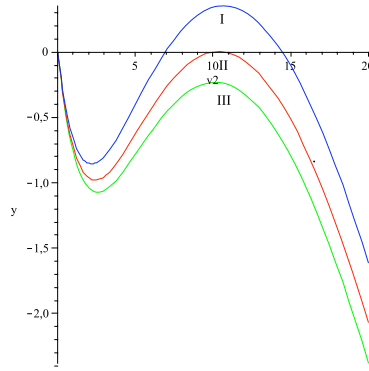


Figure 2.19: Each of the plots corresponds to the Profit  $\pi_2$  of Firm  $F_2$  when Firm  $F_1$  decides to invest  $v_1$  and Firm  $F_2$  has two possible best responses  $V_2(v_1) = \{v_2; 0\}$  with  $v_2 > 0$ , i.e.  $\pi_2(V_1(0), v_2; c_1, c_2)$ . The plot in red (II) corresponds to a pair of production costs  $(c_1, c_2) \in I_{S_1}^M$ , the plot in blue (I) corresponds to a pair of production costs  $(c_1, c_2)$  that are in the single monopoly region  $S_1^M$  and the plot in green (III) corresponds to a pair of production costs  $(c_1, c_2)$  that are in the single monopoly region  $S_2^M$ .

Let us characterize the boundary  $L_{S_1}^M$  between the single monopoly region  $S_1^M$  and the single monopoly boundary region  $S_1^B$  with initial production costs  $(c_1, c_2)$  in the Monopoly region  $M_1$ . In Lemma 2.4.4 we give the algebraic characterization of the curve  $L_{S_1}^M = \{c_1(c_2) : c_2 \in [B(L_{S_1}^M; Le_{S_1}^M), B(I_{S_1}^c; L_{S_1}^M)]\}$ . The point  $B(L_{S_1}^M; Le_{S_1}^M)$  is implicitly determined as a solution of the polynomial equations presented in Lemma 2.4.4 and Theorem 2.4.2. The point  $B(I_{S_1}^M; L_{S_1}^M)$  is determined, as before, as a solution of the polynomial equations presented in Lemma 2.4.3 and Lemma 2.4.4. Let  $L_1$  and  $N_1$  be as in Theorem 2.2.1.

**Lemma 2.4.4** *The initial production costs  $c_1 = c_1^M(c_2)$  of Firm  $F_1$  such that  $(c_1^M(c_2), c_2) \in L_{S_1}^M$ , and the best investment  $v_1 = V_1(0)$  of Firm  $F_1$  to a zero investment of Firm  $F_2$  are implicitly determined as solutions of the following polynomial equations:*

$$2\beta_1 v_1^3 + 6\beta_1 \lambda_1 v_1^2 + L_1 v_1 + N_1 = 0, \quad (2.27)$$

where

$$v_1 = \frac{\gamma \lambda_1 (c_2 - \alpha_2) - 2\beta_2 \lambda_1 (c_1 - \alpha_1)}{2\epsilon_1 \beta_2 (c_L - c_1) + 2\beta_2 (c_1 - \alpha_1) - \gamma (c_2 - \alpha_2)} \quad (2.28)$$

**Proof:** By Theorem 2.2.1,  $\partial \pi_{1, M_1}(v_1, 0; c_1, c_2) / \partial v_1 = 0$  can be written as equation (2.27). Take  $a_1 = c_1 - (\epsilon_1 (c_1 - c_L) v_1) / (\lambda_1 + v_1)$  and  $a_2 = c_2$ , by Lemma 2.2.1, we get

$$\left( \frac{\gamma}{2\beta_2} (c_2 - \alpha_2) - (c_1 - \alpha_1) \right) (\lambda_1 + v_1) = \epsilon_1 (c_L - c_1) v_1 \quad (2.29)$$

Thus (2.28) follows from (2.29). □

### Boundary of the single monopoly boundary region $S_1^B$

The upper boundary of the single monopoly boundary region  $U_{S_1}^B$  is the lower boundary of the single monopoly region  $L_{S_1}^M$  and has already been characterized in the beginning of this Section. Let us characterize the boundary  $L_{S_1}^B$  between the single monopoly boundary region  $S_1^B$  and the single duopoly region  $S_1^D$  for initial production costs  $(c_1, c_2)$  in the monopoly region  $M_1$ . In Lemma

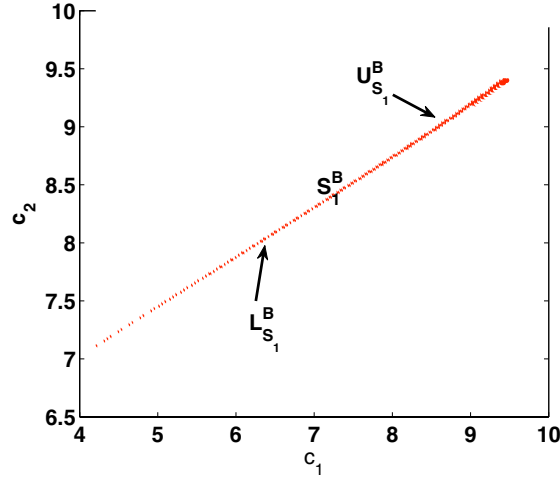


Figure 2.20: Full characterization of the boundaries of the single monopoly boundary region  $S_1^B$ : the upper boundary  $U_{S_1}^B$  and the lower boundary  $L_{S_1}^B$ .

2.4.5 we give the algebraic characterization of the curve  $L_{S_1}^B = \{c_1(c_2) : c_2 \in [B(L_{S_1}^D; L_{S_1}^B), B(L_{S_1}^B; d_3)]\}$ . The point  $B(L_{S_1}^D; L_{S_1}^B)$  is implicitly determined as a solution of the polynomial equations presented in Lemma 2.4.6 and Lemma 2.4.5. The point  $B(L_{S_1}^B; d_3)$  is implicitly determined as a solution of the polynomial equations presented Lemma 2.4.5 and Theorem 2.4.1.

Let  $A_1, E_1, F_1, G_1$  and  $H_1$  be as in Theorem 2.4.1.

**Lemma 2.4.5** *The initial production costs  $c_1 = c_1^M(c_2)$  of Firm  $F_1$  such that  $(c_1^M(c_2), c_2) \in L_{S_1}^B$  and the best investment  $v_1 = V_1(0)$  of Firm  $F_1$  to a zero investment of Firm  $F_2$  are implicitly determined as solutions of the following polynomial equations:*

$$A_1 c_1^2 + E_1 c_1 c_2 + F_1 c_1 + G_1 c_2 + H_1 = 0 \quad (2.30)$$

and

$$v_1 = \frac{\gamma\lambda_1(c_2 - \alpha_2) - 2\beta_2\lambda_1(c_1 - \alpha_1)}{2\epsilon_1\beta_2(c_L - c_1) + 2\beta_2(c_1 - \alpha_1) - \gamma(c_2 - \alpha_2)} \quad (2.31)$$

**Proof:** By Theorem 2.4.1,  $\partial\pi_{1,D}(v_1, 0; c_1, c_2)/\partial v_2 = 0$  can be written as equation (2.30). We get equation (2.31) as in Lemma 2.4.4.

□

### Boundary of the single duopoly region $S_1^D$

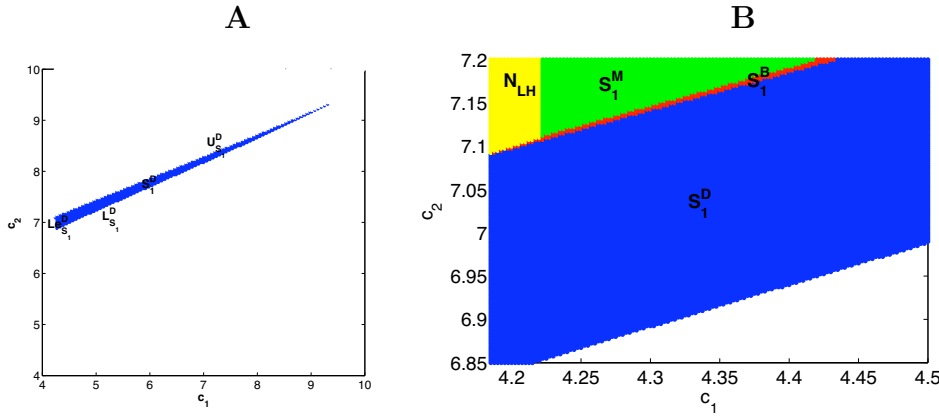


Figure 2.21: (A) Full characterization of the boundaries of the single duopoly region  $S_1^D$ : the upper boundary  $U_{S_1}^D$ ; the lower boundary  $L_{S_1}^D$ ; and the left boundary  $Le_{S_1}^D$ ; (B) Zoom of the lower part of  $Le_{S_1}^D$ .

The upper boundary of the single duopoly region  $U_{S_1}^D$  is the lower boundary of the single monopoly boundary region  $L_{S_1}^B$  and has already been characterized in this Subsection. The left boundary of the single duopoly region  $Le_{S_1}^D$  is the right boundary  $d_3$  of the nil Nash investment region  $N_{LH}$  that will be characterized in Subsection 2.4.2.

Let us characterize the boundary  $L_{S_1}^D$  between the single duopoly region  $S_1^D$  and the competitive Nash investment region  $C$  for initial production costs  $(c_1, c_2)$  in the monopoly region  $M_1$  (see Figure 2.22). In Lemma 2.4.6 we give the algebraic characterization of the curve  $L_{S_1}^D = \{c_1(c_2) : c_2 \in [B(L_{S_1}^B; L_{S_1}^D), B(L_{S_1}^D; d_3)]\}$ . The point  $B(L_{S_1}^B; L_{S_1}^D)$  is implicitly determined as a solution of the polynomial equations presented in Lemma 2.4.5 and Lemma 2.4.6. The point  $B(L_{S_1}^D; d_3)$  is implicitly determined as a solution of the polynomial equations presented in Lemma 2.4.6 and Theorem 2.4.1.

**Lemma 2.4.6** *The initial production costs  $c_1 = c_1^M(c_2)$  of Firm  $F_1$  such that  $(c_1^M(c_2), c_2) \in L_{S_1}^D$ , the best investment  $v_1 = V_1(0)$  of Firm  $F_1$  to a zero investment of Firm  $F_2$  and the best investment of Firm  $F_2$   $V_2^+ \in V_2(V_1(0))$  are implicitly determined as solutions of the following polynomial equations:*

$$\begin{aligned} K_7 W_1^4 W_2^4 &+ K_8 W_1^4 W_2^3 + K_9 W_1^3 W_2^4 + K_{10} W_1^3 W_2^3 - ((4\beta_1\beta_2 - \gamma^2)^2/\beta_2) W_2^3 W_1^2 + \\ &+ K_{11} W_1^2 W_2^2 + K_{12} W_1 W_2^2 + K_{13} W_2 W_1^2 + \\ &+ \lambda_2^2 \epsilon_2^2 (c_2 - c_L) W_1^2 + \lambda_1^2 \epsilon_1^2 (c_1 - c_L) W_2^2 = 0 \end{aligned} \quad (2.32)$$

and

$$C W_2^3 W_1 + A_2 W_2 W_1 + B_2 W_1 - (B_2/\lambda_2) H_2 W_2 = 0 \quad (2.33)$$

and

$$C W_1^3 W_2 + A_1 W_1 W_2 + B_1 W_2 - (B_1/\lambda_1) H_1 W_1 = 0 \quad (2.34)$$

**Proof:** We get equation (2.32) as in Lemma 2.4.3.

By Theorem 2.2.2,  $\partial\pi_{2,D}(v_1, v_2; c_1, c_2)/\partial v_2 = 0$  can be written as equation (2.33).

By Theorem 2.2.2,  $\partial\pi_{1,D}(v_1, v_2; c_1, c_2)/\partial v_1 = 0$  can be written as equality (2.34).

□

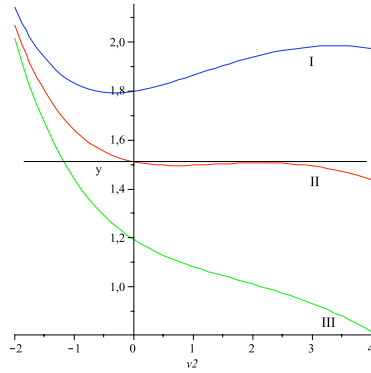


Figure 2.22: Each of the plots corresponds to the Profit  $\pi_2$  of Firm  $F_2$  when Firm  $F_1$  decides not to invest. The plot in red (II) corresponds to a pair of production costs  $(c_1, c_2) \in L_{S_1}^D$ , the plot in blue (I) corresponds to a pair of production costs  $(c_1, c_2)$  that are in the competitive Nash investment region  $C$  and the plot in green (III) corresponds to a pair of production costs  $(c_1, c_2)$  that are in the single duopoly region  $S_2^D$ .

### Boundary of the single recovery region $S_1^R$

The single recovery region  $S_1^R$  (due to the symmetry, a similar characterization holds for  $S_2^R$ ) has three boundaries: the *upper boundary*  $U_{S_1}^R$ , the *left boundary*  $L_{S_1}^R$ , and the *right boundary*  $R_{S_1}^R$  (see Figure 2.23). We are now going to characterize the upper boundary  $U_{S_1}^R$  of the single recovery region  $S_1^R$  and will leave the left and right boundaries of the single recovery region, that are also boundaries of the nil Nash investment region, to be characterized in Subsection

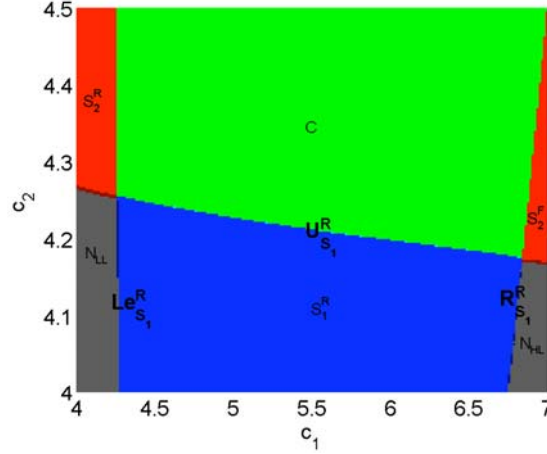


Figure 2.23: Full characterization of the boundaries of the single recovery region  $S_1^R$ : the upper boundary  $U_{S_1}^R$ ; the right boundary  $R_{S_1}^R$ ; and the left boundary  $Le_{S_1}^R$ . In green the competitive Nash investment region  $C$ , in grey the nil Nash investment region  $N$ , in red the single Nash investment region  $S_2$  for Firm  $F_2$  and in blue the single recovery region  $S_1^R$  for Firm  $F_1$ .

2.4.2 (see Figure 2.24). In Lemma 2.4.7 we give the algebraic characterization of the curve  $U_{S_1}^R = \{c_1(c_2) : c_2 \in [Q; P_3]\}$  where the point  $Q$  is characterized by being in the intersection between the competitive Nash investment region  $C$  and the nil Nash investment region  $N_{LL}$  and the point  $P_3$  is characterized by being in the intersection between the competitive Nash investment region  $C$  and the nil Nash investment region  $N_{HL}$ .

**Lemma 2.4.7** *The initial production costs  $c_1 = c_1^R(c_2)$  of Firm  $F_1$  such that  $(c_1^R(c_2), c_2) \in U_{S_1}^R$  are implicitly determined as solutions of the following polynomial equations:*

$$A_2 c_2^2 + E_2 c_1 c_2 + F_2 c_2 + G_2 c_1 + H_2 = 0 \quad (2.35)$$



and

$$A_1 c_1^2 + E_1 c_1 c_2 + F_1 c_1 + G_1 c_2 + H_1 = 0 \quad (2.36)$$

**Proof:** By Theorem 2.4.1, we get equations (2.35) and (2.36).

□

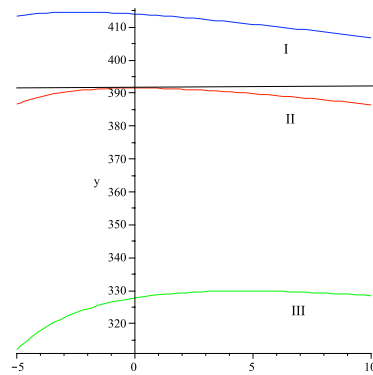


Figure 2.24: Each of the plots corresponds to the profit  $\pi_2$  of Firm  $F_2$  when Firm  $F_1$  decides not to invest, i.e.  $\pi_{2,D}(V_1(0), v_2; c_1, c_2)$ . The plot in red (II) corresponds to a pair of production costs  $(c_1, c_2) \in U_{S_1}^R$ , the plot in blue (I) corresponds to a pair of production costs  $(c_1, c_2)$  that are in the nil Nash investment region  $N_{HL}$  and the plot in green (III) corresponds to a pair of production costs  $(c_1, c_2)$  that are in the single recovery region  $S_1^R$ .

## 2.4.2 Nil Nash investment region

The *nil Nash investment region*  $N$  is the set of production costs  $(c_1, c_2) \in N$  with the property that  $(0, 0)$  is a Nash investment equilibrium. Hence, the nil Nash investment region  $N$  consists of all production costs  $(c_1, c_2)$  with the property that

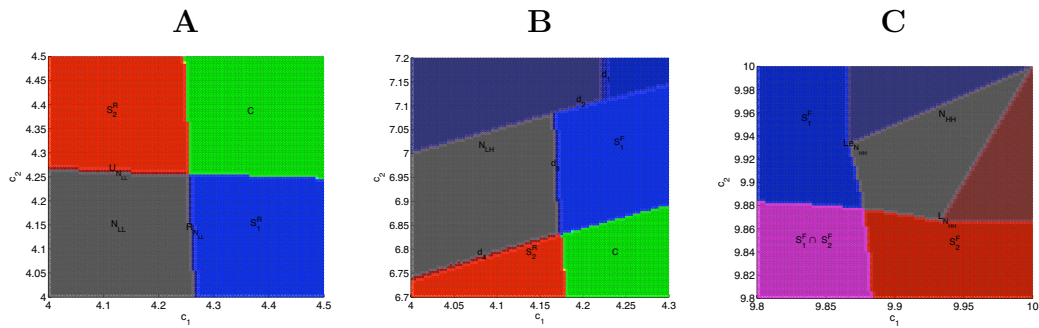


Figure 2.25: Full characterization of the nil Nash investment region  $N$  in terms of the Firms' initial production costs  $(c_1, c_2)$ : **(A)** The subregion  $N_{LL}$  of the nil Nash investment region  $N$  is colored grey corresponding to initial production cost such that the Firms do not invest and do not produce; **(B)** The subregion  $N_{LH}$  of the nil Nash investment region  $N$  is colored grey corresponding to initial production cost such that the Firms do not invest and do not produce and dark blue corresponding to cases where the Firms do not invest but Firm  $F_1$  produces a certain amount  $q_1$  greater than zero; **(C)** The subregion  $N_{HH}$  of the nil Nash investment region  $N$  is colored grey corresponding to initial production cost such that the Firms do not invest and do not produce; dark blue corresponding to cases where the Firms do not invest but Firm  $F_1$  produces a certain amount  $q_1$  greater than zero and dark red corresponding to cases where the Firms do not invest but Firm  $F_2$  produces a certain amount  $q_2$  greater than zero.

the new production costs  $(a_1(v_1), a_2(v_2))$ , with respect to the Nash investment equilibrium  $(0, 0)$ , are equal to the production costs  $(c_1, c_2)$ .

The nil Nash investment region  $N$  is the union of four disjoint sets: the set  $N_{LL}$  consisting of all production costs that are low for both Firms (see Figure 2.25 (A)); the set  $N_{LH}$  (resp.  $N_{HL}$ ) consisting of all production costs that are low for Firm  $F_1$  (resp.  $F_2$ ) and high for Firm  $F_2$  (resp.  $F_1$ ) (see Figure 2.25 (B)); and the set  $N_{HH}$  consisting of all production costs that are high for both Firms (see Figure 2.25 (C)).

In this Subsection, we characterize the boundaries of these nil Nash investment regions. The boundaries of the nil Nash investment region  $N_{HH}$  have been characterized in the previous Subsection. The left boundary  $Le_{N_{HH}}$  of the nil Nash investment region  $N_{HH}$  coincides with the upper boundary of the single monopoly region  $U_{S_1}^M$  (see Lemmas 2.4.1 and 2.4.2) and the lower boundary  $L_{N_{HH}}$  of the nil Nash investment region  $N_{HH}$  coincides with the upper boundary of the single monopoly region  $U_{S_2}^M$ . To characterize all the other boundaries of the nil Nash investment regions, we will use the following Theorems:

Let  $A_i, E_i, F_i, G_i$  and  $H_i$  be as in Theorem 2.4.1. Let us define the following parameters:

- $I_i = 4\beta_i\beta_j/\lambda_i$ ;  $A_i = -2I_i\epsilon_i\beta_i$ ;  $E_i = I_i\epsilon_i\gamma$ ;
- $G_i = -I_i\epsilon_i\gamma c_L$ ;  $F_i = 2I_i\epsilon_i\beta_i\alpha_i + 2I_i\epsilon_i c_L\beta_i - I_i\epsilon_i\gamma\alpha_i$ ;
- $K = (4\beta_i\beta_j - \gamma^2)^2$ ;  $H_i = -2I_i\epsilon_i c_L\beta_i\alpha_i + I_i\epsilon_i c_L\gamma\alpha_i - K$ .

**Theorem 2.4.1** *The solutions of  $\partial\pi_{i,D}(0, 0; c_1, c_2)/\partial v_i = 0$  are contained in*

$$A_i c_i^2 + E_i c_i c_j + F_i c_i + G_i c_j + H_i = 0.$$

**Proof:** Let us compute

$$\frac{d\pi_{i,D}}{dv_i} = \frac{\partial\pi_{i,D}}{\partial a_i} \frac{\partial a_i}{\partial v_i} + \frac{\partial\pi_{i,D}}{\partial a_j} \frac{\partial a_j}{\partial v_i} + \frac{\partial\pi_{i,D}}{\partial v_i}. \quad (2.37)$$

We have that

$$\begin{aligned} \frac{\partial\pi_{i,D}}{\partial a_i} &= -\frac{4\beta_i\beta_j(2\beta_j(\alpha_i - a_i) + \gamma(a_j - \alpha_j))}{(4\beta_i\beta_j - \gamma^2)^2} \\ \frac{\partial a_i}{\partial v_i} &= \frac{\eta_i\lambda_i}{(\lambda_i + v_i)^2} \\ \frac{\partial\pi_{i,D}}{\partial a_j} &= -\frac{2\beta_i\gamma(2\beta_j(\alpha_i - a_i) + \gamma(a_j - \alpha_j))}{(4\beta_i\beta_j - \gamma^2)^2} \\ \frac{\partial\pi_{i,D}}{\partial v_i} &= -1. \end{aligned}$$

Hence,  $d\pi_{i,D}/dv_i = 0$  if, and only if,

$$\frac{4\beta_i\beta_j\eta_i\lambda(2\beta_j(\alpha_i - a_i) + \gamma(a_j - \alpha_j))}{\lambda_i^2} = K \quad (2.38)$$

Taking  $a_i = c_i$  and  $a_j = c_j$ , we get that  $d\pi_{i,D}/dv_i = 0$  if, and only if,

$$I_i\eta_i(2\beta_i(\alpha_i - c_i) + \gamma(c_j - \alpha_j)) - K = 0$$

After algebraic manipulations, we get

$$2I_i\eta_i\beta_i\alpha_i - 2I_i\eta_i\beta_i c_i + I_i\eta_i\gamma c_j - I_i\eta_i\gamma\alpha_i - K = 0$$

which leads to

$$A_i c_i^2 + E_i c_i c_j + F_i c_i + G_i c_j + H_i = 0.$$

□

Let  $Q = \epsilon_i(\alpha_i + c_L)$  and  $R = -\epsilon_i\alpha_i c_L - 2\beta_i\lambda_i$ .

**Theorem 2.4.2** *The solution of  $\partial\pi_{i,M_i}(0, 0; c_1, c_2)/\partial v_i = 0$ , is contained in*

$$c_i = (-Q + \sqrt{Q^2 - 4PR})/(-2\epsilon_i). \quad (2.39)$$

**Proof:** Let us compute

$$\frac{d\pi_{i,M_i}}{dv_i} = \frac{\partial\pi_{i,M_i}}{\partial a_i} \frac{\partial a_i}{\partial v_i} + \frac{\partial\pi_{i,M_i}}{\partial v_i}.$$

Since

$$\partial\pi_{i,M_i}(v_i, 0; c_1, c_2)/\partial v_i = (\epsilon_i\lambda_i(\alpha_i - a_i)(c_i - c_L)) / (2\beta_i(\lambda_i + v_i)^2) - 1,$$

$d\pi_{i,M_i}(v_i, 0; c_1, c_2)/dv_i = 0$  if, and only if,

$$\epsilon_i\lambda_i(\alpha_i - a_i)(c_i - c_L) = 2\beta_i(\lambda_i + v_i)^2.$$

Letting  $v_i = 0$  ( $a_i = c_i$ ), we get

$$\epsilon_i\lambda_i(\alpha_i - c_i)(c_i - c_L) = 2\beta_i\lambda_i^2$$

that can be written as

$$-\epsilon_i\lambda_i c_i^2 + \epsilon_i\lambda_i(\alpha_i + c_L)c_i - \epsilon_i\lambda_i\alpha_i c_L - 2\beta_i\lambda_i^2 = 0.$$

Choose the positive solution, we get

$$c_i = (-Q + \sqrt{Q^2 - 4PR})/(-2\epsilon_i).$$

□

We begin by characterizing the boundary of the nil Nash investment region  $N_{LL}$  that is composed by a *right boundary*  $R_{N_{LL}}$  and a *upper boundary*  $U_{N_{LL}}$ . The right boundary of the nil Nash investment region  $N_{LL}$  (see Figure 2.25 (A)) is given by the curve (see Theorem 2.4.1 and Figure 2.26)

$$\frac{\partial \pi_{1,D}}{\partial v_1}(0, 0; c_1, c_2) = 0.$$

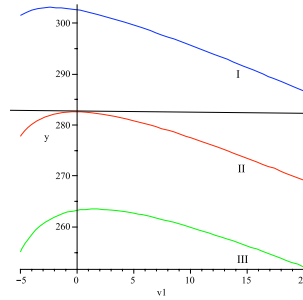


Figure 2.26: Each of the plots corresponds to the profit  $\pi_1$  of Firm  $F_1$  when Firm  $F_2$  decides not to invest, i.e.  $\pi_{1,D}(V_1(0), 0; c_1, c_2)$ . The plot in red (II) corresponds to a pair of production costs  $(c_1, c_2) \in R_{N_{LL}}$ , the plot in blue (I) corresponds to a pair of production costs  $(c_1, c_2)$  that are in the nil Nash investment region  $N_{LL}$  and the plot in green (III) corresponds to a pair of production costs  $(c_1, c_2)$  that are in the single recovery region  $S_1^R$ .

Furthermore, the upper boundary of the region  $N_{LL}$  is given by the curve (see Theorem 2.4.1 and Figure 2.27)

$$\frac{\partial \pi_{2,D}}{\partial v_2}(0, 0; c_1, c_2) = 0$$

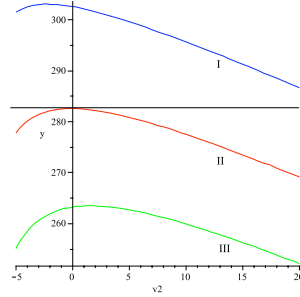


Figure 2.27: Each of the plots corresponds to the profit  $\pi_2$  of Firm  $F_2$  when Firm  $F_1$  decides not to invest, i.e.  $\pi_{2,M_2}(0, V_2(0); c_1, c_2)$ . The plot in red (II) corresponds to a pair of production costs  $(c_1, c_2) \in U_{N_{LL}}$ , the plot in blue (I) corresponds to a pair of production costs  $(c_1, c_2)$  that are in the nil Nash investment region  $N_{LL}$  and the plot in green (III) corresponds to a pair of production costs  $(c_1, c_2)$  that are in the single recovery region  $S_2^R$ .

We will refer to the boundaries of the region  $N_{LH}$  as  $d_1$ ,  $d_2$ ,  $d_3$  and  $d_4$  (see Figure 2.25 (B)). The arc  $d_1$  is given by the curve (see Theorem 2.4.2 and Figure 2.28)

$$\frac{\partial \pi_{1,M_1}}{\partial v_1}(0, 0; c_1, c_2) = 0$$

The arc  $d_2$  is a segment line  $l_{M_1}$  characterized in Lemma 2.2.2. The arc  $d_2$  is described above. The arc  $d_3$  is given by the curve (see Theorem 2.4.1 and Figure 2.29)

$$\frac{\partial \pi_{1,D}}{\partial v_1}(0, 0; c_1, c_2) = 0$$

and the arc  $d_4$  is given by the curve (see Theorem 2.4.1 and Figure 2.30)

$$\frac{\partial \pi_{2,D}}{\partial v_2}(0, 0; c_1, c_2) = 0$$

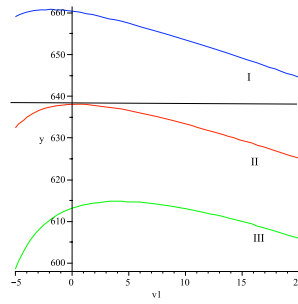


Figure 2.28: Each of the plots corresponds to the profit  $\pi_1$  of Firm  $F_1$  when Firm  $F_2$  decides not to invest, i.e.  $\pi_1(V_1(0), 0; c_1, c_2)$ . The plot in red (II) corresponds to a pair of production costs  $(c_1, c_2) \in d_1$ , the plot in blue (I) corresponds to a pair of production costs  $(c_1, c_2)$  that are in the nil Nash investment region  $N_{LH}$  and the plot in green (III) corresponds to a pair of production costs  $(c_1, c_2)$  that are in the single favorable region  $S_1^F$ .

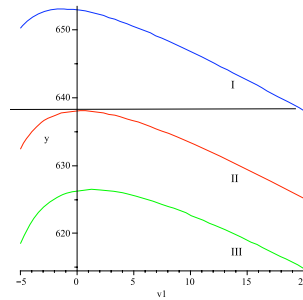


Figure 2.29: Each of the plots corresponds to the profit  $\pi_1$  of Firm  $F_1$  when Firm  $F_2$  decides not to invest, i.e.  $\pi_{1,D}(V_1(0), 0; c_1, c_2)$ . The plot in red (II) corresponds to a pair of production costs  $(c_1, c_2) \in d_3$ , the plot in blue (I) corresponds to a pair of production costs  $(c_1, c_2)$  that are in the nil Nash investment region  $N_{LH}$  and the plot in green (III) corresponds to a pair of production costs  $(c_1, c_2)$  that are in the single favorable region  $S_1^F$ .



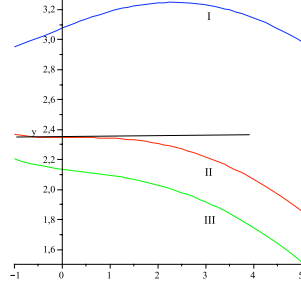


Figure 2.30: Each of the plots corresponds to the profit  $\pi_2$  of Firm  $F_2$  when Firm  $F_1$  decides not to invest, i.e.  $\pi_{2,D}(0, V_2(0); c_1, c_2)$ . The plot in red (II) corresponds to a pair of production costs  $(c_1, c_2) \in d_4$ , the plot in blue (I) corresponds to a pair of production costs  $(c_1, c_2)$  that are in the single recovery region  $S_2^R$  and the plot in green (III) corresponds to a pair of production costs  $(c_1, c_2)$  that are in the nil Nash investment region  $N_{LH}$ .

### 2.4.3 Competitive Nash investment region

The *competitive Nash investment region*  $C$  consists of all production costs  $(c_1, c_2)$  such that there is a Nash investment equilibrium  $(v_1, v_2)$  with the property that  $v_1 > 0$  and  $v_2 > 0$ . Hence, the new production costs  $a_1(v_1)$  and  $a_2(v_2)$  of Firms  $F_1$  and  $F_2$  are smaller than the actual production costs  $c_1$  and  $c_2$  of the Firms  $F_1$  and  $F_2$ , respectively.

In Figure 2.31, the boundary of region  $C$  consists of four piecewise smooth curves: The curve  $C_1$  is characterized by  $a_1(v_1) = c_1$  i.e.  $v_1 = 0$ ; the curve  $C_2$  is characterized by  $a_2(v_2) = c_2$  i.e.  $v_2 = 0$ ; the curve  $C_3$  corresponds to points  $(c_1, c_2)$  such that the new production costs  $(a_1(v_1), a_2(v_2))$  have the property that  $\pi_1(a_1, a_2) = \pi_1(c_1, c_2)$ ; and the curve  $C_4$  corresponds to points  $(c_1, c_2)$  such that the Nash investment equilibrium  $(a_1(v_1), a_2(v_2))$  has the property that  $\pi_1(a_1, a_2) = \pi_1(c_1, a_2)$ . The curve  $C_2$  (respectively  $C_1$ ) is the common boundary between the competitive Nash investment region  $C$  and the single recovery region  $S_2^R$  (respectively  $S_1^R$ ). The boundary  $C_3$  can be decomposed in three parts  $C_3^D$ ,

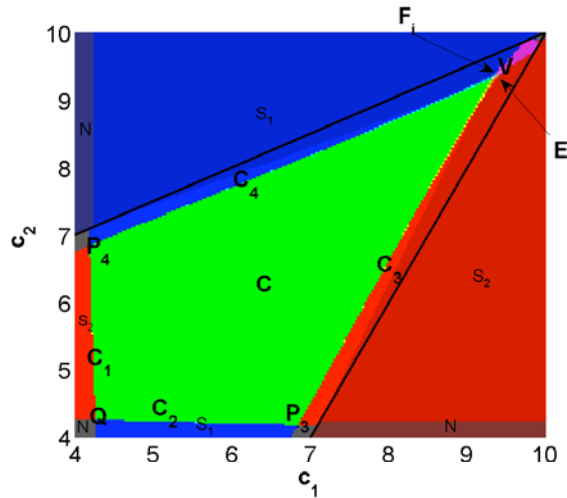


Figure 2.31: Firms' investments in the competitive Nash investment region. The competitive Nash investment region is colored green, the single Nash investment region  $S_1$  (respectively  $S_2$ ) is colored blue (respectively red) and the nil Nash investment region  $N$  is colored grey.

$C_3^B$  and  $C_3^M$ . The boundary  $C_3^D$  consists of all points in  $C_3$  between the points  $P_3$  and  $E_3$  (see Figure 2.31). The boundary  $C_3^D - \{P_3\}$  has the property of being contained in the lower boundary of the single duopoly region  $S_2^D$  of Firm  $F_2$ . The boundary  $C_3^B$  consists of all points in  $C_3$  between the points  $E_3$  and  $F_3$  (see Figure 2.31). The boundary  $C_3^B$  has the property of being contained in the lower boundary of the single monopoly boundary region  $S_2^B$  of Firm  $F_2$ . The boundary  $C_3^M$  consists of all points in  $C_3$  between the points  $F_3$  and  $V$  (see Figure 2.31). The boundary  $C_3^M$  has the property of being contained in the lower boundary of the single monopoly boundary region  $S_2^B$  of Firm  $F_2$ . Due to the symmetry, a similar characterization holds for the boundary  $C_4$ . The points  $P_3$ ,  $P_4$ ,  $Q$  and  $V$  are the corners of the competitive Nash investment region  $C$  (see Figure 2.31). The point  $Q$  is characterized by being in the intersection between the competitive Nash investment region  $C$  and the nil Nash region  $N_{LL}$ . The point  $P_3$  (respe-

ctively  $P_4$ ) is characterized by being in the intersection between the competitive Nash investment region  $C$  and the nil Nash investment region  $N_{HL}$  (respectively  $N_{LH}$ ). The point  $E_3$  in the boundary of the competitive Nash investment region  $C$  is characterized by belonging to the boundaries of the single duopoly region  $S_2^D$  and the single monopoly boundary region  $S_2^B$  (see Figure 2.31). The point  $F_3$  in the boundary of the competitive Nash investment region  $C$  is characterized by belonging to the boundaries of the single monopoly boundary region  $S_2^B$  and the single monopoly region  $S_2^M$  (see Figure 2.31).

## 2.5 FOP-Model regions with multiple Nash equilibria

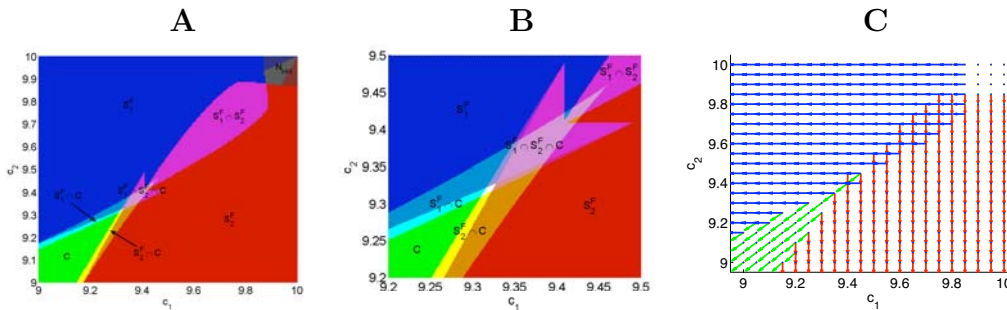


Figure 2.32: (A) Nash investment regions in the high production costs region,  $c_i \in [9, 10]$ , with  $i \neq j$ ; (B) Zoom of (A) in the region where there are three Nash investment equilibria; (C) Dynamics on the production costs in the high production costs region,  $c_i \in [9, 10]$ , with  $i \neq j$ : in blue, the dynamics in the single Nash investment region for Firm  $F_1$ ,  $S_1$  where only Firm  $F_1$  invests; in red the dynamics in the single Nash investment region for Firm  $F_2$ ,  $S_2$  where only Firm  $F_2$  invests; and in green the dynamics in the competitive Nash investment region  $C$  where both Firms invest.

Let us consider the region of high production costs, that can correspond to

the production of new technologies, where there are multiple Nash investment equilibria. Recall that  $S_i^c = R - S_i$  and  $C^c = R - C$ . In this section, we study the production costs that correspond to the existence of multiple Nash investment equilibria. We find a region  $S_1^F \cap S_2^F \cap C$  with a competitive Nash investment equilibrium, a single favorable Nash investment equilibrium to Firm  $F_1$  and a single favorable Nash investment equilibrium to Firm  $F_2$  (see Figure 2.35); a region  $S_1^F \cap S_2^F \cap C^c$  where there are, simultaneously, a single favorable Nash investment equilibrium to Firm  $F_i$  and a single favorable Nash investment equilibrium to Firm  $F_2$  (see Figure 2.33); and a region  $S_i^F \cap C \cap S_j^c$ , with  $i \neq j$ , where there are two Nash investment equilibria, one favorable to Firm  $F_1$  and a competitive one (see Figure 2.34).

This shows the high complexity of the R&D strategies of the Firms, for high values of initial production costs.

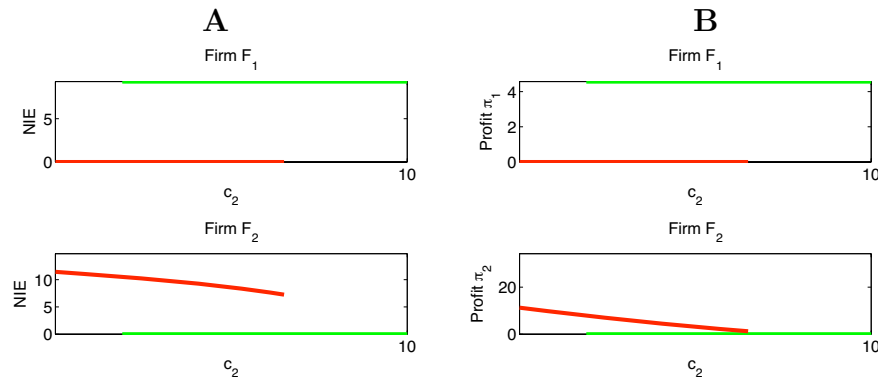


Figure 2.33: We fix the initial production cost of Firm  $F_1$ ,  $c_1 = 9.7$  and plot (A) the Nash investment equilibria (NIE) of Firm  $F_1$  and the Nash investment equilibria of Firm  $F_2$ ; (B) the profit of Firm  $F_1$  and the profit of Firm  $F_2$  where green means that the pair  $(c_1, c_2)$  belongs to the single Nash investment region  $S_1$  and red means that the pair  $(c_1, c_2)$  belongs to the single Nash investment region  $S_2$ .

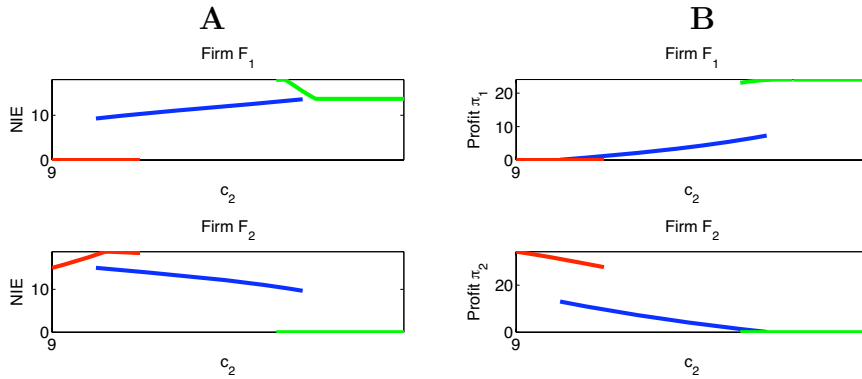


Figure 2.34: We fix the initial production cost of Firm  $F_1$ ,  $c_1 = 9.2$  and plot (A) the Nash investment equilibria (NIE) of Firm  $F_1$  and the Nash investment equilibria of Firm  $F_2$ ; (B) the profit of Firm  $F_1$  and the profit of Firm  $F_2$  where green means that the pair  $(c_1, c_2)$  belongs to the single Nash investment region  $S_1$ , red means that the pair  $(c_1, c_2)$  belongs to the single Nash investment region  $S_2$  and blue means that the pair  $(c_1, c_2)$  belongs to the competitive Nash investment region  $C$ .

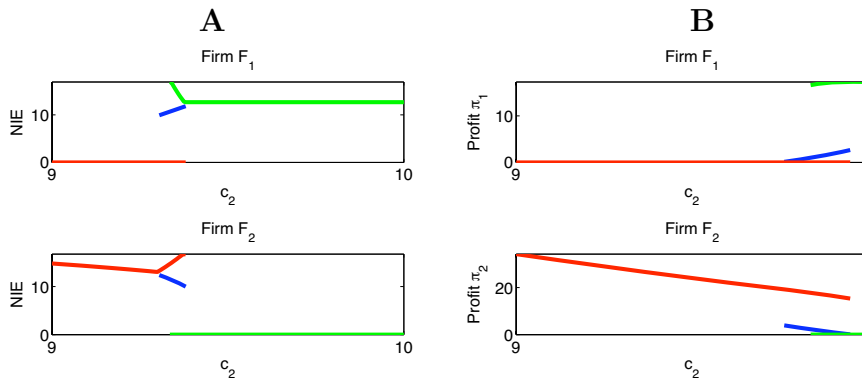


Figure 2.35: We fix the initial production cost of Firm  $F_1$ ,  $c_1 = 9.35$  and plot (A) the Nash investment equilibria (NIE) of Firm  $F_1$  and the Nash investment equilibria of Firm  $F_2$ ; (B) the profit of Firm  $F_1$  and the profit of Firm  $F_2$  where green means that the pair  $(c_1, c_2)$  belongs to the single Nash investment region  $S_1$ , red means that the pair  $(c_1, c_2)$  belongs to the single Nash investment region  $S_2$  and blue means that the pair  $(c_1, c_2)$  belongs to the competitive Nash investment region  $C$ .

## 2.6 FOP-Model R&D deterministic dynamics

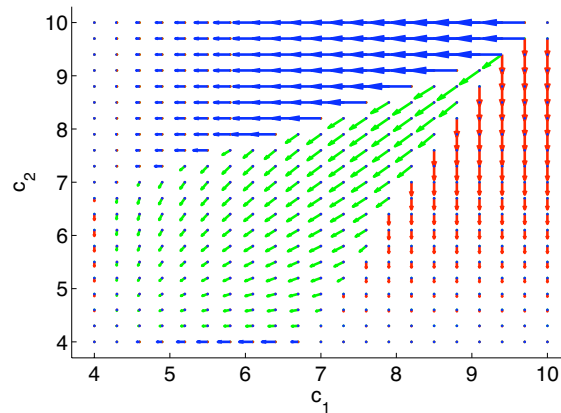


Figure 2.36: Dynamics on the production costs in terms of the initial production costs  $(c_1, c_2)$ : in blue, the dynamics in the single Nash investment region for Firm  $F_1$ ,  $S_1$  where only Firm  $F_1$  invests; in red the dynamics in the single Nash investment region for Firm  $F_2$ ,  $S_2$  where only Firm  $F_2$  invests; and in green the dynamics in the competitive Nash investment region  $C$  where both Firms invest.

The R&D deterministic dynamics on the production costs of the duopoly competition appear from the Firms deciding to play a perfect Nash equilibrium in the Cournot competition with R&D cost reduction investment programs, period after period. The nil Nash investment region is the set of equilibria for these dynamics. It is unusual in dynamical systems to have a non-isolated set of equilibrium points. We notice that we have a single Nash investment region coexisting with a competition Nash investment region, and we have the single Nash investment regions for both Firms coexisting with the competitive Nash investment region. This is due to the complex investment structure that we have to deal in these problems. For simplicity, we will study, separately, the R&D deterministic dynamics in the competitive, in the single and in the nil Nash investment regions,

using the corresponding Nash investment equilibrium.

The R&D deterministic dynamics in the single Nash investment region is implicitly determined by Theorems 2.2.1 and 2.2.2. Let  $S_1 = S_1^F \cup S_1^R$  be the single Nash investment region of Firm  $F_1$ . If  $(c_1, c_2) \in S_1^F$ , then only Firm  $F_1$  invests along the time. Furthermore, at some period of time, the pair of new production costs falls in the monopoly region and so Firm  $F_2$  is driven out of the market by Firm  $F_1$ . The production costs approach, along the time, the region  $N_{LH}$  (see Figure 2.36). Hence, the production costs of Firm  $F_1$  approach low costs of production but the production costs of Firm  $F_2$  are always fixed at high production costs. If  $(c_1, c_2) \in S_1^R$  then only Firm  $F_1$  invests along the time. So, Firm  $F_1$  will recover, along the time, from its disadvantageous position. The production costs approach, along the time, the nil Nash investment region  $N_{LL}$  (see Figure 2.36). Hence Firm  $F_1$  is able to recover, along the time, to the region where both Firms have low production costs.

The R&D deterministic dynamics in the competitive Nash investment region is implicitly determined by Theorems 2.2.1 and 2.2.2. In the competitive Nash investment region both Firms invest, along the time, and the production costs converge to the nil Nash investment region  $N_{LL}$ . Hence, the production costs of both Firms are driven by the *R&D* deterministic dynamics to low production costs.

When the production costs are high (see Section 2.5) we have regions with multiple Nash investment equilibria. In the region  $R_{S_1 \cap S_2}$ , the Firm that decides to invest in the first period can drive the other Firm out of the Market, and its production costs will approach, along the time, low production costs either in the nil Nash investment region  $N_{LH}$  or in the nil Nash investment region  $N_{HL}$ . Hence, the short and long term economical outcome for the Firms can depend

only upon the *R&D* investment decision of both Firms at period one. In Figure 2.37, we observe that for some production cost  $c_2$ , the Firms face two possible dynamics depending on which of the two possible equilibria  $S_1$  or  $S_2$  they decide to choose. In the region  $R_{S_i \cap C}$ , with  $i \neq j$ , if both Firms decide to implement their *R&D* cost reduction investment programs according to the Nash investment strategy in the competitive Nash investment region  $C$ , both Firms will stay in the market, along the time, and their production costs will approach low production costs. However, if one of the Firms decides not to invest in period one, this Firm can be driven out of the Market and the production costs of the other Firm will approach, along the time, low production costs. In Figure 2.38, we observe that for some production cost  $c_2$ , the Firms face two possible dynamics depending on which of the two possible equilibria  $S_1$  or  $C$  decide to choose. Finally, in Figure 2.39 we see that for some production cost  $c_2$ , the Firms face three possible dynamics depending on which of the three possible equilibria  $S_1$  or  $C$  or  $S_2$  decide to choose.



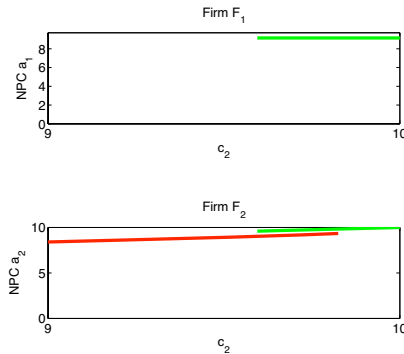


Figure 2.37: Plot of the New production cost (NPC) of Firm  $F_1$  and the New production cost of Firm  $F_2$  with the initial production cost of Firm  $F_1$   $c_1 = 9.7$  fixed where green means that the pair  $(c_1, c_2)$  belongs to the single Nash investment region  $S_1$  and red means that the pair  $(c_1, c_2)$  belongs to the single Nash investment region  $S_2$ .

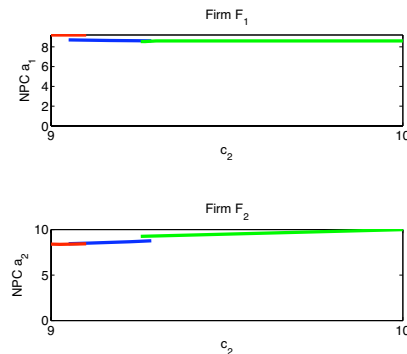


Figure 2.38: Plot of the New production cost (NPC) of Firm  $F_1$  and the New production cost of Firm  $F_2$  with the initial production cost of Firm  $F_1$   $c_1 = 9.2$  fixed where green means that the pair  $(c_1, c_2)$  belongs to the single Nash investment region  $S_1$ , red means that the pair  $(c_1, c_2)$  belongs to the single Nash investment region  $S_2$  and blue means that the pair  $(c_1, c_2)$  belongs to the competitive Nash investment region  $C$ .

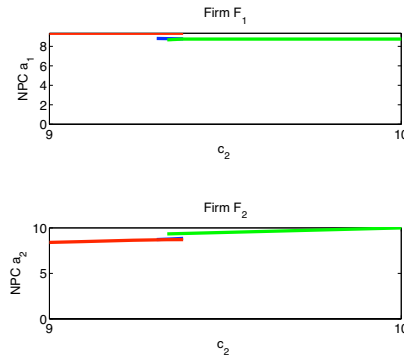


Figure 2.39: Plot of the New production cost (NPC) of Firm  $F_1$  and the New production cost of Firm  $F_2$  with the initial production cost of Firm  $F_1$   $c_1 = 9.35$  fixed where green means that the pair  $(c_1, c_2)$  belongs to the single Nash investment region  $S_1$ , red means that the pair  $(c_1, c_2)$  belongs to the single Nash investment region  $S_2$  and blue means that the pair  $(c_1, c_2)$  belongs to the competitive Nash investment region  $C$ .

## 2.7 Conclusions

In this Chapter, we presented R&D deterministic dynamics on the production costs of Cournot competitions, based on perfect Nash equilibria of R&D investment strategies of the Firms at every period. The following conclusions are valid in some parameter region of our model. We introduced a new R&D investment function inspired by the logistic equation and found all Perfect Nash investment equilibria of the Cournot competition model with R&D cost reduction investment programs.

We described four main economic regions corresponding to distinct perfect Nash equilibria: a competitive Nash investment region  $C$  where both Firms invest, a single Nash investment region for Firm  $F_1$ ,  $S_1$ , where only Firm  $F_1$  invests, a single Nash investment region for Firm  $F_2$ ,  $S_2$ , where only Firm  $F_2$  invests, and

a nil Nash investment region  $N$  where neither of the Firms invest. For the FOP-Model these four Nash investment regions appear whereas for the AJ-Model we only find three different Nash investment equilibria regions: a competitive Nash investment region  $C$ , a single Nash investment region  $S_1$  for Firm  $F_1$  and a single Nash investment region  $S_2$  for Firm  $F_2$ . The non existence of nil Nash investment region  $N$  has to do with the shape of d'Aspremont and Jacquemin's R&D cost reduction investment function that reflects an higher incentive to invest. For the FOP-Model, the nil Nash investment region has four subregions:  $N_{LL}$ ,  $N_{LH}$ ,  $N_{HL}$  and  $N_{HH}$ . The single Nash investment region can be divided into four subregions: the single favorable region for Firm  $F_1$ ,  $S_1^F$ , the single recovery region for Firm  $F_1$ ,  $S_1^R$ , the single favorable region for Firm  $F_2$ ,  $S_2^F$ , the single recovery region for Firm  $F_2$ ,  $S_2^R$ . The single favorable region  $S_1^F$  (due to the symmetry the same characterization holds for  $S_2^F$ ) is the union of three disjoint regions: the single duopoly region  $S_1^D$  where the production costs, after the investments, belong to the duopoly region  $D$ ; the single monopoly boundary region  $S_1^B$  where the production costs, after the investments, belong to the boundary of the monopoly region  $l_{M_1}$ ; and the single monopoly region  $S_1^M$  where the production costs, after the investments, belong to the monopoly region  $M_1$ .

We showed the existence of regions where the Nash investment equilibria are not unique: the intersection  $R_{S_1 \cap S_2}$  between the single Nash investment region  $S_1$  and the single Nash investment region  $S_2$  is non empty; the intersection  $R_{S_i \cap C}$ , with between the single Nash investment region  $S_i$  and the competitive Nash investment region  $C$  is non empty; the intersection  $R_{S_1 \cap C \cap S_2}$  between the single Nash investment region  $S_1$ , the single Nash investment region  $S_2$  and the competitive Nash investment region  $C$  is non empty.

In Section 2.6, we presented, for the FOP-Model, the R&D deterministic dy-

namics on the production costs of Cournot competitions, based on R&D investment strategies of the Firms and we illustrated the transients and the asymptotic limits of the R&D deterministic dynamics on the production costs. We introduced the implicit equations (see Theorems 2.2.1 and 2.2.2) determining the R&D deterministic dynamics that are distinct in the competitive Nash investment region  $C$  and in the single Nash investment regions  $S_1$  and  $S_2$ . The nil Nash investment region  $N$  determines the set of all production costs that are fixed by the dynamics and thus is the set of equilibria for the R&D deterministic dynamics. The nil Nash investment regions  $N_{LL}$ ,  $N_{HL}$  and  $N_{LH}$  will appear as the asymptotic production costs for both Firms depending upon their R&D investment strategies. The single Nash investment region  $S_i$  determines the set of production costs where the production cost of Firm  $F_j$  is constant, along the time, and only the production cost of Firm  $F_i$  evolves. We saw that if  $(c_1, c_2)$  belongs to the single favorable Nash investment region  $S_1^F$  (respectively  $S_2^F$ ), then only Firm  $F_1$  (respectively Firm  $F_2$ ) invests along the time. The production costs approach, along the time, the region  $N_{LH}$  (respectively  $N_{HL}$ ). On the other hand, we observed that if  $(c_1, c_2)$  belongs to the single recovery Nash investment region  $S_1^R$  (respectively  $S_2^R$ ) then only Firm  $F_1$  (respectively Firm  $F_2$ ) invests along the time. Hence, Firm  $F_i$  is able to recover, along the time, from its disadvantageous position approaching the region where both Firms have low production costs  $N_{LL}$ . The R&D deterministic dynamics in the competitive Nash investment region  $C$  lead both Firms, along the time, to approach the nil Nash investment region  $N_{LL}$  corresponding to a case where both Firms have low production costs.

Interestingly, for high initial production costs, that can correspond to the production of new technologies, the single favorable regions of both Firms and the competitive Nash investment region have non-empty intersection. Hence,

in this region, depending upon the Nash investment strategy chosen from the three possible Nash investment equilibria, the time evolution of the production costs will approach three distinct economic equilibria regions called  $N_{LL}$ ,  $N_{LH}$  and  $N_{HL}$ . Hence, our analysis showed that in the case of production of new technologies, corresponding to high initial production costs, the R&D investment strategies chosen by both Firms are essential for their maintenance in the market. This also shows that the market can be driven, in a short period of time to a monopoly situation.

# Chapter 3

## Edgeworthian Economies

### Models

#### 3.1 Introduction

The work presented in this Chapter is joint work with B.F. Finkenstädt, B. Oliveira, A.A. Pinto and A.N. Yannacopoulos and most of it is contained in the research article [27], in the conference proceedings [24], [25], [26], [33] and [56] and in the book chapter [28].

In most economies three basic activities occur: production, exchange and consumption. We analyze the case of a pure exchange economy where individuals trade their goods in the market place for mutual advantage. We present models of an Edgeworthian exchange economy where two goods are traded in a market place.

In Section 3.3 we show that for a specific class of random matching Edgeworthian economies, the expectation of the limiting equilibrium price coincides with

that of related Walrasian economies.

In Sections 3.7 and 3.8 two new modifications to the model are introduced. In both these models, participants do not necessarily trade according to their bilateral Walras equilibrium price. We associate to each participant either a low or high bargaining skill factor bringing up a game alike the “prisoner’s dilemma”. The exact location in the core where the trade takes place is decided by both participants’ bargaining skills. If a more skilled participant meets a less skilled participant, trade occurs with an advantage to the more skilled bargainer (see Section 3.7). However, if both participants are too skilled, they are penalized by not being allowed to trade. If the pair randomly chosen to trade is formed by two low skilled bargainers, they will trade according to the usual bilateral Walras equilibrium price.

We analyze the effect of the participants’s bargaining skills in the variation of their utilities. Finally, in Section 3.8, we let the bargaining skills of the participants evolve, along the trades, according to two predefined rules and analyse how these bargaining skills evolve depending on these rules.

## 3.2 The Edgeworth model and some necessary results

We consider agents with preferences  $\succ_i$  that can be described by Cobb-Douglas type utility functions  $U_i(x_i, y_i) = x_i^{\alpha_i} y_i^{1-\alpha_i}$ .

Assume the following model for an exchange economy with 2 durable goods. Out of an initial collection of agents we pick  $N$  agents, through a sampling scheme with or without replacement.

The Cobb-Douglas utility function is a model which is so well rooted in eco-

conomic theory that its use hardly needs to be justified. As stated in the excellent review paper of Lloyd [45] the Cobb-Douglas function has been around for ages, even well before its formal statement by Cobb and Douglas, and its roots are inherent in the works of Mill, Pareto, Wicksell, Von Thünen, etc, and for various reasons serves as the standard test bed for a great number of studies in mathematical economics. One of these reasons is its mathematical simplicity, which however, captures important theoretical issues such as constant maximal rate of substitution etc. However, this is not the sole reason for its generalized use. Recent results of Voorneveld [80] show that the utility function being of the Cobb-Douglas form is equivalent to the preferences of the agents having the property of strict monotonicity, homotheticity in each coordinate and upper semicontinuity. These properties are rather generic properties for the preferences, which can be seen as very reasonable modelling assumptions. Furthermore, there is empirical evidence [62], according to which with very large and increasing per capita income the utility function becomes asymptotically indistinguishable from Cobb-Douglas. These very interesting results shed new light on the Cobb-Douglas utility function and provides further justification for its use as a standard model, apart from its apparent analytical simplicity.

Then these agents, at subsequent time instants, meet randomly in pairs and exchange goods so that their utility levels are maximized. When the pair  $(i, j)$  meets, they trade at the *bilateral equilibrium price*  $p$  which is given by

$$p = \frac{\alpha_i y_i + \alpha_j y_j}{(1 - \alpha_i) x_i + (1 - \alpha_j) x_j} \quad (3.1)$$

and their demands in the two goods  $(x_i, y_i)$  and  $(x_j, y_j)$  are such that the utilities of the agents are maximized under the constraints available as if only these two agents were participating in the market. The bilateral equilibrium price,



determines the unique point in the core such that the market “locally” clears. In some sense, the agents behave in a myopic way, interacting only in pairs, and not foreseeing the future interactions or keeping memory of their past encounters.

The randomness of the encounters introduces some randomness into this market. The agents start with a set of initial endowments  $(x_i(0), y_i(0))$ , then they trade in random pairs and after the  $t$  trade they end up with a consumption bundle  $(x_i(t), y_i(t))$  which are traded in the bilateral equilibrium price  $p(t)$ , given by the formula (3.1) with  $x_i, x_j, y_i, y_j$  substituted by  $x_i(t-1), x_j(t-1), y_i(t-1), y_j(t-1)$ . On each trade only two randomly chosen agents  $i, j$  exchange goods, and the consumption bundles of all the other agents  $k \neq i, j$  remain unchanged, i.e.  $(x_k(t-1), y_k(t-1)) = (x_k(t), y_k(t))$ . On account of the random pairing of the agents, the demand of the agents on the two goods is a stochastic process, and that turns the price  $p(t)$  into a stochastic process as well.

An interesting question that arises in this context is the following:

Does there exist a limiting price  $p_\infty = \lim_{t \rightarrow \infty} p(t)$  and if so how would that compare to the Walrasian equilibrium price, where all agents meet at once and trade in one go?

An answer to the first question has been given by a number of authors, see for example [36] and references therein. According to this bibliography,  $p_\infty$  exists almost surely, and it is a random variable. However, it depends on the actual game of the play, that is the exact order of the random pairing of the agents.

The aim of the present work is to provide some results on the expectation of this random variable  $p_\infty$ , and how this compares to the Walrasian price. In particular, under some rather general symmetry conditions on the initial endowments of the agents and distribution of initial preferences, we show that the

expectation of the logarithm of  $p_\infty$  equals the logarithm of the Walrasian price for the same initial endowments of the agents. This is an interesting result, in the sense that even though the agents meet and trade myopically in random pairs, they somehow “self-organize” and the expected limiting price equals that of a market where a central planner announces prices and all the agents conform to them through utility maximization, as happens in the Walrasian model.

The main reason why organizing behavior is observed is the symmetry in the endowments and preferences of the agents that, as will become clear from our analysis in the next section, poses global constraints in the market, in the sense that it enforces each agents to have a *mirror*, or a *dual agent*.

### 3.3 The main result

We introduce the concept of *duality* in the market.

We assume that the collection of agents is completely characterized by their preferences  $\alpha$ , and their endowments  $(x, y)$  in the 2 goods. We may define a probability distribution function on  $(\alpha, x, y)$  space,  $f(\alpha, x, y)$  which provides the probability that a chosen agent has preferences in  $(\alpha, \alpha + d\alpha) \times (x, x + dx) \times (y, y + dy)$ . We assume that the probability distribution has compact support, and the support in  $(x, y)$  is bounded away from zero.

**Definition 3.3.1** *We say that a market satisfies the **p** - statistical duality condition if the probability function has the symmetry property*

$$f(\alpha, x, y) = f\left(1 - \alpha, \frac{y}{p}, px\right)$$

where  $p \in \mathbb{R}$ .

The p-statistical duality property means that each agent with characteristics  $(\alpha, x, y)$  has a mirror agent with characteristics  $(1 - \alpha, y/p, px)$  with the same probability under  $f$ . The class of probability functions  $f(\alpha, x, y)$  of the form  $f_1(\alpha)f_2(x, y)$  with the property that  $f_1(\alpha) = f_1(1 - \alpha)$  and  $f_2(x, y) = f_2(y/p, px)$  satisfies the p-statistical duality. A common probability function  $f_2$ , satisfying the above condition, is the uniform distribution. Another common example of a probability function satisfying the p-statistical duality is used in Corollary 3.3.1, below, and determines the most well known matching technology used in random matching games with  $N$  agents.

Statistical duality guarantees that the prices observed in the random matching Edgeworthian economy coincide in expectation with those of the Walrasian economy. For each collection of agents, let  $p_w$  denote the Walrasian equilibrium price of the market.

**Theorem 3.3.1** *Assume a market consisting of a finite number  $N$  of agents, such that p-statistical duality holds for the initial endowments, then*

$$\mathbb{E}[\ln(p(t))] = \bar{\mathbb{E}}[\ln(p_w)] = \ln(p), \text{ for all } t \in \{1, 2, \dots, +\infty\}.$$

*Furthermore,*

$$\mathbb{E}[\ln(p_\infty)] = \ln(p)$$

*where  $\bar{\mathbb{E}}$  is the expectation over the distribution of agents and  $\mathbb{E}$  is expectation over the distribution of agents and over all possible runs of the game.*

In Theorem 3.3.1, the advantage of using the logarithm of the price is that if we consider the other good to be the numeraire, the absolute value of the logarithm

of the price keeps the same and just the sign of the value of the logarithm of the price changes.

A relevant and well known example of an economy with the p-statistical duality property is an economy where with probability 1 we start with a sample of  $N = 2M$  agents where  $M$  agents have characteristics  $(a_i, x_i, y_i), i = 1, \dots, M$ , and the remaining  $M$  agents have characteristics  $(a_{i+M}, x_{i+M}, y_{i+M}) = (1 - a_i, y_i/p, p x_i), i = 1, \dots, M$ . In other words, in this economy, each agent has a dual agent, i.e. agent  $i$  is dual to agent  $i + M$  where  $i = 1, \dots, M$ . This corresponds to choosing  $f$  to consist of  $2M$  Dirac masses and choosing  $N$  agents out an initial collection of  $N$ .

**Corollary 3.3.1** *Assume a market consisting of a finite number  $N = 2M$  of agents, such that  $M$  agents have characteristics  $(a_i, x_i, y_i), i = 1, \dots, M$ , and the remaining  $M$  agents have characteristics  $(a_{i+M}, x_{i+M}, y_{i+M}) = (1 - a_i, y_i/p, p x_i), i = 1, \dots, M$ , then*

$$\mathbb{E}[\ln(p(t))] = \ln(p_w) = \ln(p), \text{ for all } t \in \{1, 2, \dots, +\infty\}.$$

*Furthermore,*

$$\mathbb{E}[\ln(p_\infty)] = \ln(p)$$

*where  $\mathbb{E}$  is the expectation over all possible runs of the game.*

*Proof:* The distribution function  $f$  consists of  $2M$  Dirac masses and satisfies the p-statistical duality because every agent has a dual.

□

The theorem can also be shown to hold for a generalized random matching economy in which agents do not only meet in pairs. In this game, we initially pick  $N$  agents and then for each trading date we pick randomly  $M \leq N$  agents, that decide to trade on the competitive price for the local market consisting only of these  $M$  agents. The number  $M$ , may change with  $t$ . Then, under our statistical duality condition, it may be shown that the stated result holds.

### 3.4 Beyond the p-statistical duality

We consider an example of an economy where with probability 1 we start with a sample of  $N = 2M$  agents where  $M$  agents are of type  $A$  with characteristics  $(\alpha_A, x_A, y_A)$ , and the remaining  $M$  agents are of type  $B$  and have characteristics  $(\alpha_B, x_B, y_B)$ . For simplicity, we consider that the initial endowments of the two goods are  $x_i = y_i = 1/N$  for all agents. In other words, in this economy, each agent has a dual agent, i.e. agents of type  $A$  are dual to agent of type  $B$ . This corresponds to choosing  $f$ , in definition 3.3.1, to consist of  $2M$  Dirac masses and choosing the agents out an initial collection of  $N$ . Hence, letting  $p_w^{A,B}$  be the Walrasian equilibrium price of the market, we observe that the expected value  $\bar{\mathbb{E}}[\ln(p_\infty^{A,B})]$  over the distribution of agents is equal to  $\ln(p_\infty^{A,B})$ . Let  $p_\infty^{A,B} = \lim_{t \rightarrow \infty} p(t)$  be the limiting price, for a given run of the game, where  $p(t)$  is the bilateral equilibrium price at trade  $t$ . Our object of study is the value  $d_{\alpha_A, \alpha_B} = \mathbb{E}[\ln(p_\infty^{A,B})] - \ln(p_w^{A,B})$  where  $\mathbb{E}[\ln(p_\infty^{A,B})]$  is the expectation over all runs of the game.

In Figure 3.1, we consider the simple case where  $d_\alpha = d_{\alpha-0.25, \alpha+0.25}$  and  $\alpha \in ]0, 1[$ . The p-statistical duality holds for  $\alpha = 0.5$  giving  $d_{0.5} = 0$ . We observe that when we deviate  $\alpha$  from 0.5, breaking the p-statistical duality, the value of  $d_\alpha$  varies continuously with  $\alpha$ . Furthermore, for values of  $\alpha$  close to 0.5,  $d_\alpha$  looks

as a contact with order greater than one to the horizontal line at 0. Hence, these numerical results give evidence that Theorem 3.3.1 is robust in the sense that  $d_{\alpha_A, \alpha_B}$  is small for small deviations from the p-statistical duality.

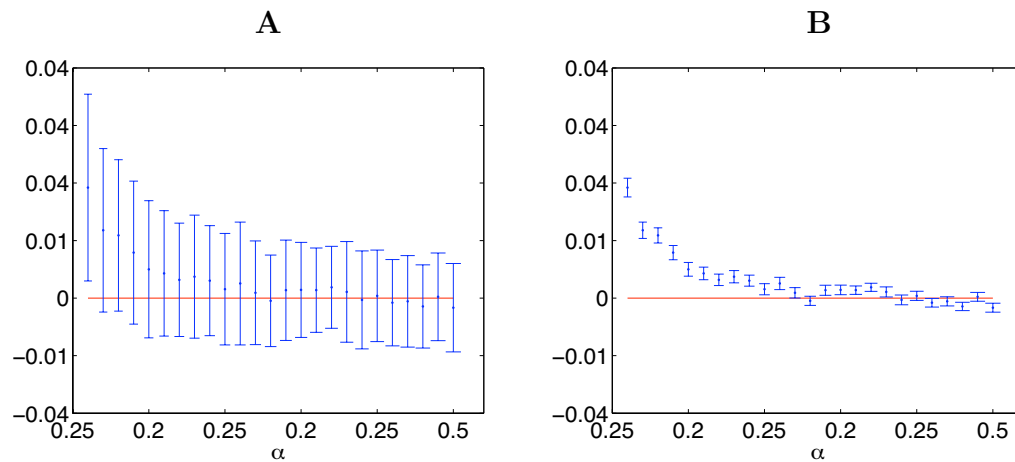


Figure 3.1: The horizontal line, in red, corresponds to  $d = 0$ . **(A)** The error bar is, as usual, centered in the mean and the upper (resp. lower) limit is the mean plus (resp. minus) the standard deviation; **(B)** The error bar is centered in the mean and the upper (resp. lower) limit is the mean plus (resp. minus) the standard deviation over the square root of the number of runs (100).

## 3.5 Proof of Theorem 3.3.1

The proof uses the following lemma which follows from Proposition 3, Chapter 1 of [36].

**Lemma 3.5.1** *There exists a random variable  $p_\infty(\omega)$  such that*

$$\lim_{t \rightarrow \infty} p(t, \omega) = p_\infty(\omega), \quad a.s. \quad (3.2)$$

where by  $\omega$  we denote a particular realization of the game, that is an initial choice of  $N$  agents and the subsequent random pair matchings.

To facilitate the presentation of the proof of Theorem 3.3.1 we need the following notation.

We will identify an agent  $A_i$  at time  $t$ , hereafter denoted by  $A_i(t)$ , with the triple  $(\alpha_i, x_i(t), y_i(t))$  consisting of her preference and her consumption bundle at time  $t$ .

We say that agent  $A_i$  at time  $t$ , which we will hereafter denote by  $A_i(t)$  is *dual* to agent  $A_j(t)$  at time  $t$ , if  $\alpha_j = 1 - \alpha_i$  and  $(x_i(t), y_i(t)) = (y_j(t)/p, p x_j(t))$ . We denote that by  $\bar{A}_i(t) = A_j(t)$ .

The initial choice of agents is a random event which will be denoted by  $\omega_A$ . We can define the random variable  $\mathcal{A}(\omega_A) = \{A_1, A_2, \dots, A_N\}$  which is the initial choice of agents that will participate in the market.

Having initially chosen the group of agents  $\mathcal{A} = \{A_1, \dots, A_N\}$ , denote by  $\omega_r$  the infinite sequence of pairs  $\omega_r = (\omega_r(1), \omega_r(2), \dots)$  where  $\omega_r(t)$  is the pair  $(i(t), j(t))$ ,  $i(t) \neq j(t)$ , corresponding to the pair of agents  $(A_{i(t)}, A_{j(t)})$  that have been randomly chosen to trade at time  $t$ .

A full run of the game is the sequence  $\omega_A \omega_r$  that is an initial choice of agents and an infinite sequence of random matchings. A finite time run of the game is the sequence  $\omega_A \omega_r |_t$  where  $\omega_r |_t$  is the restriction of  $\omega_r$  for the first  $t$  random matchings.

**Proof of Theorem 3.3.1:** Suppose that we have two initial sets of agents  $\mathcal{A} = \{A_1, A_2, \dots, A_N\}$  and  $\mathcal{B} = \{B_1, \dots, B_N\}$ , such that every agent  $B_i = \bar{A}_i$  is the dual agent of  $A_i$ . Choose a run of the play  $\omega_r$ . After each trade  $t + 1$ , the consumption bundles of the agents  $(i, j)$  that have exchanged will be given by

the following formulae

$$\begin{aligned} x_i(t+1) &= \alpha_i \left( \frac{y_i(t)}{p_{ij}(t)} + x_i(t) \right) \\ y_i(t+1) &= (1 - \alpha_i) (p_{ij}(t) x_i(t) + y_i(t)) \end{aligned} \quad (3.3)$$

and similarly for  $j$  where

$$p_{ij}(t) = \frac{\alpha_i y_i(t) + \alpha_j y_j(t)}{(1 - \alpha_i) x_i(t) + (1 - \alpha_j) x_j(t)}.$$

We observe from (3.3) that, if  $\omega(t) = (i(t), j(t))$  and  $(\bar{A}_{i(t-1)}(t-1), \bar{A}_{j(t-1)}(t-1)) = (B_{i(t-1)}(t-1), B_{j(t-1)}(t-1))$  then

$$(\bar{A}_{i(t)}(t), \bar{A}_{j(t)}(t)) = (B_{i(t)}(t), B_{j(t)}(t)). \quad (3.4)$$

That means that the random dynamical system defined by equations (3.3) is equivariant under the duality transformation.

By statistical duality, for each run of the economy  $\omega := \omega_{\mathcal{A}}\omega_r$  we have a dual run  $\bar{\omega} := \omega_{\bar{\mathcal{A}}}\omega_r$  with the same probability  $P(\omega_{\mathcal{A}}\omega_r |_t) = P(\omega_{\bar{\mathcal{A}}}\omega_r |_t)$ . Therefore, by (3.4), the statistical duality is invariant over time. Again, by (3.4), we obtain that

$$\ln(p(\omega_{\mathcal{A}}\omega_r |_t)) + \ln(p(\omega_{\bar{\mathcal{A}}}\omega_r |_t)) = 2 \ln(p) \quad (3.5)$$

which implies, by statistical duality, that  $\mathbb{E}[\ln(p(t, \omega))] = \ln(p)$ , for all  $t \in \mathbb{N}$ . Observe that equation (3.5) reflects the invariance of the maximal rate of substitution for dual pairings.

Consider now the Walrasian price  $p_W$  for the initial choice of agents  $\mathcal{A}$ . In this case, we assume that all agents trade simultaneously in one time step. The



Walrasian price is given by the formula

$$p_W = \frac{\sum_{i=1}^N \alpha_i y_i}{\sum_{i=1}^N (1 - \alpha_i) x_i}.$$

Taking logarithms in this formula and averaging over all possible choices of the initial agents, we obtain that statistical duality implies that  $\bar{\mathbb{E}}[\ln(p_W)] = \ln(p)$ .

Let us now consider the case where  $t = \infty$ . There exists a constant  $K \geq 0$  such that for all  $t$ , we have that  $|\ln(p(t, \omega))| \leq K$  almost surely. The boundedness of the price follows from the assumption that all the distribution of endowments for the agents has compact support which is bounded away from 0 for all  $t$ . Then by a direct application of Lebesgue's dominated convergence theorem we have that

$$\mathbb{E} \left[ \lim_{t \rightarrow \infty} \ln(p(t, \omega)) \right] = \lim_{t \rightarrow \infty} \mathbb{E} [\ln(p(t, \omega))] = \mathbb{E} [\ln(p_\infty(\omega))]$$

from which follows that

$$\mathbb{E} [\ln(p_\infty(\omega))] = \bar{\mathbb{E}} [\ln(p_W)] = \ln(p)$$

This concludes the proof of the theorem.  $\square$

### 3.6 An extension to Arrow-Debreu economies

The results presented may have an interesting extension to the study of economies in the presence of uncertainty, within the framework of the Arrow-Debreu model.

Consider a economy with uncertainty, in which two states of the world are possible. Only one of these states may occur in each time instance, with probability  $(\alpha, 1 - \alpha)$ , respectively. In this model we consider good 1 and good 2 as

consumption levels of a single consumption good at each state of the world. We allow each agent to have her own personalized view concerning probability the occurrence of future states of the world.

Consider that agents, make their decisions according to an expected utility function of the logarithmic form,

$$E[\ln(C)] = \alpha \ln(x) + (1 - \alpha) \ln(y)$$

where  $C = (x, y)$  is now the random variable that describes consumption at different states of the world.

Notice, the formal similarity of the above model with that of the logarithm of the Cobb-Douglas function with two physical goods. Within the context of the present Arrow-Debreu type model, the preferences  $\alpha$  of the agents have to be interpreted as personalized views concerning the probability of occurrence of the different states of the world, whereas the two goods have to be interpreted as consumption levels of the same physical good, in different states of the world. The concept of statistical duality makes sense here, if interpreted as follows: For every agent having a certain idea about the probability of occurrence of the future states of the world, there is a mirror agent, having the opposite ideas about them, as well as a “reflected” and properly dilated initial endowment, providing her the ability to consume in different states of the world. This spread in ideas about states of the world, reflects in some way the absence of information in the economy. Therefore, this model may be a good model for markets in which there is no clear idea concerning the future states of the world that are about to emerge. As such it may provide a good model for markets where there is not enough data on which a detailed study that will allow us to predict the probability of future states can be based. Theorem 3.3.1 is directly applicable for this model. The

consequences of the theorem are interesting. For instance, one may conclude that in this model, the effect of the symmetry is to make the market converge to some Walrasian equilibrium, out of which an “average” Arrow-Debreu measure may be extracted, which depends on the statistics of the views of each agent, concerning the states of the world, as well as on the initial endowments. Therefore, the model may allow some understanding of the dynamics, of how beliefs survive and propagate through the market, and may serve as a paradigm for evolutionary finance.

### 3.7 Trade deviating from the bilateral Walras equilibrium

The model with *trade deviating from bilateral equilibrium* is similar to the Edgeworth model. The difference is that, in this model, we introduce a new parameter  $g_i \in \{0, 1\}$  representing the bargaining skill of each participant. If two less skilled  $g_i = g_j = 0$  participants meet they will trade in the point of the core determined by their bilateral Walras equilibrium price, as in the Edgeworth model. However, if a more skilled participant  $g_i = 1$  meets a less skilled  $g_j = 0$  participant, they will trade in a point of the core between the point determined by their bilateral Walras equilibrium price and the interception of the core with the indifference curve of the less skilled participant, as can be seen in Figure 3.2 traducing an advantage to the more skilled participant. Finally, if both participants are highly skilled  $g_i = g_j = 1$  they are penalized by not being able to trade. This is similar to the “prisoner’s dilemma”, where two non cooperative players are penalized, a non cooperative player has a better payoff than a cooperative player, and two cooperative players have a better payoff than when they meet a non cooperative

player but still worse than the payoff of the non cooperative player.

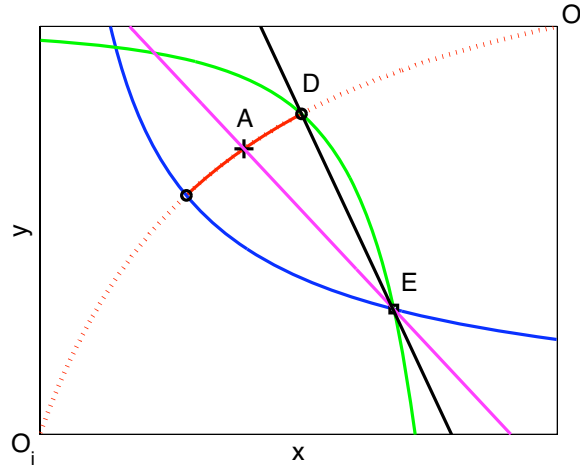


Figure 3.2: Edgeworth Box with the indifference curves for the more skilled participant  $i$  (blue curve) and for the less skilled participant  $j$  (green curve). The red curve is the core and the red dots represent the contract curve. The slope of the pink segment line is the bilateral Walras equilibrium price. The slope of the black segment line is a price that gives advantage to the more skilled participant. The interception point  $D$  of the black line with the core indicates the final allocations from the trade deviating from the bilateral Walras equilibrium. The point  $E$  indicates the initial endowments.

We study the effect of the bargaining skills in the increase of the value of the utility of the participants. Let the variation of the utility function of a participant  $u_f - u_0$  be the difference between the limit value of the utility function and the initial value of the utility function. We present, in Figure 3.3, two cumulative distribution functions of the variation of the utility functions one corresponding to the less skilled participants (black) and the other corresponding to the more skilled participants (red). This function indicates the proportion of participants that have variations of the utility function less than or equal to its argument. In Figure 3.3 (A) there are 20% of highly skilled participants. We observe that

the median of the variation of the utility function is higher for the more skilled participants. On the other hand, in Figure 3.3 (B) there are 80% of highly skilled participants, and we observe that the median of the variation of the utility function is lower for the more skilled participants. We notice that the strategy followed the minority is the one that provides a higher median variation in the utility function.

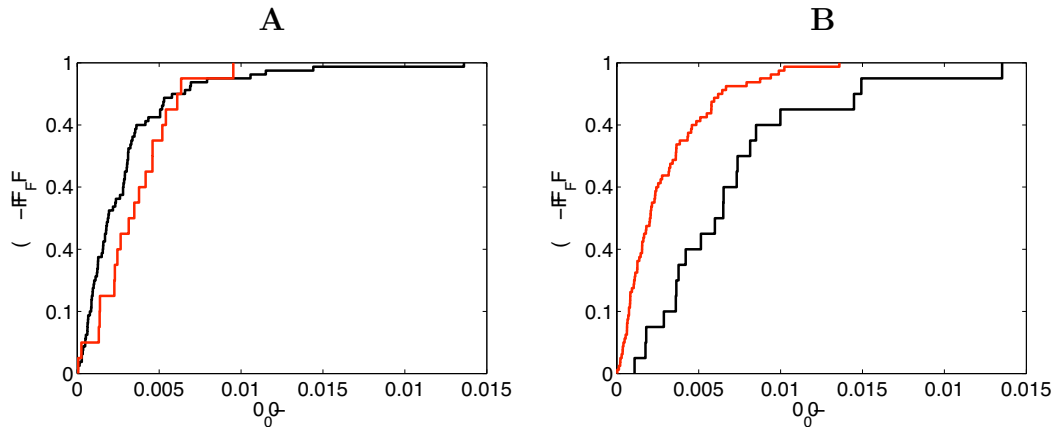


Figure 3.3: Cumulative distribution function of the variation of the utility function (defined as  $u_f - u_0$ ) for the less skilled participants (black) and for the more skilled participants (red). (A) Simulation with 20% of highly skilled participants and 80% of less skilled participants; (B) Simulation with 80% of highly skilled participants and 20% of less skilled participants.

### 3.8 Evolution of the bargaining skills

In this Section, at each iteration, a random pair of participants  $(i, j)$  is chosen with trade occurring deviating from the bilateral Walras equilibrium price (as in the previous Section). In this Section we consider that the bargaining skill  $g$  is a continuous variable, where higher values mean better bargaining skills. Without loss of generality we can consider that  $g_i \geq g_j$ . We impose that trade

only occurs if  $g_i + g_j \leq 1$  and  $g_i - g_j \in [0, 1]$ . The pair trades to the point in the core determined by the price  $p_g = \eta p + (1 - \eta)m_j$  where  $p$  is the bilateral Walras equilibrium price,  $\eta = g_i - g_j$  and  $m_j$  is the maximum price at which the participant  $j$  accepts to trade determined by the interception of the core with the indifference curve of participant  $j$ . After the trade we allow evolution on the bargaining skills of the participants according to two distinct rules: a) the bargaining skills of the participants increase if they were not able to trade and decreases if they were able to trade; b) the bargaining skills of the participants decreases if they were not able to trade and increases otherwise. In case a) if the sum of their bargaining skills is above a cut point, the participants are not allowed to trade and both participants bargaining skills are increased. Otherwise, if the sum of their bargaining skills is below the cut point, the participants will be allowed to trade with advantage to the more skilled participant. After the trade, the bargaining skills of both participants decrease. In this case we observe (see Figure 3.4 (A)) that the participants bargaining skills converge to one of two limit values (close to 0 or close to 1). In case b) if the sum of their bargaining skills is above a cut point, the participants are not allowed to trade and their bargaining skills are decreased. Otherwise, if the sum of their bargaining skills is below the cut point, the participants will be allowed to trade with advantage to the more skilled participant. After the trade, the bargaining skills of both participants increase. In this case (see Figure 3.4 (B)) we observe that the bargaining skills converge to one limit value (close to 1/2).

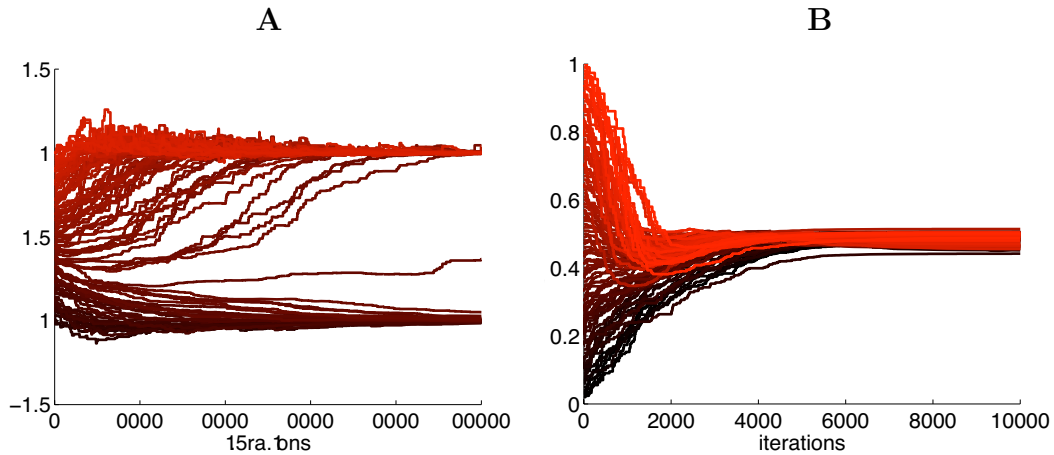


Figure 3.4: Variation of the bargaining skills with time. **(A)** The bargaining skills decrease when trade is allowed and increase otherwise; **(B)** The bargaining skills increase when trade is allowed and decrease otherwise.

### 3.9 Conclusions

In this Chapter we have proven that, under symmetry conditions, prices in a random exchange economy with two goods, where the agents preferences are characterized by the Cobb-Douglas utility function, converge to the Walrasian price. In Section 3.7 we associate a bargaining skill to each participant which brings up a game alike the Prisoner's Dilemma. When we considered a group of less skilled bargainers and a group of more skilled bargainers, the group in minority has a higher median increase in the value of the utilities. In Section 3.8 we studied the possibility of the participants adapting their bargaining skills along the time. We considered two distinct evolutionary rules: when the bargaining skills decrease with the trade, the bargaining skills of the participants converge, in time, to one of two possible limit values; when the bargaining skills increase with trade, we observe that the bargaining skills converge, in time, to a single intermediate value.

# Chapter 4

## Immune Response Models

### 4.1 Introduction

The work presented in this Chapter is joint work with N.J. Burroughs, B. Oliveira and A.A. Pinto and most of it is contained in the research articles [13], [14] and [15] and in the book chapter [32].

We analyse the effect of the Regulatory T cells (Tregs) in the local control of the immune responses by T cells. We study the model presented in [11]. We obtain an explicit formula for the level of antigenic stimulation of T cells as a function of the concentration of T cells and the parameters of the model. The relation between the concentration of T cells and the antigenic stimulation of T cells is an hysteresis, that is unfold for some parameter values. We study the appearance of autoimmunity from cross-reactivity between a pathogen and a self antigen or from bystander proliferation. We also study an asymmetry in the death rates. Under this asymmetry we show that the antigenic stimulation of Tregs is able to control locally the population size of Tregs. Other effects of this



asymmetry are a faster immune response and an improvement in the simulations of the bystander proliferation. The rate of variation of the levels of antigenic stimulation determines if the outcome is an immune response or if Tregs are able to maintain control due to the presence of a transcritical bifurcation for some tuning between the antigenic stimuli of T cells and Tregs. This behavior is explained by the presence of a transcritical bifurcation.

#### 4.1.1 Immune response model

There are a number of different (CD4) T cell regulatory phenotypes reported; we study a model of Tregs, which are currently identified as CD25<sup>+</sup> T cells, although this is not a definitive molecular marker. At a genetic level, these Tregs express Foxp3, a master regulator of the Treg phenotype inducing CD25, CTLA-4 and GITR expression, all correlating with a suppressive phenotype [68].

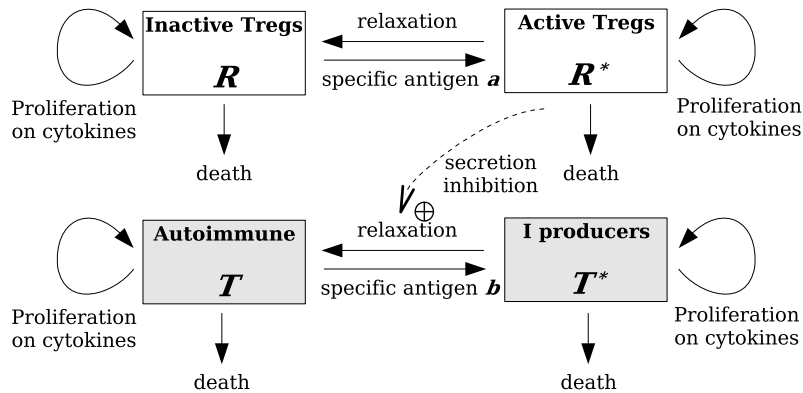


Figure 4.1: Model schematic showing growth, death and phenotype transitions of the Treg populations  $R, R^*$ , and autoimmune T cell  $T, T^*$  populations. Cytokine dynamics are not shown: IL-2 is secreted by activated T cells  $T^*$  and adsorbed by all the T cell populations equally.

We model a population of Tregs (denoted  $R, R^*$ ) and conventional T cells ( $T, T^*$ ) with processes shown schematically in Figure 4.1. Both populations require antigenic stimulation for activation, Tregs being activated by self antigens. Levels of antigenic stimulation are denoted  $a$  and  $b$  for Tregs and conventional T cells respectively. On activation conventional T cells both secrete IL-2 and acquire proliferative capacity in the presence of IL-2 while Tregs proliferate in the presence of IL-2, although less efficiently than normal T cells [74], and they do not secrete IL-2. Activated Tregs suppress IL-2 secretion [74] thereby inhibiting T cell growth. However, if IL-2 is present (CD4) T cells can still proliferate [68, 69]. In the model we assume that T cells activated by exposure to their specific antigen have a cytokine secreting state (a normal activated state) and a non secreting state to which they revert at a constant rate  $k$ . Thus in absence of antigen growth halts. Tregs also induce a transition to the (inhibited) nonsecreting state and this transition rate is assumed proportional to the Treg population density. This transition can either be through direct cell:cell contact or be induced by soluble inhibitors [68], both of which give identical mass action kinetics over suitable density ranges. T cells regain secretion status on CD28 coreceptor stimulation [76], which we assume correlates with antigen exposure through an increased conjugate formation rate. Thus in the presence of costimulation and Tregs, the T cell population would be a mixture of partially inhibited, and normal T cells. Although we assume an antigen dependent rate of secretion inhibition reversion, similar results would be obtained with a constant reversion rate, i.e. if costimulation exposure is independent of antigen density. Note that exogenous IL-2 does not reverse the suppressed phenotype, i.e. secretion status is not reacquired on cell proliferation [76].

Regulatory T cells are assumed to be in homeostasis, thus Treg density is controlled through some type of (nonlinear) competition. Homeostatic mechanisms of Tregs are currently poorly understood. In [11] it is used a generic mechanism that utilizes a cytokine (denoted  $J$ ), analogous to interleukine 7 which is known to homeostatically regulate memory T cells [70]. We assume the cytokine is secreted by the local tissues, thereby sustaining a local population of Tregs activated by a probably tissue specific profile of self antigens. Tregs compete for this cytokine by adsorption and thus population homeostasis is achieved.

In Section 4.3 we discuss an asymmetry in the model where we assume that the secreting T cells  $T^*$  have a lower death rate than the non secreting T cells  $T$  and that the active Tregs  $R^*$  also have a lower death rate than inactive Tregs  $R$  [13]. We also consider an inflow  $R_{input}$  of tregs instead of the  $J$  cytokine (both mechanisms yield similar results). This asymmetry in the death rates and the inflow  $R_{input}$  of Tregs allow the antigenic stimulation  $a$  of Tregs to regulate the size of the local population of Tregs. We also include a growth limitation mechanism and we use a (quadratic) Fas-FasL death mechanism [52], that is assumed to act on all T cells equally. Results will be similar with any saturation mechanism. Finally, we include an influx of (auto) immune T cells into the tissue ( $T_{input}$  in cells per ml per day), which can represent T cell circulation or naive T cell input from the thymus.

A set of ordinary differential equations is employed to study the dynamics, with a compartment for each T cell population (inactive Tregs  $R$ , active Tregs  $R^*$ , non secreting T cells  $T$ , secreting activated T cells  $T^*$ ), interleukine 2 density  $I$  and the homeostatic Treg cytokine  $J$ ,

$$\frac{dR}{dt} = (\epsilon\rho(I+J) - \beta(R + R^* + T + T^*) - \hat{d})R + \hat{k}(R^* - aR),$$

$$\begin{aligned}
\frac{dR^*}{dt} &= (\epsilon\rho(I+J) - \beta(R + R^* + T + T^*) - \hat{d})R^* - \hat{k}(R^* - aR), \\
\frac{dJ}{dt} &= \hat{\sigma}(S - (\hat{\alpha}(R + R^*) + \hat{\delta})J), \\
\frac{dT}{dt} &= (\rho I - \beta(R + R^* + T + T^*) - d)T + k(T^* - bT + \gamma R^* T^*) + T_{input}, \\
\frac{dT^*}{dt} &= (\rho I - \beta(R + R^* + T + T^*) - d)T^* - k(T^* - bT + \gamma R^* T^*), \\
\frac{dI}{dt} &= \sigma(T^* - (\alpha(R + R^* + T + T^*) + \delta)I).
\end{aligned} \tag{4.1}$$

Parameters are defined in Table 4.1. The model has components that have been used in previous models, for instance cytokine dependent growth [18, 48], cytokine kinetics [78], Fas-FasL mediated death [16], and positive feedback of T cells on Tregs [42, 43], in [11] this is explicitly though IL-2.

The only important aspects of this model are a mechanism to sustain a population of Tregs, secretion inhibition of T cells with a rate that correlates with Treg population size, and growth and competition for IL-2 with a higher growth rate of T cells relative to Tregs. Other aspects of the model can be altered with only quantitative differences in behavior.

### 4.1.2 Dynamics of the model

To establish the model dynamics, in [11] it was initially simulated an influx of an autoimmune population of T cells into a tissue where the Tregs are at homeostatic equilibrium. This could model adoptive transfer experiments where there is no native circulation/production of these (foreign) T cells, i.e.  $T_{input} = 0$ . There are two possible outcomes depending on the strength of activation and initial conditions: the autoimmune population is controlled with elimination of autoimmune T cells and the Treg population reverting to an homeostatic state; or the autoimmune population expands and escapes control. Escape can only

Parameter	Symbol	Range	Value
<b>T cell <math>T, T^*</math></b>			
T cell Maximum growth rate <sup>1</sup>	$\rho/\alpha$	$< 6 \text{ day}^{-1}$	$4 \text{ day}^{-1}$
Death rate of T cells	$d = \hat{d}$	$0.1-0.01 \text{ day}^{-1}$ [50]	$0.1 \text{ day}^{-1}$
Capacity of T cells <sup>2</sup>	$\rho/(\alpha\beta)$	$10^6 - 10^7 \text{ cells/ml}$ [51]	$10^7 \text{ cells/ml}$
Input rate	$T_{input}$	$0 - 10^4 \text{ cells/ml/day}$	$0,100 \text{ cells/ml per day}$
Secretion reversion (constant) <sup>3</sup>	$k$	hrs-days	$0.1 \text{ hr}^{-1}$
Antigen stimulation level	$bk$	$0.001-200 \times a\hat{k}$	Bifurcation parameter
<b>Tregs <math>R, R^*</math></b>			
Growth rate ratio $T_{reg}:T$	$\epsilon$	$< 1$	0.6
Homeostatic capacity $R_{hom}$	$(\epsilon\rho S/\hat{d} - \hat{\delta})/\hat{\alpha}$	$10 - 10^5 \text{ cells/ml}$	$10^4 \text{ cells/ml}$
Relaxation rate	$\hat{k}$	hrs-days	$0.1 \text{ hr}^{-1}$
Death rate ratio $T_{reg}:T$	$\hat{d}/d$		1
$T_{reg}$ antigen stimulation level	$a\hat{k}$	0-10 per day	1 per day
Secretion inhibition <sup>4</sup>	$\gamma$	$0.1-100 \times R_{hom}^{-1}$	$10 R_{hom}^{-1}$
<b>Cytokines</b>			
Max. cytokine concentration <sup>5</sup>	$1/\alpha$	100-500 pM	200 pM
IL-2 secretion rate	$\sigma$	<sup>6</sup> $0.07, 2 \text{ fgms h}^{-1}$ [79]	$10^6 \text{ molecs s}^{-1} \text{ cell}^{-1}$
Relative adsorbance $J$ to IL-2	$\hat{\sigma}\hat{\alpha}/\sigma\alpha$	$< 1$	0.1
Relative secretion rate of $J$	$\hat{\sigma}/\sigma$	$< 1$	0.01
Cytokine decay rate	$\sigma\delta = \hat{\sigma}\hat{\delta}$	hrs-days	$1.5 \text{ hr}^{-1}$ [3]

<sup>1</sup> Minimum duration of SG<sub>2</sub>M phase  $\alpha\rho^{-1} \approx 3hrs$ .

<sup>2</sup> Maximum T cell density for severe infections (based on LCMV).

<sup>3</sup> This is in absence of Tregs.

<sup>4</sup> This is in terms of the homeostatic Treg level  $R_{hom}$  which we set to  $10^4$  cells per ml.

<sup>5</sup> This is taken as 20 times the receptor affinity (10pM [46]).

<sup>6</sup> Naive and memory cells respectively. This corresponds to  $3000-10^5$  molecules per h, IL-2 mass 15-18 kDa.

Table 4.1: Model parameters. Reproduced from [11].

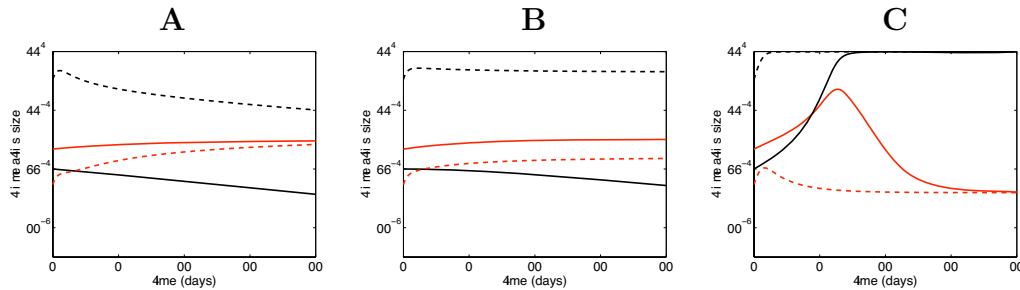


Figure 4.2: Time series plots for T cell populations on exposure to antigen with various antigenicities  $b$  and  $T_{input} = 0$ . Two initial conditions are shown, low initial T cell load (solid), and high initial T cell load (dashed). (A) Regulation, low  $b = 5 \times 10^{-2}$ ; (B) Escape and control, intermediate  $b = 0.5$ ; (C) Escape, high  $b = 5000$ . Total Treg (red), immune T cells (black). Reproduced from [11].

occur if the autoimmune antigenic stimulation  $b$  is above a threshold, denoted  $b_L$ . At low antigenic stimulation levels, autoimmune T cells are always eliminated for all initial loads. However, even if stimulation is above  $b_L$  escape requires the initial load to be sufficiently high. The dependence on T cell density is a quorum mechanism, specifically if there is a sufficiently high density of secreting T cells cytokine levels are high enough for cell proliferation to exceed cell death. During immune responses (escape of Treg control) the Treg population initially grows in the IL-2 rich environment (bystander growth), but as the T cell population saturates, by Fas-FasL apoptosis assumed in [11], the Treg population decays because it is assumed susceptible to Fas-FasL apoptosis similar to conventional T cells.

### 4.1.3 Bifurcation diagrams

These observations can be summarised in a plot of the equilibrium states. However above a critical antigenic load  $b_L$  two new steady states emerge (only one of

which is stable and thus realisable). To reach that state the initial load has to be sufficiently high, the load threshold lying on the basin of attraction of the escape state with  $I = T = 0$  and  $R, R^*$  at their homeostatic densities. This threshold is lowest for large  $b$  [11]. It gives the (necessary) minimum quorum size for escape  $T_{quorum}$  and is approximated by the density  $T + T^*$  of the unstable steady state. This dose dependence for proliferation is observed in transfer experiments. Experimentally, suppression *in vitro* can be overcome at high levels of antigenic stimulation [37]. This is observed here provided the initial density is higher than  $T_{quorum}$  when there is a threshold in the antigenic stimulation level  $b$  at which escape occurs. In the absence of Tregs the system shows identical bifurcation behavior but the antigenic stimulation ( $b_L$ ) and quorum ( $T_{quorum}$ ) thresholds are lower. Thus Tregs shift the growth threshold to alter the balance in favour of inhibition than immune responses. Therefore removal of Tregs (CD25<sup>+</sup>) in adoptive transfer experiments lowers the threshold for immune responses, and autoimmune populations that were previously suppressed in the presence of Tregs are then able to escape. In normal healthy tissue a continuous influx of autoimmune T cells is expected, both from the thymus and through the circulation. This is modelled as an influx term  $T_{input} > 0$  to the T cell population. This has two significant effects, firstly a non zero T cell population is sustained which means that escape is easier, and secondly, above an antigenic stimulation threshold, denoted  $b_H$ , control is impossible (see Figure 4.3). This is because the influx population alone is sufficient to satisfy the quorum condition. Thus, in the bifurcation plot (see Figure 4.3) a lower steady state equilibrium exists at low antigenic stimulation (controlled state), but only the escape/immune response state exists at high antigenic stimulation. At intermediate levels of antigenic stimulation  $b$  we have two possible stable outcomes. The state that is attained depends on the

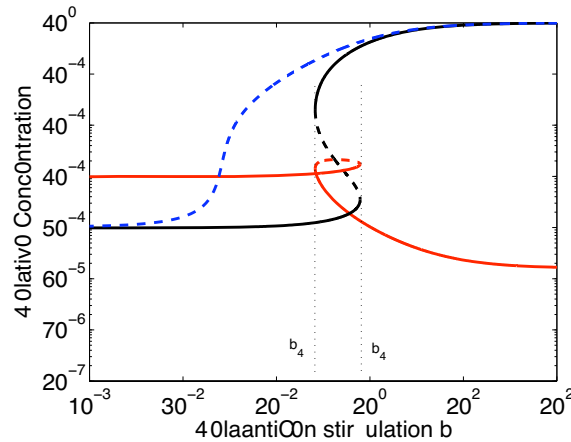


Figure 4.3: Bifurcation plots with respect to the antigenic stimulation  $b$  of T cells. Shown are two cases: Tregs present with  $R + R^*$  red,  $T + T^*$  black, and no Tregs with  $T + T^*$  blue. Stable steady states are shown as solid lines, unstable as dashed. Reproduced from [11].

initial conditions. So far it was assumed that levels of antigenic stimulation are constant, however there are likely to be both fluctuations and a slow variation over time, eg during puberty. Thus, if antigenic stimulation rises above the threshold  $b_H$  in Figure 4.3, control is lost and autoimmunity arises. Note that even if the antigenic stimulation level  $b$  falls to the original value, at which control was originally achieved, control may not be reacquired, and is only attained if stimulation falls below the second threshold  $b_L$  in Figure 4.3. This phenomena, termed hysteresis, is common in many physical and biological systems. The system displays a control state and an immune state. This biphasic behavior is a consequence of the IL-2 driven dynamics where the IL-2 concentration must be high enough such that the growth rate exceeds the death rate. This requires a sufficiently high density of secreting T cells. Thus even in the absence of Tregs, T cells can display this behavior (in fact in Figure 4.3 the parameters are such that the bifurcation points  $b_L, b_H$  are lost and hysteresis is no longer observed



although a sharp transition with  $b$  remains).

The presence of Tregs increases the thresholds  $b_L$ ,  $b_H$  in Figure 4.3, thereby enhancing the control state. The thresholds  $b_L$ ,  $b_H$  can be tuned by adjusting the Treg homeostatic population size with a larger size conferring greater protection. We note that Tregs must be less efficient at utilising IL-2 to proliferate,  $\epsilon < 1$ , eg through a lower density of surface receptors (IL-2 receptor), otherwise escape is impossible. Correspondingly, Tregs need a mechanism to sustain their numbers such that Treg die out is prevented. An homeostatic mechanism (cytokine distinct from IL-2) to maintain a local population is used. In this case conventional T cells must be less efficient at utilising this cytokine for growth than Tregs. Alternatively, a continuous input  $R_{input}$  can be used to maintain the population (see Section 4.3). This asymmetry between Tregs and conventional T cells is essential for the immune system to display both control and immune response escape. Thus, at low inflammation levels, Treg survival is predominant, while at high levels of pathogen load T cell growth is faster than Treg growth.

The bistability region vanishes when the thresholds  $b_L$  and  $b_H$  meet in a cusp bifurcation. In the immune response model, this happens for low growth rates of T cells and Tregs, for low values of the growth rate ratio between Tregs and T cells, for low values of the secretion rate of cytokine  $J$ , and for high thymic inputs.

#### 4.1.4 Dynamics of cross-reactive proliferation

Humans are continuously exposed to pathogens which invoke T cell activation and immune responses. This has consequences on Treg control of autoimmune states since immune responses produce IL-2 and thus can lead to bystander growth and loss of Treg homeostasis, or in the case of cross reactivity direct stimulation of

auto reactive T cells.

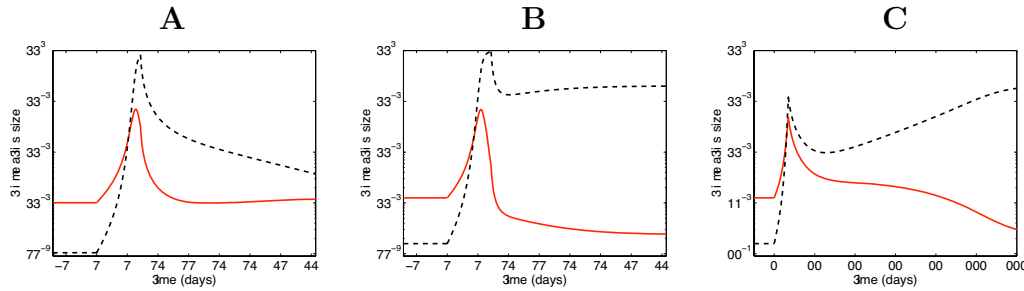


Figure 4.4: T cell cross reactivity between a pathogen and self. **(A)** Cross reactive autoimmune T cells on pathogen infection can return to a controlled state if antigenic stimulation from self ( $b = 0.1$ ) is low; **(B)** For high  $b = 0.5$  stimulation from self, an initially controlled autoimmune T cell clone escapes when infection occurs with a cross reacting pathogen; **(C)** Identical to **(B)** except infection interval is 7 days. A pathogen infection is modelled as a step increase in  $b$  to 5000 for day 0-10 (**(A)** and **(B)**), 0-7 (**(C)**) to model both the increase in antigen (cross reactive) and costimulation. Key: Red solid  $R + R^*$ , Black dashed  $T + T^*$ . Reproduced from [11].

It was simulated, in [11], a pathogen exposure in a tissue with initial Treg control of an autoimmune population where there is cross reactivity between the pathogen specific T cells and self. Depending on the strength of the autoimmune antigen it was observed either a loss of control, i.e. Tregs fail to reacquire control, or autoimmune suppression is reinstated post infection. The former case corresponds to autoimmune antigenic stimulation levels  $b_L < b < b_H$ , although escape is not guaranteed as the immune response must be of sufficient duration to allow autoimmune T cells numbers to rise and sufficiently outnumber Tregs (about 5.5 days in the simulations). Autoimmune T cells with  $b < b_L$  are always controlled post infection (see Figure 4.4 (A)). The length of the period post infection for autoimmune control to be reestablished is determined by the slow death rate of T cells. It was not included a specific downsizing mechanism or memory diffe-

rentiation in the model which would reduce this period. Escape dynamics can also show a delay in the onset of autoimmunity when infection duration is short (see Figure 4.4 (C)). Cross reactivity enhances escape, however pure bystander growth can also lead to escape although longer infection periods and higher  $b$  are required for escape (see Subsection 4.3.4). Infections transiently enhance Treg populations, either eventually returning to homeostasis, or in the case of autoimmune responses being themselves suppressed. In this model it is because of their susceptibility to Fas-FasL mediated apoptosis. Other population saturation models, specifically assumptions of the impact on Tregs of T cell saturation, can give different levels of Tregs.

## 4.2 Analysis of the model

The immune response model presented in [11] was studied in [12] with the results proven by us in [14]. We study the equilibria of the immune system in a neighbourhood of the default values for the parameters and variables. The concentration of T cells varies between a minimum value corresponding to the *homeostasis* concentration of T cells  $T_{hom}$ , i.e. when there is no antigenic stimulation of T cells ( $b = 0$ ), and a maximum value, the *capacity* of T cells  $T_{cap}$ , which is obtained for high levels of antigenic stimulation of T cells ( $b = +\infty$ ). Using Equation (4.29), the values  $T_{hom}$  and  $T_{cap}$  are implicitly determined as zeros of a polynomial. In particular, for the default values of the parameters, these values are given by  $T_{hom} = 9.6 \times 10^2$  cells per ml and  $T_{cap} = 9.7 \times 10^6$  cells per ml. When the system is at equilibrium, we present, in Theorem 4.2.1 an explicit formula for the relation between the concentration of T cells and the concentration of Tregs for values of the concentration of T cells between  $T_{hom}$  and  $T_{cap}$  (see Figure 4.5).

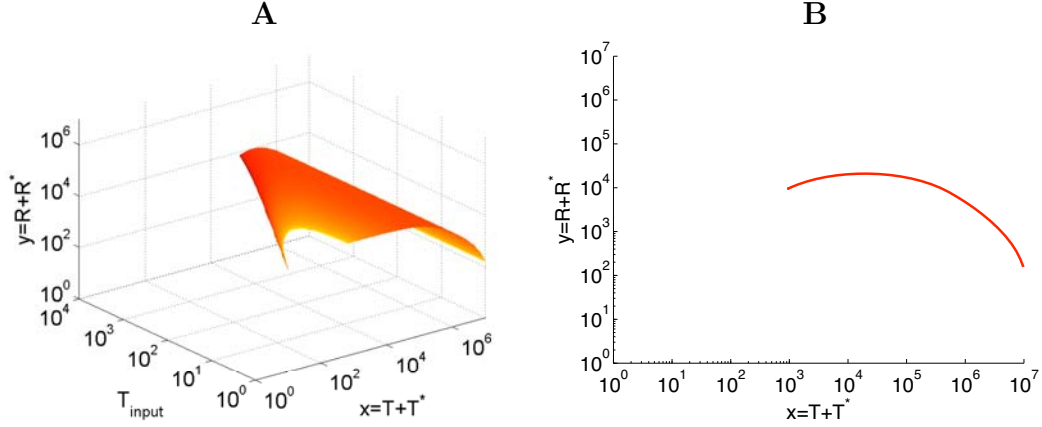


Figure 4.5: **(A)** The equilibria manifold for Thymic inputs  $T_{input} \in [1, 10000]$ . Low values of  $b$  are darker and higher values are lighter; **(B)** Cross section of the equilibria manifold for  $T_{input} = 100$ . It illustrates Theorem 4.2.1, showing the total concentration of Tregs  $y(x) = R + R^*$  as a function of the total concentration of T cells  $x = T + T^*$ . The parameters are at their default values.

Let  $Y_1, Y_2, Y_3$  be the following polynomials

$$\begin{aligned} Y_1(x) &= -\hat{\alpha}C(x) - \beta\hat{\delta}B(x) \\ Y_2(x) &= 2\hat{\alpha}\beta B(x) \\ Y_3(x) &= Y_1^2(x) - 2(\delta C(x) - \epsilon\rho Sx)Y_2(x) , \end{aligned}$$

where  $B(x) = (1 - \epsilon)x$  and  $C(x) = \epsilon T_{input} + B(x)(\beta x + d)$ .

Let  $X_1, X_2, X_3$  be the following polynomials

$$\begin{aligned} X_1(y) &= BC(y)D(y) - \epsilon\rho S \\ X_2(y) &= -2\beta BC(y) \\ X_3(y) &= X_1^2(y) - 2\epsilon T_{input}C(y)X_2(y) , \end{aligned}$$

where  $B = 1 - \epsilon$  and  $C(y) = \hat{\alpha}y + \hat{\delta}$ , and  $D(y) = \beta y + d$ .

Let  $x = T + T^*$  be the total concentration of T cells and  $y = R + R^*$  be the total concentration of Tregs.

**Theorem 4.2.1** *When the system is at equilibrium, the concentration of Tregs  $y = R + R^*$  is given by the Treg curve*

$$y(x) = \frac{Y_1(x) + \sqrt{Y_3(x)}}{Y_2(x)}, \quad (4.2)$$

where  $x = T + T^*$  is the total concentration of T cells. Conversely, the concentration of T cells  $x(y)$  is determined by

$$x = X_-(y) = \frac{X_1(y) - \sqrt{X_3(y)}}{X_2(y)} \quad \text{or} \quad (4.3)$$

$$x = X_+(y) = \frac{X_1(y) + \sqrt{X_3(y)}}{X_2(y)} \quad (4.4)$$

where  $y = R + R^*$  is the total concentration of Tregs.

For simplicity of notation we write  $y(x)$  instead of  $y = Y(x)$ . We also write  $x(y)$  when either  $x = X_-(y)$  or  $x = X_+(y)$  should be used.

**Proof:** At equilibrium we have that:

$$\hat{\sigma}(S - (\hat{\alpha}y + \hat{\delta})J) = 0, \quad (4.5)$$

$$\sigma(T^* - (\alpha(x + y) + \delta)I) = 0 \quad (4.6)$$

$$(\epsilon\rho(I+J) - \beta(x + y) - d)R + \hat{k}(R^* - aR) = 0, \quad (4.7)$$

$$(\epsilon\rho(I+J) - \beta(x + y) - d)R^* - \hat{k}(R^* - aR) = 0, \quad (4.8)$$

$$(\rho I - \beta(x + y) - d)T + k(T^* - bT + \gamma R^* T^*) + T_{input} = 0, \quad (4.9)$$

$$(\rho I - \beta(x + y) - d)T^* - k(T^* - bT + \gamma R^* T^*) = 0. \quad (4.10)$$

From (4.5), we get

$$J = \frac{S}{\hat{\alpha}y + \hat{\delta}}. \quad (4.11)$$

From (4.6), we have

$$T^* = I(\alpha(x + y) + \delta). \quad (4.12)$$

Adding (4.7) and (4.8), we obtain

$$\epsilon\rho(I + J) - \beta(x + y) - d = 0 \quad (4.13)$$

(or  $y = 0$ ).

Subtracting (4.8) from (4.7), we get

$$(\epsilon\rho(I + J) - \beta(x + y) - d)(R - R^*) + 2\hat{k}(R^* - aR) = 0. \quad (4.14)$$

From (4.13) and (4.14), we have

$$R^* = aR. \quad (4.15)$$

Let  $A = a/(a + 1)$ . From (4.15), we get

$$R^* = Ay. \quad (4.16)$$

Adding (4.9) and (4.10), we obtain

$$\rho I - \beta(x + y) - d + \frac{T_{input}}{x} = 0 \quad (4.17)$$

(or  $x = 0$ ).

Subtracting (4.17) from (4.13), we get

$$\epsilon\rho J - (1 - \epsilon)\rho I - \frac{T_{input}}{x} = 0. \quad (4.18)$$

Subtracting (4.10) from (4.9), we have

$$(\rho I - \beta(x + y) - d)(T - T^*) + 2k(T^* - bT + \gamma R^* T^*) + T_{input} = 0. \quad (4.19)$$

From (4.17) and (4.19), we have

$$T^*(kx(1 + \gamma R^*) + T_{input}) = kxbT. \quad (4.20)$$

From (4.20), we get

$$T^* = \frac{kbx^2}{kx(1 + b + \gamma R^*) + T_{input}}. \quad (4.21)$$

From (4.16) and (4.21), we obtain

$$T^* = \frac{kbx^2}{kx(1 + b + \gamma Ay) + T_{input}}. \quad (4.22)$$

From (4.12) and (4.22), we get

$$I(\alpha(x + y) + \delta) = \frac{kbx^2}{kx(1 + b + \gamma Ay) + T_{input}}. \quad (4.23)$$

Replacing (4.11) and (4.23) in (4.18), we have

$$\frac{\epsilon\rho S}{\hat{\alpha}y + \hat{\delta}} - \frac{(1 - \epsilon)\rho kbx^2}{(\alpha(x + y) + \delta)(kx(1 + b + \gamma Ay) + T_{input})} - \frac{T_{input}}{x} = 0. \quad (4.24)$$

Replacing (4.23) in (4.17), we obtain

$$\frac{\rho k b x^2}{(\alpha(x+y) + \delta)(kx(1+b + \gamma Ay) + T_{input})} - \beta(x+y) - d + \frac{T_{input}}{x} = 0 . \quad (4.25)$$

From (4.25), we get

$$\frac{\rho k b}{(\alpha(x+y) + \delta)(kx(1+b + \gamma Ay) + T_{input})} = \beta(x+y) + d - \frac{T_{input}}{x} . \quad (4.26)$$

Replacing (4.26) in (4.24), we have

$$\frac{\epsilon \rho S}{\hat{\alpha} y + \hat{\delta}} - (1 - \epsilon)(\beta(x+y) + d - \frac{T_{input}}{x}) - \frac{T_{input}}{x} = 0 . \quad (4.27)$$

From (4.27), we obtain

$$x \epsilon \rho S - (1 - \epsilon)(\beta(x+y)x + dx - T_{input})(\hat{\alpha} y + \hat{\delta}) - T_{input}(\hat{\alpha} y + \hat{\delta}) = 0 , \quad (4.28)$$

which, solving (4.28) for  $y$  and considering only the positive root, proves equality (4.2).

□

The maximum concentration  $R_{max}$  of Tregs is a zero of a fourth order polynomial and, so,  $R_{max}$  has an explicit solution. In particular, for the default values of the parameters, the maximum concentration  $R_{max}$  of Tregs is given by  $R_{max} = 2.1 \times 10^4$  cells per ml, and the corresponding concentration of T cells is  $1.9 \times 10^4$  cells per ml. The minimum concentration  $R_{min}$  of Tregs is 156 cells per ml, and the corresponding concentration of T cells is given by  $T_{cap} = 9.7 \times 10^6$  cells per ml.

When the system is at equilibrium, we obtain the level of the antigenic stimulation  $b(x, y(x))$  of T cells from the concentration  $x$  of T cells, using the auxiliary



Treg curve  $y(x)$  computed in Theorem 4.2.1 (see Figure 4.6). The *antigen function*  $b(x, y)$  is given by

$$b(x, y) = \frac{\varphi(x, y)(kx(1 + \gamma Ay) + T_{input})}{k(1 - \epsilon)\rho x^3(\hat{\alpha}y + \hat{\delta}) - kx\varphi(x, y)}, \quad (4.29)$$

where  $A = a/(1 + a)$  and  $\varphi(x, y) = (\epsilon\rho Sx - T_{input}(\hat{\alpha}y + \hat{\delta}))(\alpha(x + y) + \delta)$ .

**Theorem 4.2.2** *Let  $b(x, y)$  be the antigen function, and let  $x(y)$  and  $y(x)$  be as in Theorem 4.2.1. The level of the antigenic stimulation of T cells is given by  $b(x, y(x))$ , or, equivalently, by  $b(x(y), y)$ , when the system is at equilibrium (stable or unstable). Conversely, given an antigenic stimulation level  $b$  of T cells, the concentration  $x$  of T cells and the concentration  $y$  of Tregs are zeros of the twelfth order polynomials that can be explicitly constructed.*

**Proof:** From (4.18), we have

$$I(1 - \epsilon)\rho x = J\epsilon\rho x - T_{input}. \quad (4.30)$$

Replacing (4.11) in (4.30), we get

$$I = \frac{\epsilon\rho Sx - T_{input}(\hat{\alpha}y + \hat{\delta})}{(1 - \epsilon)\rho x(\hat{\alpha}y + \hat{\delta})}. \quad (4.31)$$

Replacing (4.31) in (4.23), we obtain

$$(\epsilon\rho Sx - T_{input}(\hat{\alpha}y + \hat{\delta}))(\alpha(x + y) + \delta) = \frac{(1 - \epsilon)\rho kbx^3(\hat{\alpha}y + \hat{\delta})}{kx(1 + b + \gamma Ay) + T_{input}}. \quad (4.32)$$

Hence, solving (4.32) for  $b$ , we prove equality (4.29).

□

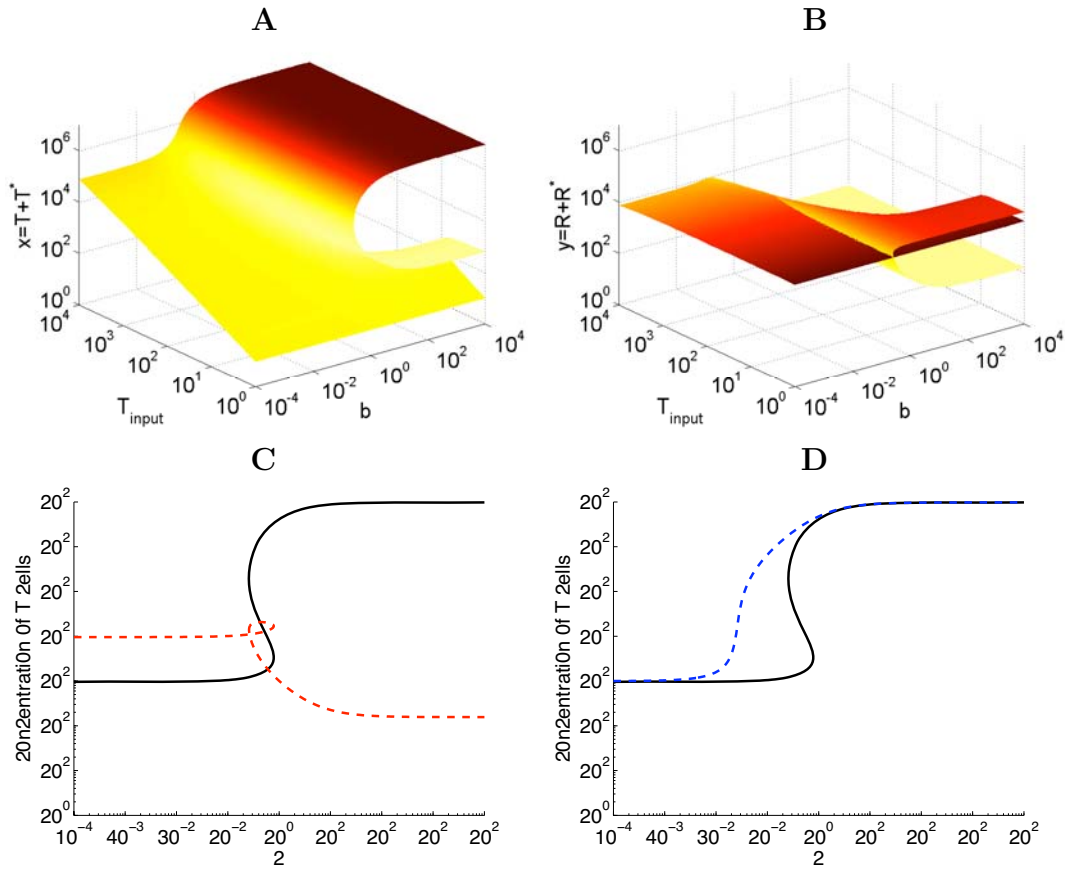


Figure 4.6: The hysteresis of the equilibria manifold for Thymic inputs  $T_{input} \in [1, 10000]$ , with the other parameters at their default values. These figures show the relation between the antigenic stimulation level  $b$ , the concentration of T cells  $x = T + T^*$ , and the concentration of Tregs  $y = R + R^*$ . The hysteresis unfolds for high values of the parameter  $T_{input}$ . (A) Low values of  $y = R + R^*$  are darker and higher values are lighter; (B) Low values of  $x = T + T^*$  are darker and higher values are lighter; (C) Cross section of the equilibria manifold for  $T_{input} = 100$ , illustrating Theorem 4.2.2, with the concentration of T cells  $x$  (black solid line) and the concentration of Tregs  $y$  (redred dashes); (D) Cross section of the equilibria manifold for  $T_{input} = 100$ , illustrating Theorem 4.2.3, with the concentration of T cells  $x$  (blueblue dashes) for the simplified model without Tregs. We also show the concentration of T cells  $x$  (black solid line) from Theorem 4.2.2.

In Theorem 4.2.3, we obtain the level of the antigenic stimulation of T cells from the concentration  $x$  of T cells, for the simplified model without Tregs. The antigen function  $\tilde{b}(x)$  in the absence of Tregs is given by

$$\tilde{b}(x) = \frac{(\alpha x + \delta)(kx + T_{input})(\beta x^2 + dx - T_{input})}{kx(\rho x^2 + (T_{input} - \beta x^2 - dx)(\alpha x + \delta))}. \quad (4.33)$$

**Theorem 4.2.3** *Let us consider the simplified model with the concentration of Tregs equal to zero (i.e.  $y = 0$ ). The level of the antigenic stimulation of T cells is given by  $\tilde{b}(x)$ , when the system is at equilibrium (stable or unstable). Conversely, given an antigenic stimulation level  $b$ , the concentration  $x$  of T cells is a zero of the fourth order polynomial that can be explicitly constructed.*

**Proof:** At equilibrium we have that:

$$\sigma(T^* - \alpha x + \delta)I = 0, \quad (4.34)$$

$$(\rho I - \beta x - d)T + k(T^* - bT) + T_{input} = 0, \quad (4.35)$$

$$(\rho I - \beta x - d)T^* - k(T^* - bT) = 0. \quad (4.36)$$

From (4.34), we have

$$T^* = I(\alpha x + \delta). \quad (4.37)$$

Adding (4.35) and (4.36), we obtain

$$\rho I - \beta x - d + \frac{T_{input}}{x} = 0 \quad (4.38)$$

(or  $x = 0$ )

Subtracting (4.36) from (4.35), we have

$$(\rho I - \beta x - d)(T - T^*) + 2k(T^* - bT) + T_{input} = 0. \quad (4.39)$$

From (4.38) and (4.39), we have

$$T^*(kx + T_{input}) = kxbT . \quad (4.40)$$

From (4.40), we obtain

$$T^* = \frac{kbx^2}{kx(1+b) + T_{input}} . \quad (4.41)$$

From (4.37) and (4.41), we get

$$I(\alpha x + \delta) = \frac{kbx^2}{kx(1+b) + T_{input}} . \quad (4.42)$$

From (4.17), we have

$$I = \frac{\beta x^2 + dx - T_{input}}{\rho x} . \quad (4.43)$$

Finally, from (4.42) and (4.43), we get

$$\tilde{b}(x) = \frac{(\alpha x + \delta)(kx + T_{input})(\beta x^2 + dx - T_{input})}{kx(\rho x^2 + (T_{input} - \beta x^2 - dx)(\alpha x + \delta))} . \quad (4.44)$$

□

When the system is at equilibrium, the threshold values of antigen stimulation  $b_L$  and  $b_H$  of T cells are determined using zeros of a polynomial. The *antigen threshold function*  $V(x, y, z)$  is equal to  $V_6(y, z)x^6 + \dots + V_0(y, z)$ , where the

functions  $V_0(y, z), \dots, V_6(y, z)$  are given by the polynomials

$$V_0(y, z) = kC^2F^2T_{input}^3$$

$$V_1(y, z) = 2kCFT_{input}^2H$$

$$V_2(y, z) = kT_{input}(H^2 + CFT_{input}(3\rho CE - \gamma ACFkz - 2\alpha G))$$

$$V_3(y, z) = kT_{input}(2FG(\alpha G - \rho CE + \gamma BCFkz) + 2\rho CEFk(1 + \gamma Ay) - \alpha CT_{input}(2\gamma AFkz + \rho Ez - 2\rho E + 2\alpha G))$$

$$V_4(y, z) = k(C(-G(\rho E(\alpha T_{input}(1 - z) + kF(1 + \gamma Ay)) - 4kz\alpha\gamma AFT_{input}) - kCT_{input}(\alpha\rho E(z - 1)(1 + \gamma Ay) + z\gamma A(\rho EF + \alpha^2 T_{input}))) + G(-kz\gamma BF^2G + \alpha^2 GT_{input} - \rho z\hat{\alpha}EFT_{input}))$$

$$V_5(y, z) = \rho Gk(\gamma BFk(\hat{\delta}\rho E - 2\alpha G) + \rho E(k\alpha C(1 + \gamma Ay) - k\hat{\alpha}F - \alpha\hat{\alpha}T_{input}))z$$

$$V_6(y, z) = \alpha Gk^2(-\alpha\gamma AG + E\rho(\gamma\hat{\delta}A - \hat{\alpha}))z,$$

where  $A = a/(1 + a)$ ,  $B = \beta\delta - \alpha d$ ,  $C(y) = \hat{\alpha}y + \hat{\delta}$ ,  $D(y) = \beta y + d$ ,  $E = 1 - \epsilon$ ,  $F(y) = \alpha y + \delta$ ,  $G = \epsilon\rho S$  and  $H(y) = \alpha C(y)T_{input} - F(y)G$ .

**Theorem 4.2.4** *When the system is at equilibrium, a threshold of the antigenic stimulation  $b_M$  of  $T$  cells exists, if, and only if, there is a zero  $x_M \in [T_{hom}, T_{cap}]$  of the antigen threshold function  $V(x, y(x), y'(x))$ . This zero is such that  $b_M = b(x_M, y(x_M))$ , where  $M \in \{L, H\}$ . The equality  $V(x, y(x), y'(x)) = 0$  is equivalent to  $\tilde{V}(x) = 0$ , where  $\tilde{V}(x)$  is a polynomial that can be explicitly constructed.*

**Proof:** By equality (4.29), we have that  $b(x, y) = N(x, y)/D(x, y)$ , where  $N$  and  $D$  are the following cubic polynomials in  $x$  and  $y$

$$N(x, y) = (\epsilon\rho Sx - T_{input}(\hat{\alpha}y + \hat{\delta}))(\alpha(x + y) + \delta)(kx(1 + \gamma Ay) + T_{input})$$

$$D(x, y) = k(1 - \epsilon)\rho x^3(\hat{\alpha}y + \hat{\delta}) - kx(\epsilon\rho Sx - T_{input}(\hat{\alpha}y + \hat{\delta}))(\alpha(x + y) + \delta).$$

If  $T_{input} > 0$ , the points  $x_L$  and  $x_H$  exist if, and only if, the function  $db(x, y(x))/dx$  have two distinct positive zeros. The values  $x_L$  and  $x_H$  are these zeros. If  $T_{input} = 0$ , the point  $x_L$  exists if, and only if, the function  $db(x, y(x))/dx$  has one positive zero. Furthermore,  $x_L$  is such zero. From equation (4.29), we have that  $b(x, y) = N(x, y)/D(x, y)$ , with  $N(x, y)$  and  $D(x, y)$  cubic polynomials in  $x$  and  $y$ . Hence,  $db(x, y(x))/dx$  is equal to  $V(x, y(x), y'(x))$  where

$$V(x, y, z) = \frac{\partial N(x, y)}{\partial x} D(x, y) - N(x, y) \frac{\partial D(x, y)}{\partial x} + \left( \frac{\partial N(x, y)}{\partial y} D(x, y) - N(x, y) \frac{\partial D(x, y)}{\partial y} \right) z .$$

Since

$$\begin{aligned} \frac{\partial N(x, y(x))}{\partial x} &= \epsilon \rho S V W + \alpha U V + k U W (1 + \gamma A y) \\ \frac{\partial N(x, y(x))}{\partial y} &= -\hat{\alpha} V W T_{input} + \alpha U V + k x \gamma A U W \\ \frac{\partial D(x, y(x))}{\partial x} &= -k U W - k x \epsilon \rho S W - k x \alpha U + 3 k \rho (1 - \epsilon) (\hat{\alpha} y + \hat{\delta}) x^2 \\ \frac{\partial D(x, y(x))}{\partial y} &= k x \hat{\alpha} W T_{input} - k x \alpha U + k \hat{\alpha} \rho (1 - \epsilon) x^3 . \end{aligned}$$

where  $U(x, y) = \epsilon \rho S x - T_{input}(\hat{\alpha} y + \hat{\delta})$ ,  $V(x, y) = k x (1 + \gamma A y) + T_{input}$  and  $W(x, y) = \alpha(x + y) + \delta$ , we get that the expression  $V(x, y, z)$  for the antigen threshold function follows.

□

For the parameters that unfold the hysteresis, the antigenic thresholds  $b_L$  and  $b_H$  form a cusp. The *cusp bifurcation* at the antigenic stimulation  $b_C$  of T cells is an origin of the unfold of the hysteresis, with respect to a parameter, and, so, biologically relevant. The concentration  $x_C$  of T cells corresponding to levels of

the antigenic stimulation  $b_C = b(x_C, y(x_C))$  satisfies the following equalities

$$\begin{aligned} V(x, y(x), y'(x)) &= 0 \text{ and} \\ W(x, y(x), y'(x), y''(x)) &= 0, \end{aligned} \tag{4.45}$$

where

$$W(x, y, z, v) = \sum_{i=1}^n V_i(y, z) \frac{x^{i-1}}{i} + \sum_{i=0}^n \frac{\partial V_i(y, z)}{\partial y} x^i z + \frac{\partial V_i(y, z)}{\partial z} x^i v.$$

In Figure 4.7, the antigenic thresholds  $b_H$  and  $b_L$  and the ratio  $b_H/b_L$  decrease with  $T_{input}$ . The cusp  $b_C$  occurs at  $T_{input} \approx 650$  cells per ml, unfolding the hysteresis. When  $T_{input}$  gets close to the value 10.34 cells per ml the threshold  $b_H$  tends to infinity. The concentration  $x(b_L)$  of T cells decreases and the concentration  $x(b_H)$  of T cells increases with  $T_{input}$ . The concentration  $y(b_L)$  of Tregs increases with  $T_{input}$  and the concentration  $y(b_H)$  of Tregs has a maxima for  $T_{input} \approx 500$  cells per ml.

### 4.3 Asymmetry in the immune response model

In [13] we introduce an asymmetry reflecting that the difference between the growth and death rates can be higher for the active T cells and the active Tregs than for the inactive T cells and inactive Tregs. This asymmetry can be explained by the effect of memory T cells. The memory T cells last longer than the other T cells and react more promptly to their specific antigen [64]. This results in a positive correlation between the antigenic stimulation and the difference between growth rate and the death rate of T cells.

This asymmetry brings up the relevance of the antigenic stimulation of Tregs

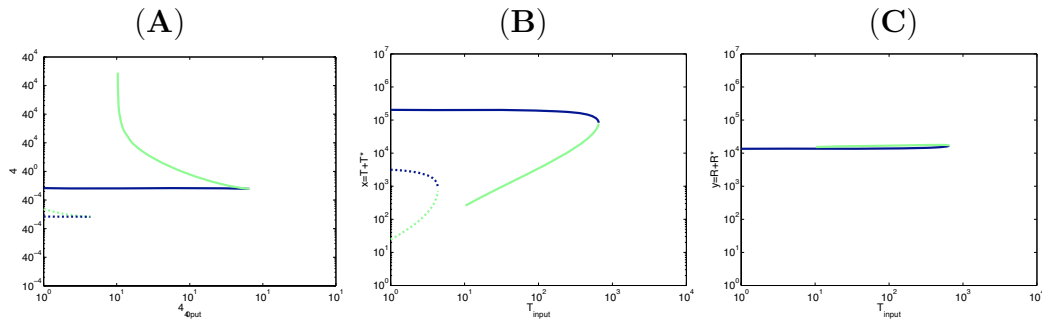


Figure 4.7: Dependence of the thresholds with the Thymic input parameter  $T_{input} \in [1, 650]$  with the other parameters at their default values. The model with Tregs is with bold lines and the simplified model without Tregs is with dotted lines. **(A)** The thresholds of the antigenic stimulation  $b_L$  (dark blue) and  $b_H$  (light green); **(B)** The concentration  $x(b_L)$  (dark blue) of T cells and the concentration  $x(b_H)$  (light green) of T cells; **(C)** The concentration  $y(b_L)$  (dark blue) of Tregs and the concentration  $y(b_H)$  (light green) of Tregs.

in the control of the local Treg population size. Hence, under homeostasis, a larger antigenic stimulation of Tregs results in a larger Treg population size. Furthermore, there is a positive correlation between the antigenic stimulation of Tregs and the thresholds  $b_L$  and  $b_H$  of antigenic stimulation of T cells. Hence, organs with different antigenic stimulation of Tregs have different levels of protection against the development of an immune response by T cells, under the presence of their specific antigen.

We study the effect of a positive correlation between the antigenic stimulation of T cells and the antigenic stimulation of Tregs, due to the antigen presenting cells (APC), such as dendritic cells, present both self antigens and foreign antigens [42, 43]. Here, with a structurally different model, we attain the same conclusions, as in [44], due to the asymmetry in the difference between the growth and death rates. We find, for some parameter values, that slow rates of increase of



the antigenic stimuli do not lead to an immune response, but fast rates of increase of the antigenic stimuli can trigger an immune response. This behavior is mathematically explained by the presence of a transcritical bifurcation.

### 4.3.1 The model

The model proposed consists of a set of ordinary differential equations similar to the one presented in [11], with a compartment for each T cell population (inactive Tregs  $R$ , active Tregs  $R^*$ , non secreting T cells  $T$ , secreting activated T cells  $T^*$ ) and interleukine 2 density  $I$ :

$$\begin{aligned}\frac{dR}{dt} &= (\epsilon\rho I - \beta(R + R^* + T + T^*) - d_R)R + \hat{k}(R^* - aR) + R_{input}, \\ \frac{dR^*}{dt} &= (\epsilon\rho I - \beta(R + R^* + T + T^*) - d_{R^*})R^* - \hat{k}(R^* - aR), \\ \frac{dT}{dt} &= (\rho I - \beta(R + R^* + T + T^*) - d_T)T + k(T^* - bT + \gamma R^* T^*) + T_{input}, \\ \frac{dT^*}{dt} &= (\rho I - \beta(R + R^* + T + T^*) - d_{T^*})T^* - k(T^* - bT + \gamma R^* T^*), \\ \frac{dI}{dt} &= \sigma(T^* - (\alpha(R + R^* + T + T^*) + \delta)I).\end{aligned}$$

The parameters range are as in Table 4.1. The new parameters considered here are  $R_{input} = T_{input} = 100$  cells/ml/day which gives a homeostatic concentration  $R_{hom}$  of Tregs of  $1.36 \times 10^3$  cells/ml in the absence of antigenic stimulation of T cells ( $b = 0$ ). And the parameters for the asymmetry in the death rates  $d_R = d_T = 0.1$  per day,  $d_{R^*} = d_{T^*} = 0.01$  per day. The new aspect of this model, comparing with the model presented in Section 4.1.1, is the asymmetry in the difference between the growth and death rates.

With this kind of asymmetry present for the T cells, the increase of the population of T cells with the increase of the antigenic stimulation  $b$  of T cells is

caused both by the increase in cytokine secretion (similarly to the model presented in Section 4.1.1) and by the decrease in the average death rate of T cells. Hence, there is an improvement in the efficiency of the response of the immune system for high antigenic stimulations (high values of the parameter  $b$ ).

In the case of the cross reactive direct stimulation, the results obtained with this model are similar to the ones presented in the Subsection 4.1.4. However, when a bystander proliferation is considered, higher death rate of the non secreting T cells provokes lower concentrations of the bystander T cells, thus improving the results obtained (see [15]). In [13] we study the effects of different tunings between the antigenic stimulation  $a$  of Tregs and the antigenic stimulation  $b$  of T cells, by considering (for simplicity) a linear relation between  $a$  and  $b$ , eg due to an increase in the number of antigen presenting cells. The protection of the tissues against autoimmunity is enhanced by this relation between the stimuli  $a$  and  $b$  since both antigenic thresholds  $b_L$  and  $b_H$  increase. This positive correlation between the stimulation of T cells and the stimulation of Tregs resembles some features of a different model [44] and, as in their case, we show, in the presence of the asymmetry of the death rates, that the time rate of variation of stimulation of the immune system can determine the presence or absence of an immune response. We find that for some tuning between the antigenic stimulation  $a$  of Tregs and the antigenic stimulation  $b$  of T cells, a high rate of variation of the stimulation provokes an immune response, contrasting with a low rate of variation of the stimulation which does not provoke an immune response. A mathematical explanation for the fact that fast and slow variations of the antigenic stimulation result in different outcomes is that for a given tuning and a given antigenic stimulation  $b$  of T cells we are in the presence of a transcritical bifurcation. Small perturbations of the tuning can bring the unfold of the transcritical

bifurcation allowing the appearance of immune responses bursts for much lower values of the antigenic stimulation of T cells than before the unfolding. The period of time necessary for the appearance of the burst depends on the size of the perturbations.

### 4.3.2 Bifurcation diagrams

We study the positive correlation between the antigenic stimulation  $a$  of Tregs and the antigenic stimulation  $b$  of T cells. Since both are presented by the antigen presenting cells (APC). For simplicity, we study a linear relation between these stimuli in the form:  $a = a_0 + mb$ . If the levels of antigenic stimulation  $a$  of the Tregs and the levels of antigen stimulation  $b$  of the T cells are independent, i.e. the slope  $m$  is equal to zero, an hysteresis is present regardless of the value of the antigenic stimulation  $a$  of the Tregs. The two antigenic thresholds  $b_L$  and  $b_H$  bound the bistability region of the hysteresis. We observe that the thresholds  $b_L$  and  $b_H$  of antigenic stimulation of T cells and the ratio  $b_H/b_L$  increase with the antigenic stimulation  $a$  of the Tregs. Similarly to the case when the antigenic stimulation  $a$  of the Tregs is independent of the antigenic stimulation  $b$  of T cells (see Figure 4.8 (A)), an hysteresis is present for small values  $0 \leq m < m_S$  of the slope  $m$ . We observe, when  $m = m_S$ , the appearance of a saddle-node bifurcation point, disconnected from the hysteresis (see Figure 4.8 (B)). For values of the slope  $m_S < m < m_X$ , a loop is present, disconnected from the hysteresis (see Figures 4.8 (C) and (D)). When  $m = m_X$ , a transcritical bifurcation appears when the loop touches the hysteresis at the threshold  $b_H$  of the hysteresis (see Figure 4.8 (E)). For values of  $m > m_X$  the loop merges with the hysteresis, corresponding to a system with a wider hysteresis (see Figure 4.8 (F)).

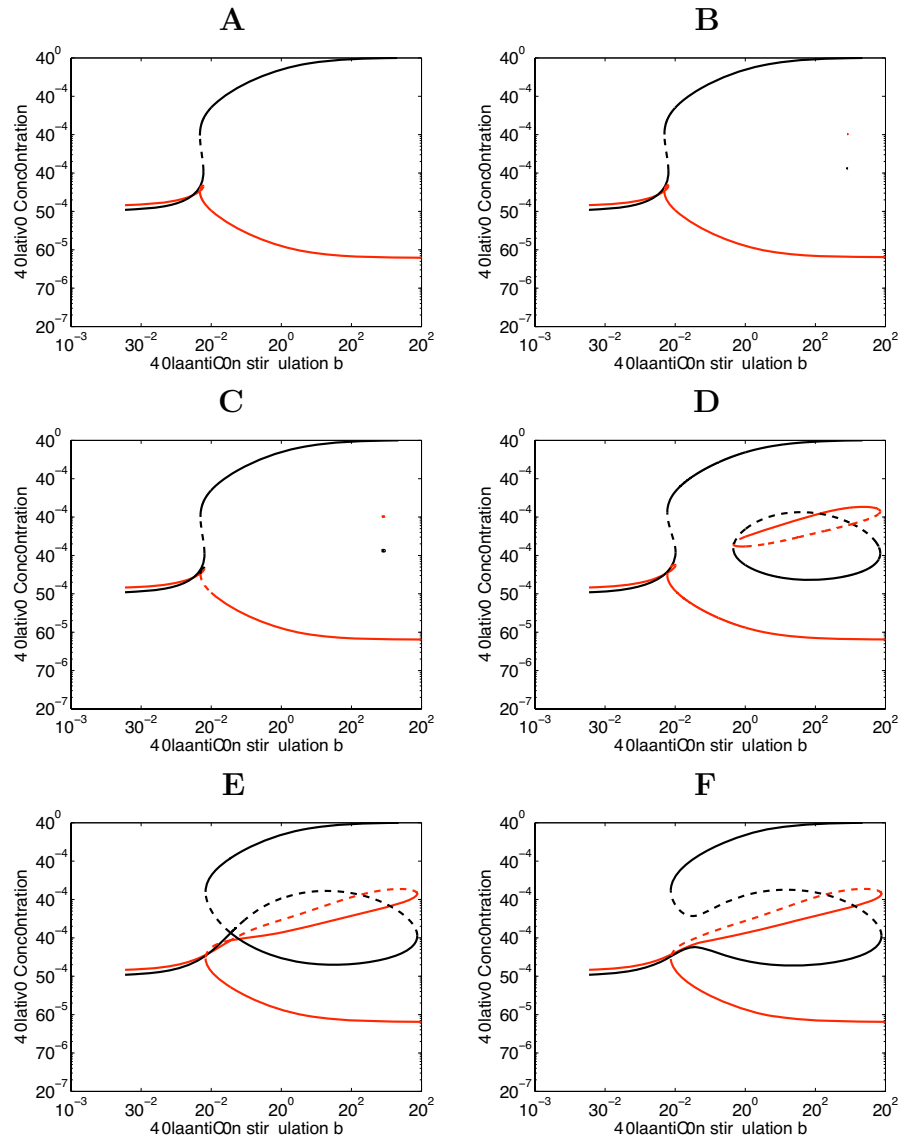


Figure 4.8: Equilibria for different tunings  $a = a_0 + mb$  of the antigenic stimulations, with  $a_0 = 1/2.4$ . From A to F the slope  $m$  increases. Black lines: concentration of T cells, Red lines: concentration of Tregs. Solid lines indicate stable equilibria and dashed lines indicate unstable equilibria. (A) ( $m = 0$ ) we see the hysteresis similar to the one observed in [11]; (B) ( $m = 0.164428$ ) we see the appearance of a saddle node point; (C) ( $m = 0.165$ ) the point increases to a loop limited by two folds; (D) ( $m = 1$ ) the loop is bigger; (E) ( $m = 1.64298$ ) the loop touches the hysteresis threshold  $b_H$  in a transcritical bifurcation; (F) ( $m = 2$ ) the loop has merged with the hysteresis. Further increases of the slope will not make qualitative differences in the figure.

If we consider that in the “normal” state of the immune system there is a positive correlation between the antigen thresholds  $a$  and  $b$  as in Figure 4.8 (F), the slope  $m$  can be related to autoimmunity, since a reduction of the slope will decrease the antigenic threshold  $b_H$  of T cells. In particular when the slope  $m = m_X$  there is a discontinuity in  $b_H$  with slopes below  $m_X$  creating thresholds  $b_H$  400 times lower than the thresholds  $b_H$  for slopes above  $m_X$ .

### 4.3.3 Fast and slow variation of antigenic stimulation

The antigenic stimulation of T cells and Tregs is likely to change with time either rapidly, eg due to an infection with the consequent immune response as an outcome, or slowly, caused by the natural modifications of the organism with age and with the T cells being kept in control by the Tregs. We model these situations by considering that the antigenic stimulation  $b$  of T cells varies between  $b_0 < b_L$  and  $b_\infty > b_H$  in an interval of time. To compute the value of  $b$ , we choose the following log-sigmoid function of time:

$$\log b(t) = \log b_0 + \frac{\log b_\infty - \log b_0}{1 + e^{-(t-t_M)/\tau}},$$

with  $b_0 = 0.01$ ,  $b_\infty = 10$  and  $t_M = 100$ . This function passes through the median  $b = \sqrt{b_0 b_\infty} = 0.316\dots$  at a time  $t_M = 100$  days. The derivative of this function is inversely proportional to the parameter  $\tau$ , meaning that the steepness factor  $\tau$  is related to the typical time of increase of  $b$ , with higher values of the steepness factor  $\tau$  being related to slow variations of  $b$ . We also consider that the antigen stimulation  $a$  of Tregs varies with the antigen stimulation  $b$  of T cells in the linear relation:  $a(b) = a_0 + mb$ , with  $a_0 = 1/2.4$  and slope  $m = 2$ , as in Figure 4.8 (F).

In the model with asymmetric death rates with a slope  $m$  above the value of

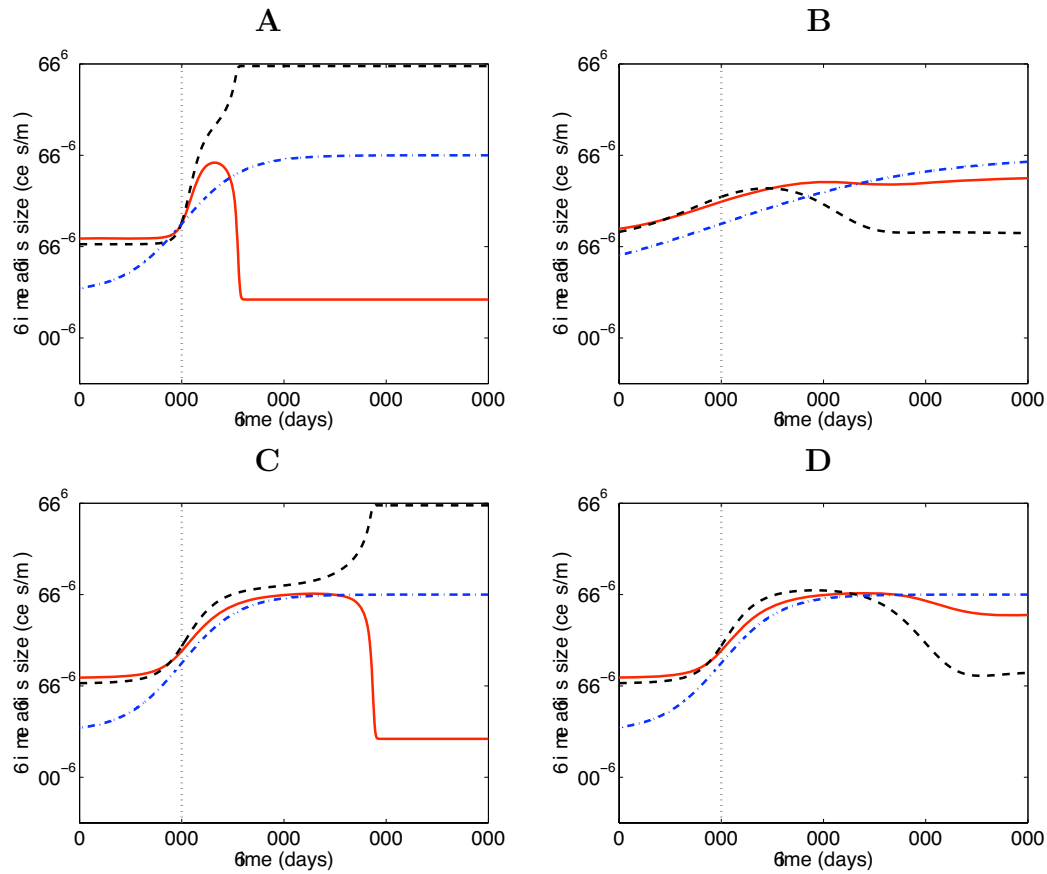


Figure 4.9: Effect of different rates of increase of  $b$ . The level of antigenic stimulation  $b$  of T cells varies between 0.01 and 10 in a log-sigmoid function of time with steepness factor  $\tau$ . The antigenic stimulation  $a$  of Tregs is  $a(b) = 1/2.4 + 2b$ . Black dashes: total concentration of T cells ( $T + T^*$ ). Red line: total concentration of Tregs ( $R + R^*$ ). Blue dash-dots: antigenic stimulation  $b$  of T cells (presented as  $b/100$  to fit in the window). Vertical grey dots: median time of the variation (100 days). (A) Fast variations of the antigenic stimulation ( $\tau = 10$  days) give an immune response; (B) For slow variations of the antigenic stimulation ( $\tau = 100$  days) the T cells remain controlled. For intermediate rates of variation either there is an immune response ((C)  $\tau = 28$  days) or a controlled state ((D)  $\tau = 29$  days).

the transcritical bifurcation  $m > m_X = 1.64\dots$ , we observe that a fast variation of the antigenic stimulation triggers an immune response (see Figure 4.9 (A)), i.e. the concentration  $T + T^*$  of T cells is high, near the capacity value  $T_{cap}$ , with a transient increase in the concentration  $R + R^*$  of Tregs. On the other hand, in a slow variation of the antigenic stimulation (see Figure 4.9 (B)), the concentration  $T + T^*$  of T cells has a temporary small increase and the increase in the concentration  $R + R^*$  of Tregs is able to sustain a controlled state, thus resulting in a subclinical behaviour that enhances the protection of the tissue against autoimmunity. We observe that there is a threshold value of the steepness factor ( $\tau_0 \approx 28.5$  days) such that an immune response arises for lower values of the steepness factor and that a controlled state is maintained for higher steepness factors (see Figures 4.9 (C) and (D)).

#### 4.3.4 Dynamics of bystander proliferation

The asymmetry maintains the basic features of the model, namely, the existence of a controlled stable steady state (with low concentration of T cells) and the existence of an immune response stable steady state (with high concentration of T cells), depending on the antigenic stimulation  $b$  of T cells and the initial conditions. The thresholds  $b_L$  and  $b_H$  of antigenic stimulation of T cells, are similar to the ones presented in Subsection 4.1.2.

The simulations of the bystander proliferation have differences between the immune response model and the model presented in this Section. In the simulations of a bystander proliferation, we considered two lines of T cells  $T_b, T_b^*$  and  $T_c, T_c^*$  that have, respectively, pathogen stimulation  $b$  and autoimmune antigen stimulation  $c$ . We study this model considering two cases: a) the symmetric case, as in [11]; b) the asymmetric case, as in [13]. The model consists of a set of

ordinary differential equations (see [11, 13] for further details) and is employed to study the dynamics, with a compartment for each T cell population (inactive Tregs  $R$ , active Tregs  $R^*$ , non secreting T cells  $T_b$  and  $T_c$ , secreting activated T cells  $T_b^*$  and  $T_c^*$ ) and interleukine 2 density  $I$ :

$$\begin{aligned}
\frac{dR}{dt} &= (\epsilon\rho I - \beta N - d_R)R + \hat{k}(R^* - aR) + R_{input}, \\
\frac{dR^*}{dt} &= (\epsilon\rho I - \beta N - d_{R^*})R^* - \hat{k}(R^* - aR), \\
\frac{dT_b}{dt} &= (\rho I - \beta N - d_T)T_b + k(T_b^* - bT_b + \gamma R^* T_b^*) + T_{input}, \\
\frac{dT_b^*}{dt} &= (\rho I - \beta N - d_{T^*})T_b^* - k(T_b^* - bT_b + \gamma R^* T_b^*), \\
\frac{dT_c}{dt} &= (\rho I - \beta N - d_T)T_c + k(T_c^* - bT_c + \gamma R^* T_c^*) + T_{input}, \\
\frac{dT_c^*}{dt} &= (\rho I - \beta N - d_{T^*})T_c^* - k(T_c^* - bT_c + \gamma R^* T_c^*), \\
\frac{dI}{dt} &= \sigma(T_b^* + T_c^* - (\alpha N + \delta)I).
\end{aligned}$$

with  $N = R + R^* + T_b + T_b^* + T_c + T_c^*$ . We chose the following values for the parameters  $R_{input} = T_{input} = 100$  cells/ml/day,  $d_R = d_T = 0.1$  per day,  $d_{R^*} = d_{T^*} = 0.01$  or  $0.1$  per day and the values of the other parameters are equal to the ones presented in Table 4.1. The important aspects of this model are a mechanism to sustain a population of Tregs, secretion inhibition of T cells with a rate that correlates with Treg population size, and growth and competition for IL-2 with a higher growth rate of T cells relative to Tregs.

We compare the dynamics of the bystander proliferation between the model with symmetric death rates and the model with asymmetric death rates. The asymmetry reflects that the difference between the growth and death rates can be higher for the active T cells and the active Tregs than for the inactive T cells and



inactive Tregs. The asymmetry in the difference between the growth and death rates brings up the relevance of the antigenic stimulation of Tregs in the control of the local Treg population size. This asymmetry can be due to the presence of memory T cells and memory regulatory T cells. We observe that the asymmetry in the model provokes slightly faster growth rate of T cells, in particular for high antigenic stimulations  $b$  of T cells due to the lower average death rate of T cells.

In the case of the cross reactive direct stimulation, the results are analogous to the immune response model [11]: the final state of the model is either a controlled state or an immune response state, the last one being achieved if the stimulation of the autoimmune antigen  $b$  is between  $b_L$  and  $b_H$  and the duration of the immune response is of sufficient duration (about 5 days in the simulations in [11]). The simulations of the bystander proliferation present differences between the symmetric case and the asymmetric case. In our simulations, we consider a tissue with initial controlled state of both T cells lines and we simulate a pathogen infection as a step increase in  $b$  from 0 to 1000 between days 0 and 7 (other choices of suitable pathogen dynamics give analogous results). If the autoimmune stimulation of T cells was too low ( $c < c_L$ ) the autoimmune T cells could not sustain autoimmunity after pathogen clearance and Tregs would be able to regain control. On the other hand, if the autoimmune stimulation of T cells was too high ( $c > c_H$ ) it would be impossible to have an initial controlled autoimmune state. In the simulations in Figure 4.10, we choose the autoimmune antigenic stimulation  $c = 0.1$  to be a constant value between the thresholds  $c_L$  and  $c_H$  of antigen stimulation. In the three simulations presented in Figure 4.10, we observe that the concentrations of the autoimmune line of T cells  $T_c$ ,  $T_c^*$  increases between days 0 and 7, because, during this period of time, there is an increase of the concentration of  $I$  cytokine secreted by the line of T cells  $T_b$ ,  $T_b^*$

that respond to the pathogen. There is also a transient increase in the population of Tregs due to the  $I$  cytokine followed by suppression of Tregs due to the Fas-FasL mediated apoptosis. In the end of the pathogen exposure (after 7 days) the secreting autoimmune T cells  $T_c^*$  generate enough  $I$  cytokine to sustain the population of autoimmune T cells  $T_c$ ,  $T_c^*$  in high concentrations, thus developing an autoimmune response.

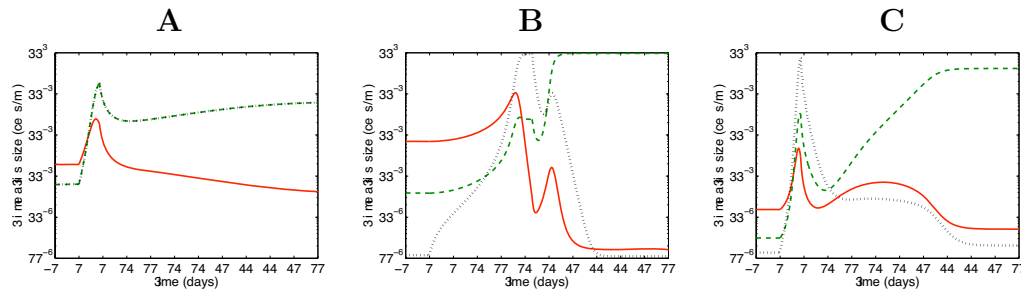


Figure 4.10: Bystander proliferation for different models. **(A)** The symmetric case: the T cells not responding to the pathogen have equal concentration to the T cells responding to the pathogen; **(B)** Only the secreting T cells  $T^*$  die slower: the T cells not responding to the pathogen have lower concentration than the T cells responding to the pathogen; **(C)** The asymmetric case: the T cells not responding to the pathogen have lower concentration than the T cells responding to the pathogen and take more time than in case B to achieve an immune response. Black dots: concentration of T cells responding to the pathogen ( $T_b + T_b^*$ ); Green dashes: concentration of T cells not responding to the pathogen ( $T_c + T_c^*$ ); Red line: concentration of Tregs ( $R + R_*$ ).

The onset of autoimmunity depends both of the duration of the pathogen exposure and of the model considered. In the symmetric case with two lines of T cells (with  $d_{R^*} = d_{T^*} = 0.1$  per day), we observe that the autoimmune response stabilizes around 10 weeks after the pathogen exposure (see Figure 4.10 (A)). In the asymmetric case, with lower death rate of secreting T cells and active Tregs ( $d_{R^*} = d_{T^*} = 0.01$  per day), the autoimmunity arises approximately 8 weeks after

the pathogen exposure (see Figure 4.10 (C)). We also consider an intermediate choice of death rates (see Figure 4.10 (B)), where the asymmetry of the death rates is present only for the T cells ( $d_{R^*} = 0.1$  per day and  $d_{T^*} = 0.01$  per day). In this case, the autoimmunity appears after about 6 weeks. The comparison of the Tregs concentrations, presented in Figures 4.10 (B) and (C), show that the asymmetry in the growth and death rates between the active and inactive regulatory T cells have implications in the concentration of the regulatory T cells after the pathogen removal. As we can see, in Figures 4.10 (B) and (C), the concentration of the regulatory T cells is higher in the presence of the asymmetry. In the case of an autoimmune response of T cells  $T_c, T_c^*$ , we observed that the concentration of both lines of T cells are always equal in the symmetric case where  $T_b + T_b^* = T_c + T_c^*$  (see Figure 4.10 (A)), because the growth rates and the death rates of the two types of T cells are equal. However, in the asymmetric case (see Figure 4.10 (C)), the line of T cells  $T_b, T_b^*$  that responds to the pathogen stimulation  $b$  has higher concentration than the other line of T cells  $T_c, T_c^*$  during the infection period (between 0 and 7 days). This is due to the lower average death rate of the line of T cells that respond to the pathogen  $T_b, T_b^*$ . For the same reason, when we consider the asymmetry of the death rates only for the T cells (see Figure 4.10 (B)), the concentration of the line of T cells  $T_b, T_b^*$  that responds to the pathogen is also higher than the other concentration of the other line of T cells  $T_c, T_c^*$  during the infection period. After the infection period, the T cells  $T_b, T_b^*$  decrease to the initial homeostatic levels. However, the autoimmune response for the T cells  $T_c, T_c^*$  appear because the antigenic stimulation  $c$  is between  $c_L$  and  $c_H$  and, also, because the IL-2 cytokine concentration is high enough to move their state, through the hysteresis unstable manifold, to the basin of attraction of the autoimmune response equilibrium state.

## 4.4 Conclusions

In this Chapter, we examined mechanisms of Treg control of immune responses through regulation of cytokine dependent T cell proliferation. In the model in [11], Tregs have two effects on cytokine levels: firstly they directly inhibit cytokine secretion; and secondly they adsorb (and thus compete for) proliferative cytokines. Both of these have an impact on T cell growth. Secretion inhibition is shown to act as a growth modulator through adjustment of a quorum threshold associated with cytokine growth dynamics. The second effect was minimal in the simulations because the Treg population was always a minor population. However, increasing the homeostatic level of Tregs would increase the impact of this competition and reduce immune response growth rates, thereby extending immune response times.

The threshold mechanism discussed here is extremely robust to model details, being effectively a model of activation and escape. Proliferation driven by a secreted cytokine is naturally population size (quorum) dependent [18] and “quorum sensing” imposes a population consensus on immune responses which are only initiated if a sufficiently high number of T cells are locally activated. A locally maintained population of Tregs raise this quorum threshold in the local tissue. Thus, immune responses are inhibited unless the number of activated T cells is sufficiently large when the immune response escapes inhibition; such escape is dependent on the higher efficiency with which conventional T cells (responders) can utilise IL-2 compared to Tregs.

The bistability presented here is, in fact, a common feature of all the current Treg models [42]. To retain a control Treg population we had to include an homeostatic mechanism such as a J cytokine or an input flux  $R_{input}$  (as in Section 4.3), eg from the thymus.

Treg induced secretion inhibition can protect different tissues from immune responses to varying degrees, by adjusting (possibly through evolutionary selection) the size and activity of the local Treg population. In Section 4.3, when we considered an asymmetry in the death rates, the size and activity of the local Treg population are controlled by the antigenic stimulation  $a$  of Tregs, by the inflow  $R_{input}$  of Tregs and by the asymmetry in the death rates of Tregs. Furthermore, the asymmetry in the death rates of T cells, caused for example by the presence of memory cells, is an improvement to the model, since high antigenic stimulations  $b$  of T cells provoke a faster increase of the concentration of T cells in the modified model. These mechanisms allow tissues that are frequently exposed to antigen, eg the gut, to have the balance more in favour of inhibition, while other tissues may have no local Treg population. Under pathogen invasion Treg control can be broken and an immune response ensue. After pathogen clearance, T cells downsize and differentiate to memory whilst Tregs ideally return to pre immune response levels through homeostatic regulation. However, since regulation is non specific, an immune response, and the associated proliferative cytokine production can induce bystander proliferation of autoimmune T cells (and Tregs), whilst enhanced levels of costimulation can abrogate inhibition which undermines control of autoimmunity. The existence of an asymmetry in the death rates of T cells is an improvement of the immune response model in the simulation of the bystander proliferation because it allows the T cells stimulated by the pathogen to have higher concentrations than the other lines of T cells. Because of the hysteresis implicit in the dynamics, the high proliferation of these bystanders during the immune response may lead to their escape from Treg control and thereby establish chronic autoimmunity.

We also considered (see [13]) that the antigenic stimulation  $a$  of Tregs is pos-

itively correlated to the antigenic stimulation  $b$  of T cells. When we considered a linear relation  $a = a_0 + mb$ , between the antigenic stimulations  $a$  and  $b$ , we observed a transcritical bifurcation at a slope  $m = m_X$  that can be related to the appearance of autoimmunity at low self antigenic stimulation  $b$  of T cells for lower slopes  $m < m_X$ . For higher slopes  $m > m_X$ , we can still see a partial effect, dependent of the rate of increase of the antigenic stimulation  $b$  of T cells with results similar to other authors [44] in a structurally different model. We observed that for slow increases of the antigenic stimulation  $b$  the Tregs are able to maintain control but for fast increases of  $b$  an immune response is triggered. Thus our model can explain the fact that autoimmunity can be associated with a prior pathogen exposure. Whilst bystander proliferation could lead to autoimmunity we found that cross reacting T cells were more prone to escape (escape at lower  $b$ ). The load threshold behavior observed in adoptive transfer experiments [69] is also explained by this quorum growth mechanism, whilst we predict a cytokine (principally IL-2) dependence of this threshold and thus its modulation under alteration of the IL-2 environment. The reverse switch from autoimmune to controlled state can be achieved if the autoimmune T cell population can be lowered sufficiently, or Treg density increased. For example, immune suppression that targets conventional T cells but not Tregs could lead to a switch. A possible target is suppression of IL-2 secretion, provided chronic autoimmune states are IL-2 dependent. However, because of the hysteresis in this system high levels of suppression are needed, whilst the observation of delayed escape and autoimmunity indicates that temporal dynamics must also be considered.



# Bibliography

- [1] C.D. Aliprantis, D. J. Brown and O.Burkinshaw, Edgeworth equilibria. *Econometrica* **55**, 1109-1137 (1987).
- [2] R. Amir, I. Evstigneev and J. Wooders, Cooperation vs. Competition in R&D: the role of Stability of Equilibrium. *Journal of Economics* **67**, 63-73 (1998).
- [3] P.M. Anderson and M.A. Sorenson, Effects of route and formulation on clinical pharmacokinetics of interleukine-2. *Clinical Pharmacokinetics* **27** 19-31 (1994).
- [4] C. d'Aspremont and A. Jacquemin, Cooperative and noncooperative R&D in duopoly with spillovers. *American Economic Review* **78**, 1133-1137 (1988).
- [5] R. Aumann, Correlated equilibrium as an expression of Bayesian rationality. *Econometrica* **55**, 1-18 (1987).
- [6] R. Aumann and L. Shapley, *Values of non atomic games*, Princeton University Press (1974).
- [7] K. Binmore and M. Herrero, Matching and bargaining in dynamic markets. *Review of Economic Studies* **55**, 17-31(1988).



- 
- [8] G.I. Bischi, M. Gallegati and A. Naimzada, Symmetry-breaking bifurcations and representative firm in dynamic duopoly games. *Annals of Operations Research* **89**, 253-272 (1999).
- [9] L. Boukas, D. Pinheiro, A.A. Pinto, S. Z. Xanthopoulos and A.N. Yannacopoulos, Dynamical Scenarios for Contingent Claims Valuation in Incomplete Markets. *Journal of Difference Equations and Applications (Accepted for publication)*, 1-20 (2009).
- [10] J.A. Brander and B.J. Spencer Strategic commitment with R&D: the symmetric case, *The Bell Journal of Economics* **14**, 225-235 (1983).
- [11] N.J. Burroughs, B.M.P.M. Oliveira and A.A. Pinto, Regulatory T cell adjustment of quorum growth thresholds and the control of local immune responses. *J. Theor. Biol.* **241**, 134-141(2006).
- [12] N.J. Burroughs, B.M.P.M. Oliveira, A.A. Pinto and H.J.T. Sequeira, Sensibility of the quorum growth thresholds controlling local immune responses. *Mathematical and Computer Modelling* **47**, 714-725 (2008).
- [13] N.J. Burroughs, B.M.P.M. Oliveira, A.A. Pinto and M. Ferreira, A transcritical bifurcation in an immune response model. *Journal of Difference Equations and Applications (Accepted for Publication)*, 1-7 (2009).
- [14] N.J. Burroughs, B.M.P.M. Oliveira, A.A. Pinto and M. Ferreira, Immune response Dynamics. *Mathematical and Computer Modelling (Accepted for Publication)*, 1-17 (2009).
- [15] N.J. Burroughs, M. Ferreira, B.M.P.M. Oliveira and A.A. Pinto, Autoimmunity arising from bystander proliferation of T cells in an immune response

- model. *Mathematical and Computer Modelling (Accepted for Publication)*, 1-10 (2009).
- [16] R.E. Callard, J. Stark and A.J. Yates, Fratricide: a mechanism for T memory-cell homeostasis. *Trends Immunol.* **24**, 370-375 (2003).
- [17] A. Cournot, *Recherches sur les Principes Mathématiques de la Théorie des Richesses*. Paris, 1838. English edition: *Researches into the Mathematical Principles of the Theory of Wealth*. Edited by N. Bacon. New York: Macmillan (1897).
- [18] R.J. de Boer, and P. Hogeweg, Immunological discrimination between self and non-self by precursor depletion and memory accumulation. *J. Theor. Biol.* **124**, 343 (1987).
- [19] R. DeBondt, Spillovers and innovative activities. In *International Journal of Industrial Organization* **15**, 1-28 (1997).
- [20] F.Y. Edgeworth, *Mathematical psychics: An essay on the application of mathematics to the moral sciences*, London: Kegan Paul (1881).
- [21] F.A. Ferreira, F. Ferreira, M. Ferreira, B.M.P.M. Oliveira and A.A. Pinto, Dynamics in a duopoly model with R&D investments. In Zita Vale et al. (eds.): *Knowledge and Decision Technologies*, Porto: Instituto Politécnico do Porto, Proc. of the 2<sup>nd</sup> ICKEDS'06, Lisbon, Portugal. ISBN: 972-8688-39-3, 199-202 (2006).
- [22] F.A. Ferreira, F. Ferreira, M. Ferreira, B. Oliveira and A.A. Pinto, Cournot Model: repeated R&D investments for non-identical firms. CD-Rom Proc. of Mathematical Methods in Engineering, Ankara, Turquia. ISBN: 975-6734-04-3 (2006).

- 
- [23] F.A. Ferreira, F. Ferreira, M. Ferreira and A.A. Pinto, Quantity competition with product differentiation. In César Sellero et al (eds.). Actas do VIII Congresso Galego de Estatística e Investigación de Operacións. Santiago de Compostela, Espanha. ISBN: 978-84-690-9136-4, 127-132 (2007).
- [24] M. Ferreira, B. Finkenstädt, B. Oliveira and A.A. Pinto, Evolution in an Edgeworthian Exchange Economy. CD-ROM Actas do I Congresso de Estatística e Investigação Operacional da Galiza e Norte de Portugal / VII Congresso Galego de Estatística e Investigación de Operacións, Guimarães, Portugal. ISBN: 972-99841-0-7 (2005).
- [25] M. Ferreira, B. Finkenstädt, B. Oliveira and A.A. Pinto, Is there an optimal greed in an Edgeworthian economy? In Zita Vale et al. (eds.): *Knowledge and Decision Technologies*, Porto: Instituto Politécnico do Porto, Proc. of the 2<sup>nd</sup> ICKEDS'06, Lisbon, Portugal. ISBN: 972-8688-39-3, 203-206 (2006).
- [26] M. Ferreira, B.F. Finkenstädt, B.M.P.M. Oliveira and A.A. Pinto, Nonlinearity in an Edgeworthian Exchange Economy. CD-Rom Proc. of Mathematical Methods in Engineering, Ankara, Turquia. ISBN: 975-6734-04-3 (2006).
- [27] M. Ferreira, B.F. Finkenstädt, B. Oliveira, A.A. Pinto and A.N. Yannacopoulos, On the convergence to Walrasian prices in random matching Edgeworthian economies. *Submitted for Publication*, 1-10 (2009).
- [28] M. Ferreira, B.F. Finkenstädt, B. Oliveira and A.A. Pinto, A modified model of an Edgeworthian Economy. Dynamics and Games in Science DYNA2008 in honor of Maurício Peixoto and David Rand, Edited by Alberto Pinto, Book Chapter (Accepted for Publication) (2009).

- [29] M. Ferreira, B.M.P.M. Oliveira and A.A. Pinto, Patents in new technologies. *Journal of Difference equations and applications* **15**, 1135-1149 (2009).
- [30] M. Ferreira, B.M.P.M. Oliveira and A.A. Pinto, Piecewise R&D Dynamics on costs. *Fasciculi Mathematici (Accepted for publication)*, 1-13 (2009).
- [31] M. Ferreira, B. Oliveira and A.A. Pinto, Survey on Patents in new technologies. Dynamics and Games in Science DYNA2008 in honor of Maurício Peixoto and David Rand, Edited by Alberto Pinto, Book Chapter (Accepted for Publication) (2009).
- [32] M. Ferreira, B. Oliveira, A.A. Pinto and N.J. Burroughs, The control of immune responses by regulatory T cells. Dynamics and Games in Science DYNA2008 in honor of Maurício Peixoto and David Rand, Edited by Alberto Pinto, Book Chapter (Accepted for Publication) (2009).
- [33] B. Finkenstädt, A.A. Pinto, M. Ferreira and B.M.P.M. Oliveira, Edgeworthian economies. *Proceedings in Applied Mathematics and Mechanics (PAMM)*, Volume 7, Issue 1, 1041305-1041306 (2007).
- [34] B.F. Finkenstädt and P. Kuhbier, On the stability of equilibria in an exchange economy: From a Walrasian tâtonnement to an individual interaction mechanism. *Unpublished Manuscript* (1995).
- [35] G. Furtado, M. Curotto de Lafaille, N. Kutchukhidze and J. Lafaille, Interleukin 2 signaling is required for CD4<sup>+</sup> regulatory T cell function *The Journal of Experimental Medicine* **196** 851-857 (2002).
- [36] D. Gale, *Strategic Foundations of Perfect Competition*, Cambridge University Press (2000).

- 
- [37] T.C. George, J. Bilsborough, J.L. Viney and A.M. Norment, High antigen dose and activated dendritic cells enable Th cells to escape regulatory T cell-mediated suppression *in vitro*. *Eur. J. Immunol* , 502-511(2003).
- [38] C.-S. Hsieh, Y. Liang, A. J. Tyznik, S. G. Self, D. Liggitt and A. Y. Rudensky, Recognition of the peripheral self by naturally arising CD25<sup>+</sup> CD4<sup>+</sup> T cell receptors. *Immunity* **21**, 267-277 (2004).
- [39] M. Kamien, E. Muller and I. Zang, Research joint ventures and R&D cartels. *American Economic Review* **82**, 1293-1306 (1992).
- [40] M. Kamien and I. Zang, Competing research joint ventures. *Journal of Economics and Management Strategy* **2**, 23-40 (1993).
- [41] M. Katz, An analysis of cooperative research and development. *Rand Journal of Economics* **17**, 527-543 (1986).
- [42] K. Leon, R. Perez, A. Lage and J. Carneiro, Modelling T-cell-mediated suppression dependent on interactions in multicellular conjugates. *J. Theor. Biol.* **207**, 231-254 (2000).
- [43] K. Leon, A. Lage and J. Carneiro, Tolerance and immunity in a mathematical model of T-cell mediated suppression. *J. Theor. Biol.* **225**, 107-126 (2003).
- [44] K. Leon, J. Faro, A. Lage and J. Carneiro, Inverse correlation between the incidences of autoimmune disease and infection predicted by a model of T cell mediated tolerance. *Journal of Autoimmunity*, 31-42 (2004).
- [45] P.J. Lloyd, The origins of the von Thünen-Mill-Pareto-Wicksell-Cobb-Douglas function. *History of Political Economy* **33**, 1-19 (2001).

- [46] J.W. Lowenthal and W.C. Greene, Contrasting interleukine 2 binding properties of the alpha (p55) and beta (p70) protein subunits of the human high-affinity interleukine 2 receptor. *The Journal of Experimental Medicine*, 1155-1169 (1987).
- [47] A. MasColell, An equivalence theorem for a bargaining set. *Journal of Mathematical Economics* **18**, 129-139 (1989).
- [48] A. R. McLean, Modelling T cell memory. *J. Theor. Biol.*, 63-74 (1994).
- [49] A. McLennan and H. Schonnenschein, Sequential bargaining as a non cooperative foundation for Walrasian equilibria. *Econometrica* **59**, 1395-1424 (1991).
- [50] C.A. Michie, A. McLean, C. Alcock and P.C.L. Beverley, Life-span of human lymphocyte subsets defined by CD45 isoforms. *Nature* **360**, 264-265 (1992).
- [51] D. Moskophidis, M . Battegay, M. Vandenbroek, E. Laine, U. Hoffmann-rohrer and R.M. Zinkernagel, Role of virus and host variables in virus persistence or immunopathological disease caused by a noncytolytic virus. *The Journal of General Virology* **76**, 381 (1995).
- [52] S. Nagata, Fas ligand-induced apoptosis. *Annu. Rev. Genet.*, 9-55 (1999).
- [53] A.A. Pinto, Game Theory and Duopoly Models, *Interdisciplinary Applied Mathematics, Springer-Verlag* (2009 - Plan Accepted).
- [54] A.A. Pinto, F.A. Ferreira, M. Ferreira and B.M.P.M. Oliveira, Cournot Duopoly with competition in the R&D expenditures. Proceedings in Applied Mathematics and Mechanics (PAMM), Volume 7, Issue 1, 1060601-1060602 (2007).

- [55] A.A. Pinto, F.A. Ferreira, M. Ferreira and B.M.P.M. Oliveira, Cournot model with investments to change the market size. Proceedings in Applied Mathematics and Mechanics (PAMM), Volume 7, Issue 1, 1041303-1041304 (2007).
- [56] A.A. Pinto, M. Ferreira, B. Finkenstädt and B.M.P.M. Oliveira, Greed in Random Matching Games. Numerical Analysis and Applied Mathematics, AIP (American Institute of Physics) Conference Proceedings, 1048, Kos, Greece, 1-4 (Accepted for Publication) (2009).
- [57] A.A. Pinto, M. Ferreira and B.M.P.M. Oliveira, R&D Dynamics on costs. Numerical Analysis and Applied Mathematics, AIP (American Institute of Physics) Conference Proceedings, 1048, Kos, Greece, 1-4 (Accepted for Publication) (2009).
- [58] A.A. Pinto, B. Oliveira, F. Ferreira and M. Ferreira, R&D investments in a duopoly model. CD-ROM Proceedings of the First Annual Meeting of the Portuguese Economic Journal. University of the Azores, Ponta Delgada, Açores, Portugal. ISBN: 978-972-8612-34-4, 1-10 (2007).
- [59] A.A. Pinto, B. Oliveira, F.A. Ferreira and M. Ferreira. Investing to survive in a duopoly model. Intelligent Engineering Systems and Computational Cybernetics, Springer Netherlands, Chapter 23 (2008).
- [60] A.A. Pinto, S.X. Xanthopoulos and A.N. Yannacopoulos, *Market games for contingent claim valuation in incomplete markets (In Preparation)*
- [61] A.A. Pinto, *Game Theory and Duopoly Models*, Interdisciplinary Applied Mathematics, Springer-Verlag (2010).

- [62] A.A. Powell, K.R. McLaren, K.R. Pearson and M. T. Rimmer, Cobb-Douglas Utility ñ Eventually, Monash University, Department of Econometrics and Business Statistics, Working Paper (2002).
- [63] D.L. Qiu, On the dynamic efficiency of Bertrand and Cournot equilibria. *Journal of Economic Theory* **75**, 213-229 (1997).
- [64] P.R. Rogers, C. Dubey and S. L. Swain, Qualitative Changes Accompany Memory T Cell Generation: Faster, More Effective Responses at Lower Doses of Antigen. *Journal of Immunology* **164**, 2338-2346 (2000).
- [65] M. de la Rosa, Sascha Rutz, H. Dorninger and A. Scheffold, Interleukin-2 is essential for CD4<sup>+</sup>CD25<sup>+</sup> regulatory T cells function. *Eur. J. Immunol.* **34**, 2480-2488 (2004).
- [66] A. Rubinstein and A. Wolinsky, Decentralized trading, strategic behaviour and the Walrasian outcome. *Review of Economic Studies* **57**, 63-78 (1990).
- [67] L. Ruff, Research and technological progress in a Cournot economy. *Journal of Economic Theory* **1**, 397-415 (1997).
- [68] S. Sakaguchi, Naturally arising CD4<sup>+</sup> regulatory T cells for immunological self-tolerance and negative control of immune responses. *Annu. Rev. Immunol.* **22**, 531-562 (2004).
- [69] E.M. Shevach, R.S. McHugh, C.A. Piccirillo and A.M. Thornton, Control of T-cell activation by CD4(+) CD25(+) suppressor T cells. *Immunological Reviews* **182**, 58-67 (2001).
- [70] K.S. Schluns, W.C. Kieper, S.C. Jameson, L. Lefrancois, Interleukin-7 mediates the homeostasis of naive and memory CD8 T cells *in vivo*. *Nat. Immunol.* **1**, 426-432 (2000).



- [71] M. Shubik, Edgeworth's market games. *Contributions to the theory of games IV*, edited by R. D. Luce and A. W. Tucker, Princeton University Press (1959).
- [72] N. Singh and X. Vives, Price and quantity competition in a differentiated duopoly. *RAND Journal of Economics* **15**, 546-554 (1984).
- [73] C. Tanchot, F. Vasseur, C. Pontoux, C. Garcia and A. Sarukhan, Cutting edge: IL-2 is critically required for the in vitro activation of CD4(+)CD25(+) T cell suppressor function. *The Journal of Immunology* **172**, 4285-4291(2004).
- [74] A.M. Thornton and E.M. Shevach, CD4<sup>+</sup>CD25<sup>+</sup> immunoregulatory T cells suppress polyclonal T cell activation *in vitro* by inhibiting interleukine 2 production. *The Journal of Experimental Medicine* **188**, 287-296 (1998).
- [75] A. M. Thornton and E. M. Shevach, *Suppressor effector function of CD4<sup>+</sup> CD25<sup>+</sup> immunoregulatory T cells is antigen nonspecific* *The Journal of Immunology* **164**, 183-190 (2000).
- [76] A.M. Thornton, E.E. Donovan, C.A. Piccirillo and E.M. Shevach, Cutting edge: IL-2 is critically required for the in vitro activation of CD4(+)CD25(+) T cell suppressor function. *The Journal of Immunology* **172**, 6519-6523 (2004).
- [77] J. Tirole, *The Theory of Industrial Organization*. MIT Press, MA (1988).
- [78] C. Utny and N.J. Burroughs, Perturbation theory analysis of competition in a heterogeneous population. *Physica D* **175** 109-126 (2003).
- [79] H. Veiga-Fernandes, U. Walter, C. Bourgeois, A. McLean and B. Rocha, Perturbation theory analysis of competition in a heterogeneous population. *Nat. Immunol.* **1**, 47-53 (2000).

- [80] M. Voorneveld, From preferences to Cobb-Douglas utility. SSE/EFI Working Paper Series in Economics and Finance **701** (2008).